Theories and Predictions of nucleon–nucleus scattering

(from 0 to 300 MeV)

K. Amos

University of Melbourne,
Australia.

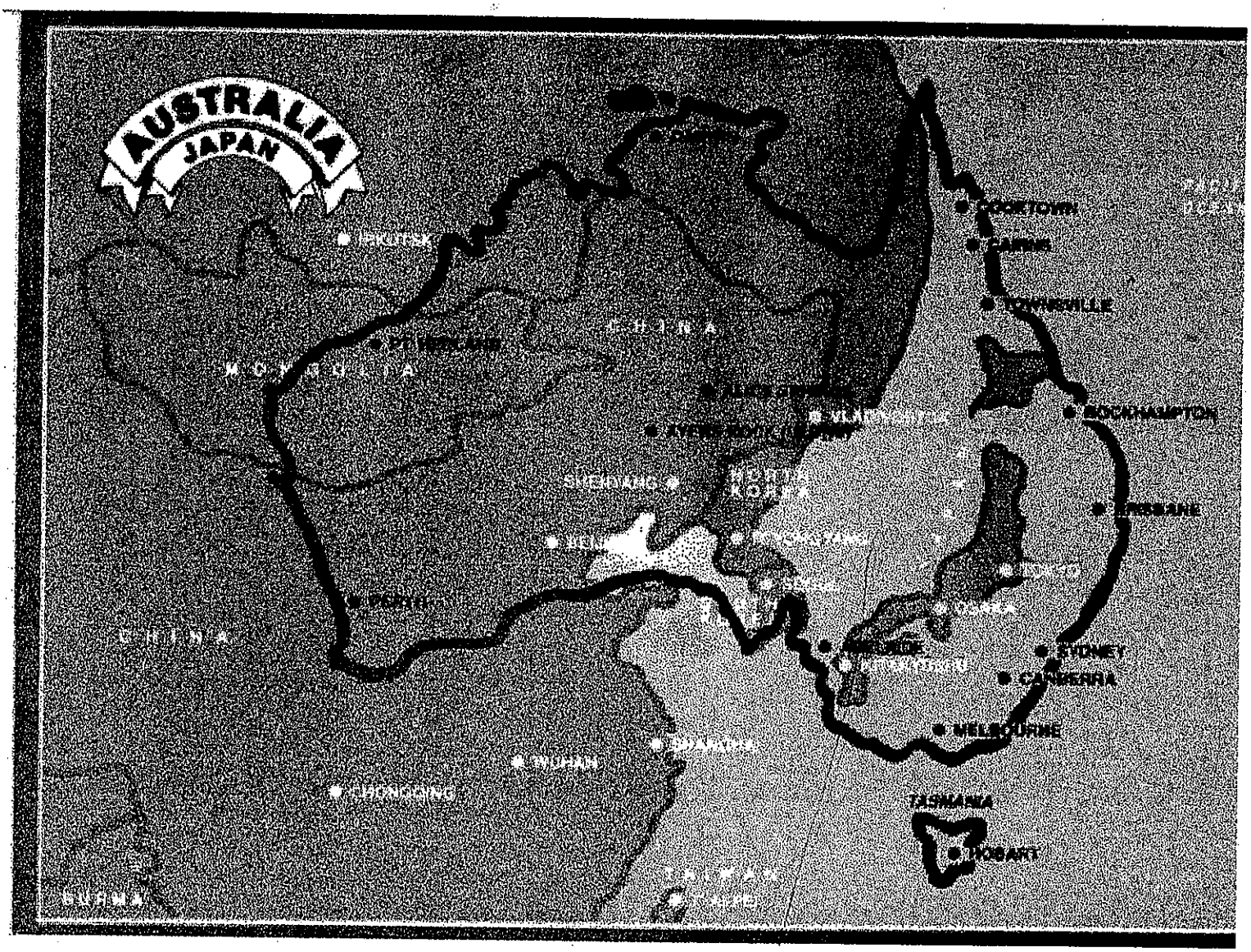
AUSTRALIA
JAPAN
IRKUTSK
CHINA
MONGOLIA
SHENYANG
BEIJING
XI'AN
CHINA
WUHAN
CHONGQING
BURMA
COOKTOWN
TOWNSVILLE
ROCKHAMPTON
BRISBANE
SYDNEY
CANBERRA
MELBOURNE
TASMANIA
HOBART

Why study nuclear interactions?

- Intrinsic knowledge

  Scattering tests theories of structure

  Gives relative motion wave functions

  Only good way I know to probe radioactive ion beam nuclei

- Astrophysics – σ_R input to:- Kubono Nilsson

  The solar model – supernova evolution

  Probe of nature of 'waiting point' nuclei

  Cosmic model – nucleosynthesis at t ~3 min.

- Radiation therapy/protection

  Dosimetry relies on neutron cross sections –

  Proton cross sections in tissue – KERMA

- Disposal of radioactive waste

  Transmutations to remove 'nasties'

  – limit radioactivities to "acceptable" times

- New power generation systems

- Aircaft/Space technologies

  Surge errors in integrated circuits Shen

  Radiation protection – astronauts/air crews

Tests of nuclear structure

Conventional tests of any (nucleonic) model description of a nucleus include:–

- Ground state binding energy, r.m.s. radii, plus any sensible higher radial moments Pandharipande
- Spectra $\Longrightarrow$ $Ex; J^{\pi}, T$ (Ex = excitation energies) Honma Shimbara Nakanishi
- Static moments, γ decay rates ; β-decay rates $\Longrightarrow$ $\mu,\ Q,\ B(EL),\ B(ML)$, $\ell n\, F_{\xi}$
- Electron scattering $\Longrightarrow F_{long}(q),\ F^{(E)}_{trans}(q),\ F^{(M)}_{trans}(q)$
- Proton/neutron scattering (elastic, inelastic, charge exchange) $\Longrightarrow$ $\frac{d\sigma}{d\Omega}(\theta), A_y(\theta), \cdots$ and RIB-hydrogen scattering (by using inverse kinematics) Matsuda Terashima
- Particle exchange reactions - heavy ion collisions $(d,p); (\alpha,p); (^{16}O, ^{12}C) \cdots \Longrightarrow$ $\frac{d\sigma}{d\Omega}(\theta)$

Typical experimental data

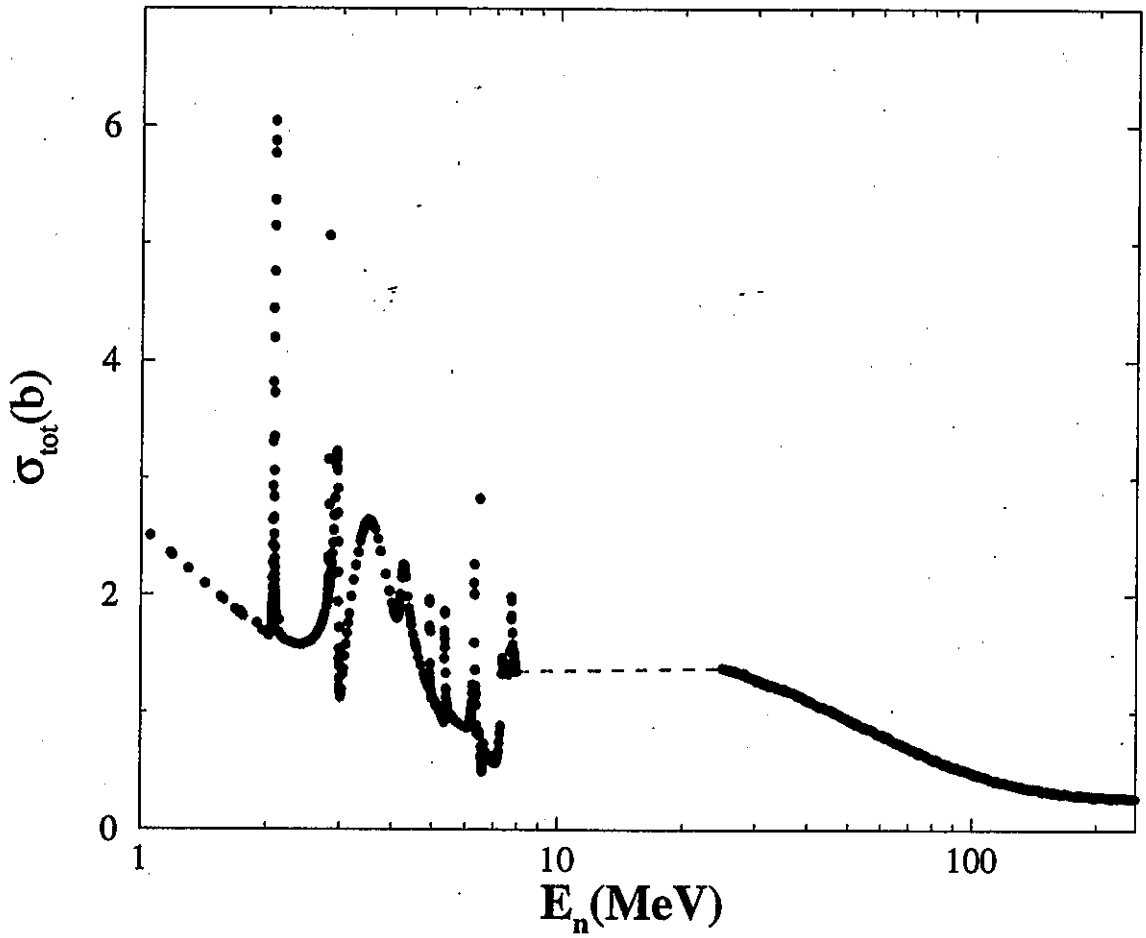

Example: Neutron total scattering from ^{12}C

Typical spectra of targets

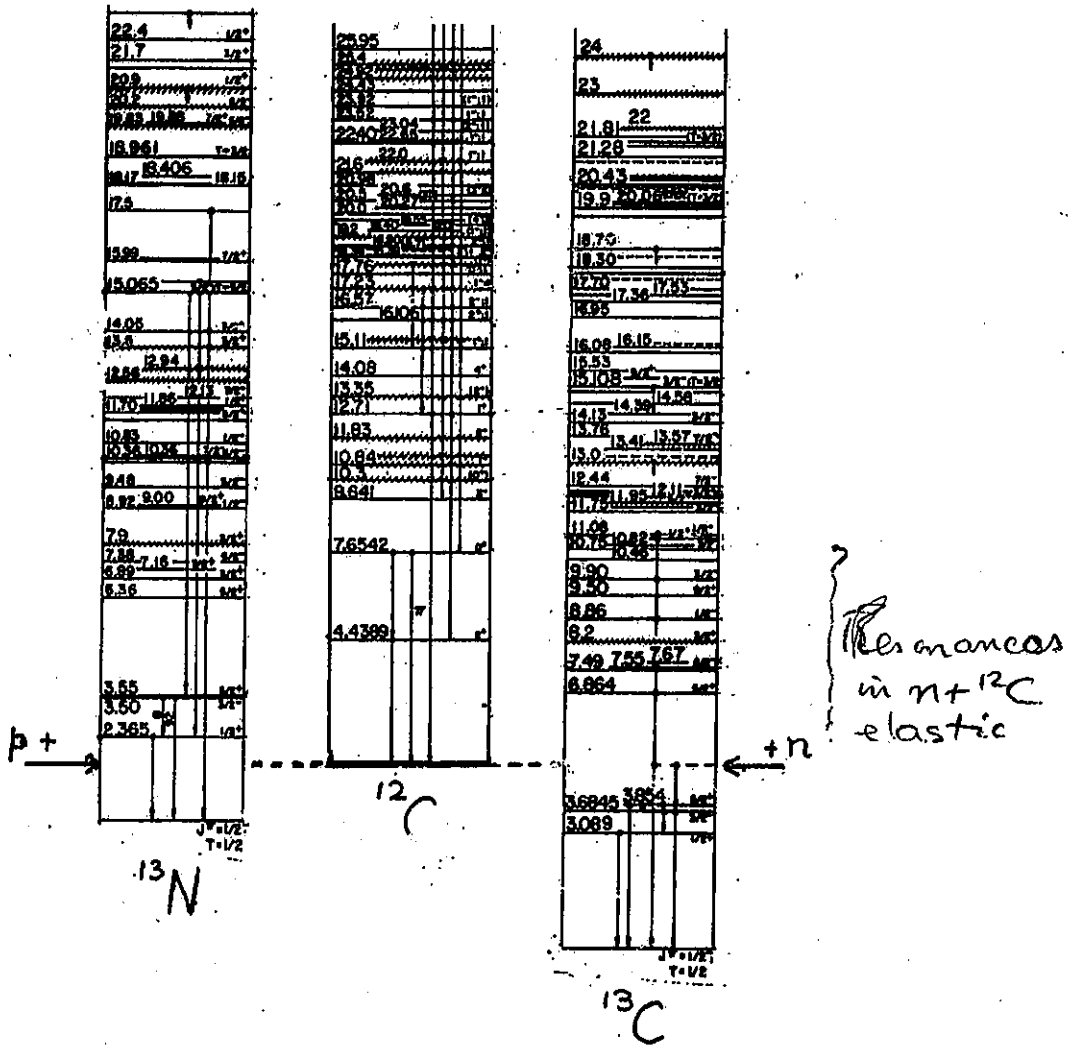

Spectra of ^{12}C, ^{13}C, and ^{13}N

(Energies relative to nucleon thresholds)

Formal theory of NA scattering

- The Schrödinger equation in operator form

$$(E - H_0)\,|\Psi_k\rangle = V\,|\Psi_k\rangle \qquad E \propto k^2 \ ,$$

- Solve formally $\quad [G_0(E) = (E - H_0)^{-1}]$

$$|\Psi_k\rangle = \frac{1}{E - H_0} V\,|\Psi_k\rangle = G_0(E) V\,|\Psi_k\rangle \ .$$

- Solution $\quad [\, G_0^{(+)}(E) = [E - H_0 + i\epsilon]^{-1}]$

$$\left|\Psi_k^{(+)}\right\rangle = |\phi_k\rangle + \frac{1}{E - H_0 + i\epsilon} V \left|\Psi_k^{(+)}\right\rangle$$

$\{H_0 - E\}|\phi_k\rangle = 0$

(Lippmann-Schwinger equation for scattering wave)

- Iterating (drop sub- and superscripts)

$$\begin{aligned} |\Psi\rangle &= [1 + GV + GVGV + \cdots]\,|\phi\rangle \\ &= \frac{1}{1 - GV}\,|\phi\rangle \\ V\,|\Psi\rangle &= [V + VGV + VGVGV + \cdots]\,|\phi\rangle \\ &= T\,|\phi\rangle \end{aligned}$$

Akaishi
Pandharipande

Formal theory of NA scattering ctnd.

- T matrix operator

$$\begin{aligned} T &\equiv V + VGV + VGVGV + \cdots \\ &= V + VGT \end{aligned}$$

Akaishi

$$\begin{aligned} T(\mathbf{k}', \mathbf{k}; E) &= V(\mathbf{k}', \mathbf{k}) \\ &\quad + \int V(\mathbf{k}', \mathbf{q}) \frac{1}{E - E_q} T(\mathbf{q}, \mathbf{k}; E)\, d\mathbf{q} \end{aligned}$$

- L-S solution

$$\left|\Psi_k^{(+)}\right\rangle = |\phi_k\rangle + \frac{1}{E - H_0 + i\epsilon} T\,|\phi_k\rangle$$

- Scattering amplitude – elastic

(no spin) second term at large distances $\Rightarrow$

$$\begin{aligned} f(\mathbf{k}', \mathbf{k}) &= -\frac{\mu}{2\pi\hbar^2} \langle \mathbf{k}'\,|T|\,\mathbf{k}\rangle \\ &= \sum_\ell (2\ell + 1)\; f_\ell\; P_\ell(\hat{\mathbf{k}}' \cdot \hat{\mathbf{k}}) \\ &= \sum_\ell (2\ell + 1) \frac{i}{2k} (1 - S_\ell)\, P_\ell(\hat{\mathbf{k}}' \cdot \hat{\mathbf{k}}) \end{aligned}$$

Hilbert-Schmidt expansion of amplitudes

- LS equation in momentum space: $(z = E + i\epsilon)$

$$\langle \mathbf{k}' | \mathsf{T}(\mathsf{z}) | \mathbf{k} \rangle = \langle \mathbf{k}' | \mathsf{V}(\mathsf{z}) | \mathbf{k} \rangle + \frac{1}{8\pi^3} \int \frac{\langle \mathbf{k}' | \mathsf{V}(\mathsf{z}) | \mathbf{q} \rangle \langle \mathbf{q} | \mathsf{T}(\mathsf{z}) | \mathbf{k} \rangle}{z - (q^2/2\mu)} \, d\mathbf{q}$$

- Spectral representation: $(\zeta = [(q^2/2\mu) + i\epsilon])$

$$\langle \mathbf{k}' | \mathsf{T}(\mathsf{z}) | \mathbf{k} \rangle = \langle \mathbf{k}' | \mathsf{V}(\mathsf{z}) | \mathbf{k} \rangle + \sum_N \frac{\chi_N(\mathbf{k}')\chi_N(\mathbf{k})}{z + \xi_N^2/2\mu} + \frac{1}{8\pi^3} \int \frac{\langle \mathbf{k}' | \mathsf{V}(\zeta) | \mathbf{q} \rangle \ \langle \mathbf{q} | \mathsf{T}(\zeta) | \mathbf{k} \rangle}{z - (q^2/2\mu)} \, d\mathbf{q}$$

- Form factors: with B.E. $= \xi_N^2/2\mu$

$$\chi_N(\mathbf{k}) = \frac{1}{2\mu} \left(k^2 + \xi_N^2\right) \ \phi_{n,\ell}(k) \ Y_{\ell m}(\Omega_N)$$

- Partial wave expansion: Only continuum case

$$T_\ell(k', k; z) = V_\ell(k', k) + \frac{1}{2\pi^2} \int \frac{V_\ell(k', q) \ T_\ell(q, k; z)}{z - q^2/(2\mu)} q^2 \, dq$$

Hilbert-Schmidt expansion ctnd.

- In operator and Weinberg expansion forms:

$$T_\ell(z) = V_\ell + \frac{V_\ell \; \mathbf{1} \; T_\ell(z)}{z - H_0} \equiv \sum_n a_{n\ell} \; g^\star_{n\ell}(k', z^\star) \; g_{n\ell}(k, z)$$

- Hilbert-Schmidt theorem (symmetric $\int^{al}$ eqns.)

  Start with symmetric form of LS eqn.

$$\overline{T_\ell(z)} = \overline{V_\ell(z)} + \overline{V_\ell(z)} \; \overline{T_\ell(z)}$$

  where with $G_0(z) = [H_0 - z]^{-1}$

$$\begin{aligned} \overline{T_\ell(z)} &= -\sqrt{G_0(z)} \; T_\ell(z) \; \sqrt{G_0(z)} \\ \overline{V_\ell(z)} &= -\sqrt{G_0(z)} \; V_\ell(z) \; \sqrt{G_0(z)} \end{aligned}$$

- Form factors: Eigenfunctions with finite norm

$$\begin{aligned} \overline{V_\ell(z)} \; \overline{g_{n,\ell}(z)} &= \eta_{n,\ell}(z) \; \overline{g_{n,\ell}(z)} \\ \langle \overline{g_{n,\ell}(z)} | \overline{g_{n',\ell}(z)} \rangle &= \delta_{nn'} \end{aligned}$$

  n: quantum numbers characterizing eigenvalues $(\eta_{n,\ell})$ in decreasing absolute magnitude

Hilbert-Schmidt expansion ctnd.

- Unsymmetric LS with $\overline{g_{n,\ell}(z)} = \sqrt{G_0(z)}\; g_{n,\ell}(z)$

$$V_\ell(z)\; G_0(z)\; g_{n,\ell}(z) = -\eta_{n,\ell}(z)\; g_{n,\ell}(z)$$

or
$$\frac{1}{2\pi^2}\int \frac{V_\ell(k,q)\mathbf{1}g_{n,\ell}(q,z)}{z - q^2/(2\mu)}\; q^2\; dq = -\eta_{n,\ell}(z)\; g_{n,\ell}(k,z)$$

Eigenvalues of $V_\ell(z)G_0(z)$ and $\overline{V_\ell(z)}$ are identical
(operators are related by a similarity transform)

Normalisation for $g_{n,\ell}$

$$\frac{1}{2\pi^2}\int g^*_{n'\ell}(q,z^*)\frac{1}{z - q^2/(2\mu)}\; g_{n\ell}(q,z)\; q^2\; dq\; = \delta_{n'n}\;.$$

- LS equation expands:

$$\sum_n a_{n\ell}\; g^*_{n\ell}(k',z^*)\; g_{n\ell}(k,z) = V_\ell(k',k)$$

$$+\sum_n a_{n\ell}\; g_{n\ell}(k,z)\left[\frac{1}{2\pi^2}\int \frac{V_\ell(k',q)\; 1g^*_{n\ell}(q,z^*)}{z - q^2/(2\mu)}\; q^2 dq\right]$$

$$= V_\ell(k',k) + \sum_n a_{n\ell}\; \eta_{n\ell}\; g^*_{n\ell}(k',z^*)\; g_{n\ell}(k,z)$$

Hilbert-Schmidt expansion ctnd.

- Rearranging: identifies separable form for V

$$V_\ell(k',k) = \sum_n a_{n\ell}\ [1-\eta_{n\ell}]\ g^\star_{n\ell}(k',z^\star)\ g_{n\ell}(k,z)$$

- Define $a_{n\ell}$: Act from right with $G_0\ g^\star_{m\ell}(k,z^\star)$ and use normalisation constraint

$$a_{m\ell} = -\frac{\eta_{m\ell}}{[1-\eta_{m\ell}]}$$

- Separable forms:

$$T_\ell(k',k;z) = -\sum_n \frac{\eta_{n\ell}}{[1-\eta_{n\ell}]} g^\star_{n\ell}(k',z^\star)\ g_{n\ell}(k,z)$$

and then one gets

$$V_\ell(k',k) = -\sum_n \eta_{n\ell}\ g^\star_{n\ell}(k',z^\star)\ g_{n\ell}(k,z)$$

$$\equiv -\sum_n \chi^*_{n\ell}(k',z^\star)\ \frac{1}{\eta_{n\ell}}\ \chi_{n\ell}(k,z)$$

Note: the rate at which the terms decrease with $\eta_{n\ell}$ determine limits to place on sums

MCAS

An algebraic solution for multi-channel scattering of nucleons with nuclei

A scattering theory for low energy collisions.
Application to nucleon-^{12}C scattering in particular

with collaborators:–

G. Pisent (INFN Padova, Italy)
L. Canton (INFN Padova, Italy)
D. van der Knijff
(Information Div., Melbourne)
J. Svenne (U. Manitoba, Canada)

Multi-channel T matrices

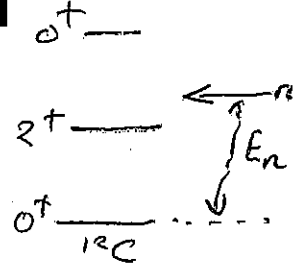

- Coupled Lippmann-Schwinger equations

$$T_{cc'}(p,q;E) = V_{cc'}(p,q)$$
$$+\mu \sum_{c''=1}^{\text{open}} \int_0^\infty V_{cc''}(p,x) \frac{1}{k_{c''}^2 - x^2 + i\epsilon} T_{c''c'}(x,q;E)\ x^2\ dx$$
$$-\mu \sum_{c''=1}^{\text{closed}} \int_0^\infty V_{cc''}(p,x) \frac{1}{h_{c''}^2 + x^2} T_{c''c'}(x,q;E)\ x^2\ dx$$

- Expand the potential matrix

$$V_{cc'}(p,q) \sim V_{cc'}^{(N)}(p,q) = \sum_{n=1}^{N} \hat{\chi}_{cn}(p)\ \eta_n^{-1}\ \hat{\chi}_{c'n}(q)$$

- The form factors $\quad (\hat{\chi}_{cn} \equiv \eta_{cn}\ g_{n,c}(z;q))$

$$\hat{\chi}_{cn}(p) = \left[\frac{2}{\pi}\right]^{\frac{1}{2}} \frac{1}{p} \int_0^\infty F_l(pr) \chi_{cn}(r)\ dr$$

- Radial terms – link to the potential matrices

$$\chi_{cn}(r) = \sum_{c'=1}^{C} V_{cc'}(r) \Phi_{c'n}(r)$$

Separable (Sturmian) expansions

If it is possible to expand

$$V_{cc'}(p,q) \equiv \int_0^\infty j_{\mathcal{L}}(pr) V_{cc'}(r) j_{\mathcal{L}}(qr) r^2 dr$$
$$= \sum_{n=1}^{N} \hat{\chi}_{cn}(p) \frac{1}{\eta_n} \hat{\chi}_{c'n}(q)$$

then (and usually N=30 suffices)

$$T_{cc'}(p,q;E) = \sum_{n,n'=1}^{N} \hat{\chi}_{cn}(p) \frac{1}{\{\eta_n \delta_{nn'} - [G_0]_{nn'}\}} \hat{\chi}_{c'n'}(q)$$

where the Green function elements are

$$[G_0]_{cc'} = \mu \sum_{c"=1}^{\text{open}} \int_0^\infty \hat{\chi}_{cn}(x) \frac{1}{k_{c"}^2 - x^2 + i\epsilon} \hat{\chi}_{cn'}(x)\ x^2\ dx$$
$$-\mu \sum_{c"=1}^{\text{closed}} \int_0^\infty \hat{\chi}_{cn}(x) \frac{1}{h_{c"}^2 + x^2} \hat{\chi}_{cn'}(x)\ x^2\ dx$$

Sturmians and expansions of $V_{cc'}$

Sturmians are solutions of eigenvalues problems

$$G_0 V_{cc'} \left|\Phi_{ci}\right\rangle = -\eta_{ci} \left|\Phi_{ci}\right\rangle$$

For given $V_{cc'}$ sets can be formed by recursion

Start with $V_{cc'} \longrightarrow V_0$ (known)

from which $\left\{\eta_{ci}^{(0)}\right\}$ and $\left\{\left|\Phi_{ci}^{(0)}\right\rangle\right\}$ all known

Iteration of forms

$$V_{cc'}^{(m+1)} = \sum_{j=1}^{\Gamma\times N} \sum_{n=1}^{N} \hat{\chi}_{cj}^{(m)}(p) \frac{1}{\eta_j^{(m)}} \hat{\chi}_{c'j}^{(m)}(q)$$

$$\hat{\chi}_{cj}^{(m)}(p) = \sum_{c'=1}^{\Gamma} V_{cc'}^{(m)} \Phi_{cj}^{(m)}(p)$$

Multi-channel S matrices

- Sturmians from eigenvalue equations

$$\sum_{c'} G_c^{(0)} V_{cc'} \left|\Phi_{c'p}\right\rangle = -\eta_p \left|\Phi_{cp}\right\rangle$$

- Separable expansion of multi-channel potential matrix leads to a multi-channel T (or S) matrix (c, c' open channels, each J^π understood)

$$\begin{aligned} S_{cc'} &= \delta_{cc'} - i\pi\mu\sqrt{k_c k_{c'}}\; T_{cc'} \\ &= \delta_{cc'} - i^{l_{c'}-l_c+1}\pi\mu \sum_{n,n'=1}^{N} \\ &\quad \times \sqrt{k_c}\hat{\chi}_{cn}(k_c)\left(\left[\boldsymbol{\eta} - \mathbf{G}_0\right]^{-1}\right)_{nn'} \hat{\chi}_{c'n'}(k_{c'})\sqrt{k_{c'}} \end{aligned}$$

- Matrix elements of $\mathbf{G}_0$ and $\boldsymbol{\eta}$

$$\begin{aligned} [\mathbf{G}_0]_{nn'} = \mu \Bigg[&\sum_{c=1}^{\text{open}} \int_0^\infty \hat{\chi}_{cn}(x) \frac{x^2}{k_c^2 - x^2 + i\epsilon} \hat{\chi}_{cn'}(x)\; dx \\ &- \sum_{c=1}^{\text{closed}} \int_0^\infty \hat{\chi}_{cn}(x) \frac{x^2}{h_c^2 + x^2} \hat{\chi}_{cn'}(x)\; dx \Bigg] \end{aligned}$$

$$[\boldsymbol{\eta}\,]_{nn'} = \eta_n\; \delta_{nn'}$$

Finding resonances

- Rapid determination of all narrow resonances
(nucleon elastic scattering from $J = 0^+$ targets)

$$1 - S_{\rm el} = i\pi\mu \sum_{nn'=1}^{M} k\, \hat{\chi}_{1n}(k) \left[(\boldsymbol{\eta} - \mathbf{G}_0)^{-1}\right]_{nn'} \hat{\chi}_{1n'}(k)$$

$$= i\pi\mu \sum_{nn'=1}^{M} k\, \frac{\hat{\chi}_{1n}(k)}{\sqrt{\eta_n}} \left[\left(\mathbf{1} - \boldsymbol{\eta}^{-\frac{1}{2}} \mathbf{G}_0 \boldsymbol{\eta}^{-\frac{1}{2}}\right)^{-1}\right]_{nn'} \frac{\hat{\chi}_{1n'}(k)}{\sqrt{\eta_{n'}}}$$

Note the diagonal (complex) matrix

$$\left[\boldsymbol{\eta}^{-\frac{1}{2}}\right]_{nn'} = \delta_{nn'} \frac{1}{\sqrt{\eta_n}} \,.$$

- To find resonances, diagonalise

$$\sum_{n'=1}^{N} \left[\boldsymbol{\eta}^{-\frac{1}{2}}\right]_{nn} [\mathbf{G}_0]_{nn'} \left[\boldsymbol{\eta}^{-\frac{1}{2}}\right]_{n'n'} \tilde{Q}_{n'r} = \zeta_r \tilde{Q}_{nr} \,,$$

(a complex, symmetric matrix)

- Resonances – get from energy evolution of ζ_r

Resonant behavior occurs when an eigenvalue of the complex ζ_r moves near (1,0) in Gauss plane.

Finding resonances ctnd.

- S-matrix has poles at corresponding energies

$$\left[\left(\mathbf{1}-\boldsymbol{\eta}^{-\frac{1}{2}}\mathbf{G}_0\boldsymbol{\eta}^{-\frac{1}{2}}\right)^{-1}\right]_{nn'} = \sum_{r=1}^{N}\tilde{Q}_{nr}\frac{1}{1-\zeta_r}\tilde{Q}_{n'r}\,.$$

- Resonance existence $\zeta_r(E_{res}) \Rightarrow (1.0 + i\delta)$

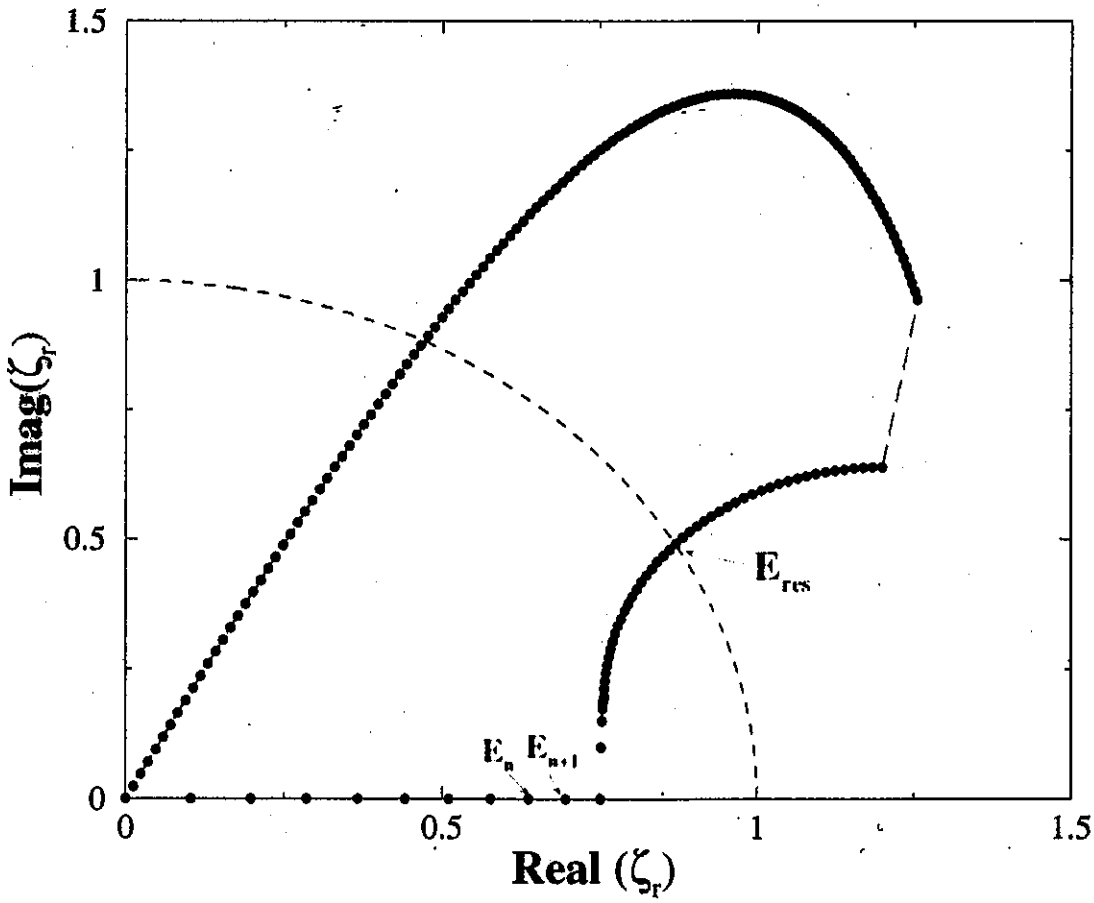

Argand plot of $\zeta_r(E)$

Resonance Location

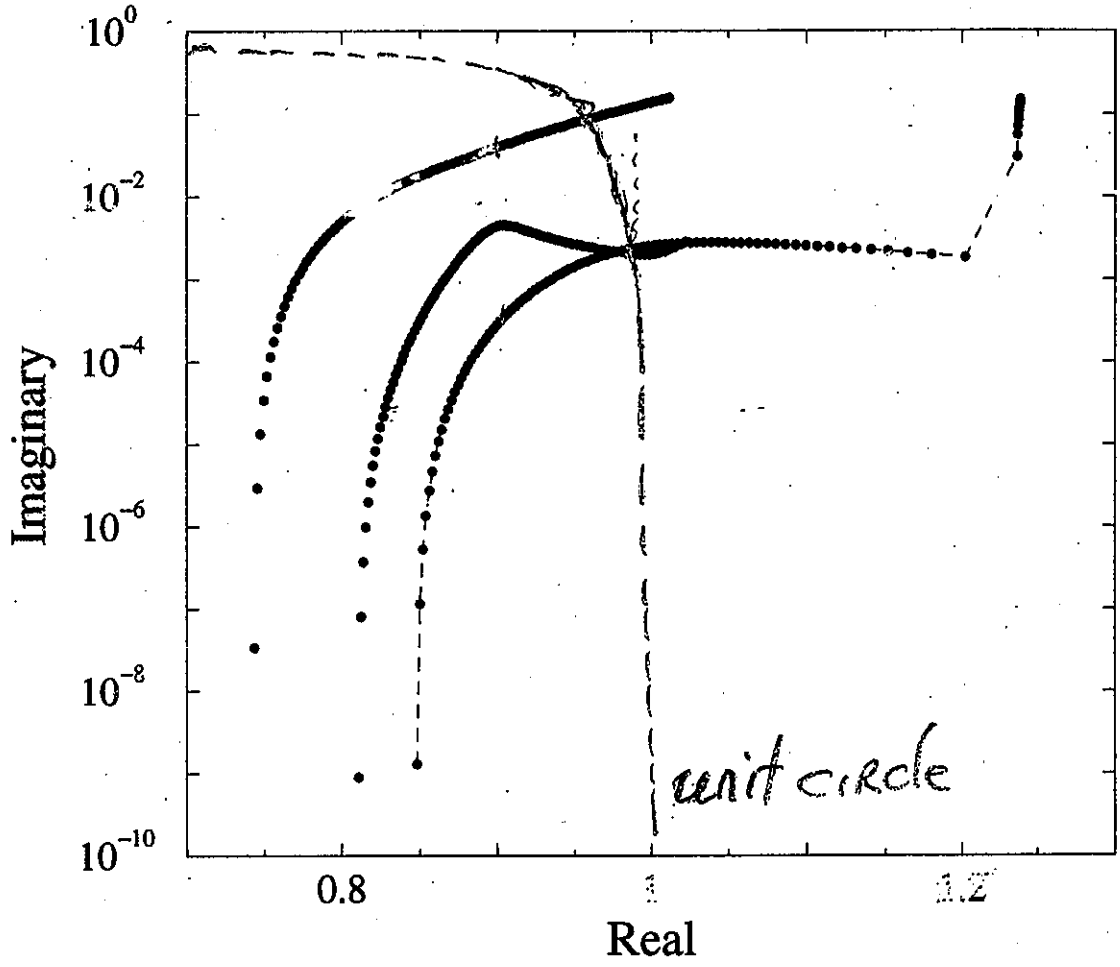

Argand plots of the $\frac{3}{2}^+$ solutions

(ζ_r for n+^{12}C scattering)

Resonance Location ctnd.

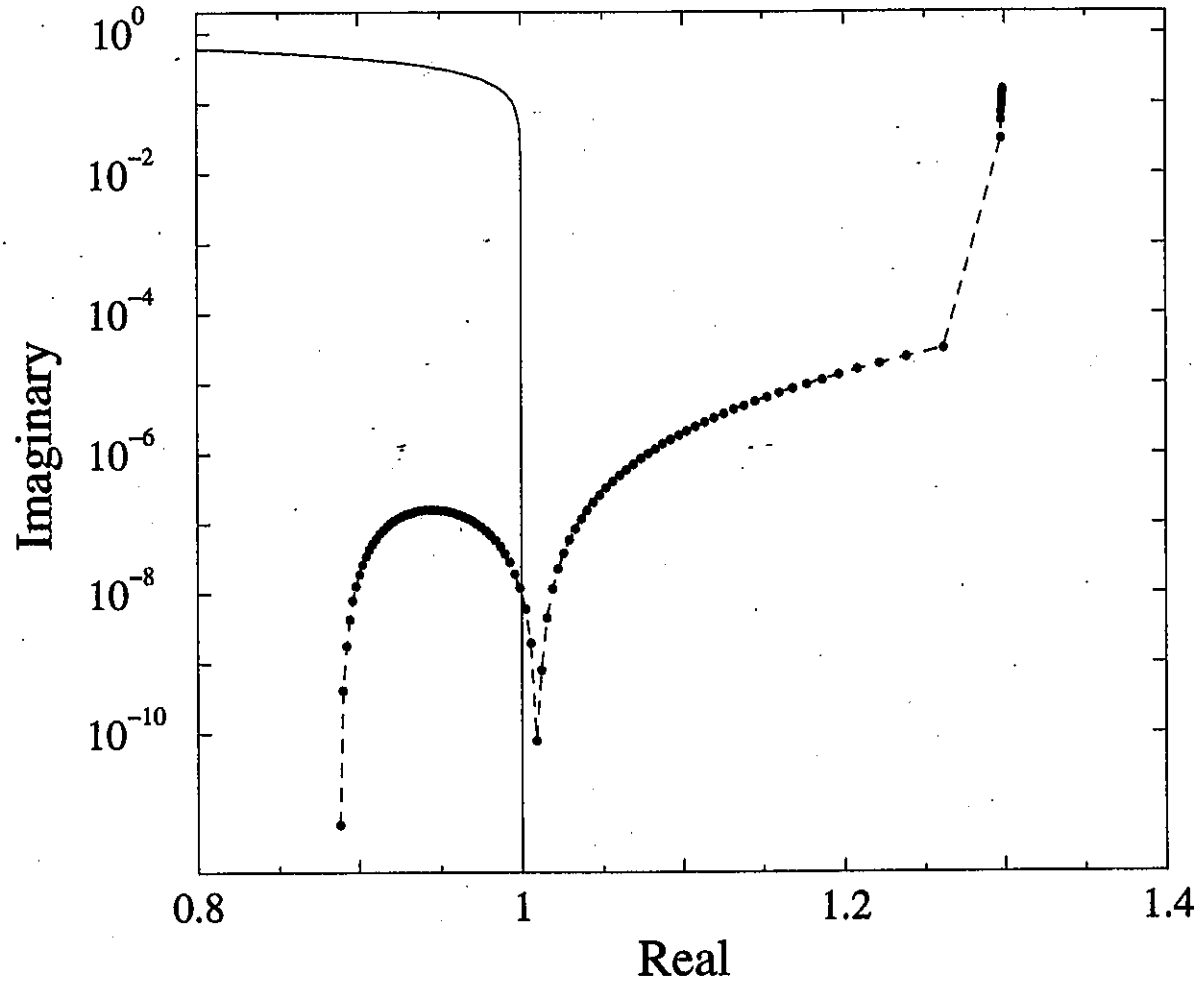

Argand plot of the $\frac{5}{2}^{+}$ solution
(ζ_r for n+^{12}C scattering)

Resonance Location ctnd.

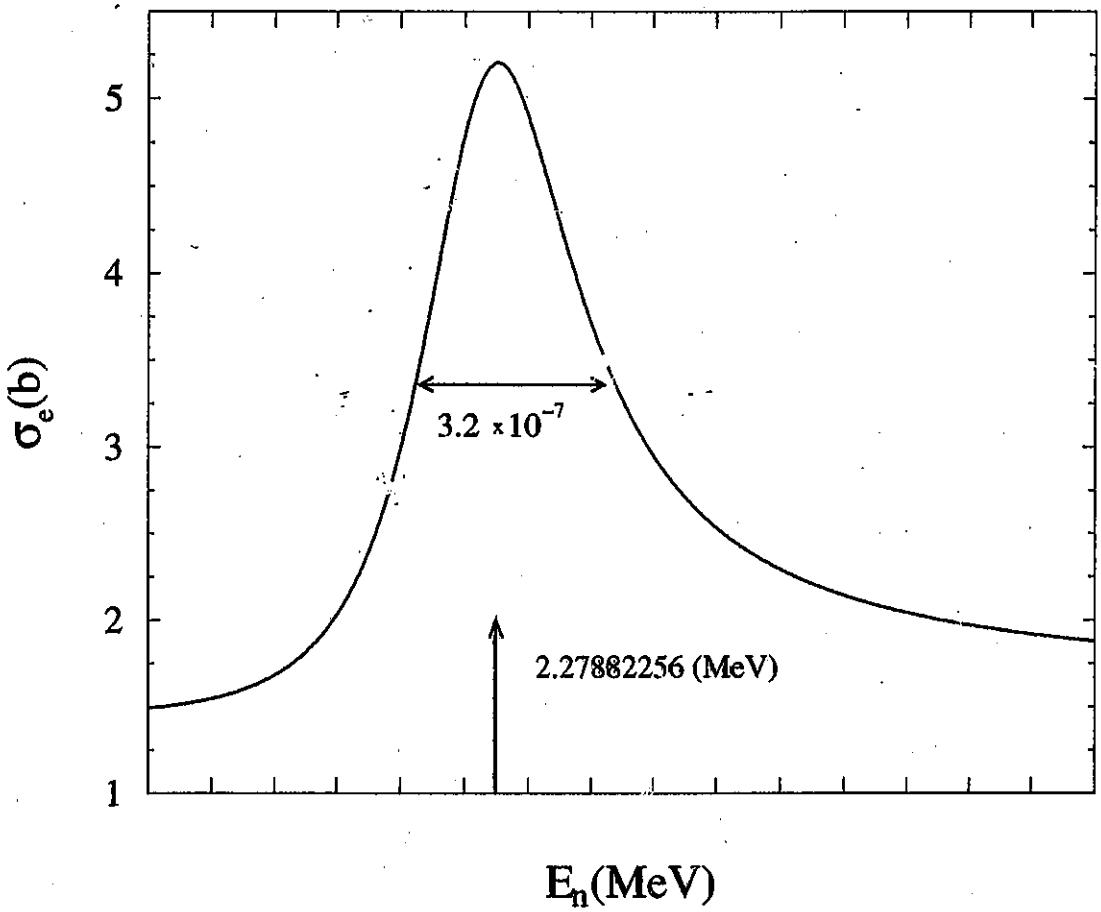

Cross section over the $\frac{5}{2}^+$ resonance

Bound state solutions

- Momentum space Schrödinger Equation:
  (after partial wave projection with B.E. = -E)

$$\Phi_\ell(p:E) = -\frac{2}{\pi}\frac{1}{(E+p^2/(2\mu))}\int V_\ell(p,q)\,\Phi_\ell(q;E)\,q^2dq$$

- Linking to complex poles of T: recast as

$$T = \frac{1}{1-VG}V$$

Simple poles when denominator has simple zeros

- Use bound state representation:
  determinants of the matrices that represent the operators vanish for specific (bound) energies
- Link to MCAS:
  Get Green fn. matrices for NEGATIVE energies all channels closed, then find zeros of $|\eta + \boldsymbol{G_r}|$

$$|\eta + \boldsymbol{G_r}| = \det\{\eta + \mathbf{G_r}\}$$

$$= \det\left\{\eta_n\delta_{nn'} + \mu\sum_c\int_0^\infty \hat{\chi}_{cn}(x)\frac{x^2}{h_c^2+x^2}\hat{\chi}_{cn'}(x)\,dx\right\}$$

Collective model for potential matrices

- Basis of channel states

$$|(\mathcal{L}s)\mathcal{J}IJ^{\pi}\rangle = \Big[|(\mathcal{L}\otimes s)_{\mathcal{J}}\rangle \otimes |\psi_I(\alpha)\rangle\Big]^{M,\pi}_{J}$$

- Potential matrix $\langle(\mathcal{L}'s)\mathcal{J}'I'|\ W(r)\ |(\mathcal{L}s)\mathcal{J}I\rangle$
  (deformation disregarded temporarily)

$$\begin{aligned} V_{c'c}(r) \quad = \quad & f(r)\Big\{V_0\delta_{c'c} + V_{ll}[\ell\cdot\ell]_{c'c} + V_{ss}[\mathbf{s}\cdot\mathbf{I}]_{c'c}\Big\} \\ & + g(r)V_{ls}[\ell\cdot\mathbf{s}]_{c'c} \end{aligned}$$

- Tamura collective model

$$f(r) = \Big[1 + e^{\left(\frac{r-R}{a}\right)}\Big]^{-1} \ ;\ g(r) = \frac{1}{r}\frac{df(r)}{dr}$$

- Rotational model$\Rightarrow$ nuclear surface

$$R = R_0(1+\epsilon)\ ;\ \epsilon = \sum_{L(=2)} \sqrt{\frac{4\pi}{2L+1}}\,\beta_L\,[\mathbf{Y}_L(\hat{r})\cdot\mathbf{Y}_L(\hat{\xi})]$$

Mass 13 bound states ctnd.

Bare results

No Pauli exclusion

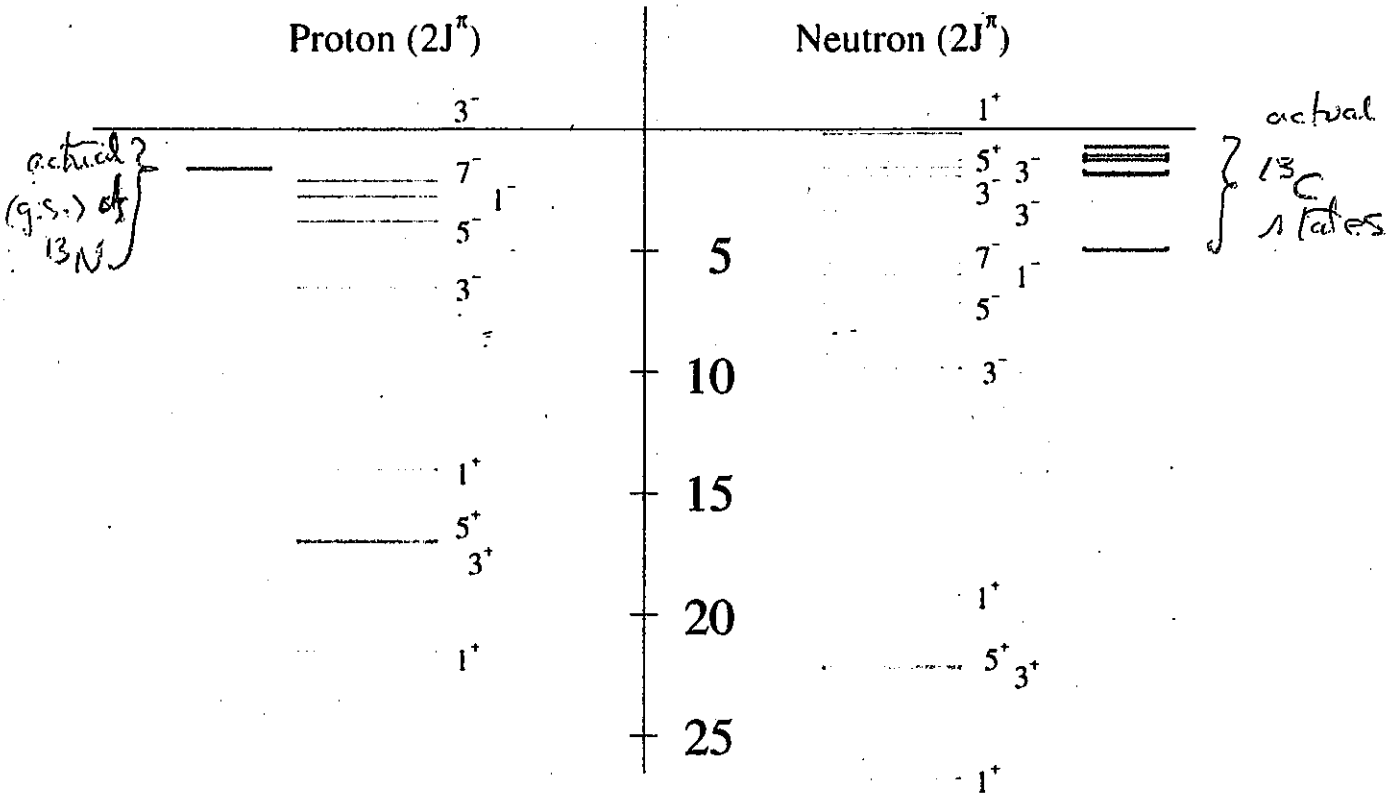

Energies in reference to p + ^{12}C and n + ^{12}C thresholds

Including the Pauli principle

•Basic collective model ⇒ Pauli principle violation:
scattering w. fn. not orthogonal to forbidden states

• Solution:

Add orthogonalizing pseudo-potential (OPP),

$$\mathcal{V}_{cc'}(r,r') = V_{cc'}(r)\ \delta(r-r') + \lambda A_c(r)A_c(r')\ \delta_{c,c'}$$

(exact if $\lambda \to \infty$; but suffice $\lambda = 100$ MeV)

• Choice for $A_c(r)$:

Use the spurious bound state functions

$$\frac{d^2A_c(r)}{dr^2} + \left[\frac{2m}{\hbar^2}\left(E - w_c(r)\right) - \frac{l(l+1)}{r^2}\right] A_c(r) = 0$$

$$w_c(r) = [V_0 + V_{ll}\,l(l+1)]f_0(r) + g_0(r)V_{sl}[\mathbf{l}\cdot\mathbf{s}]_c]$$

• MCAS new potential form factors:

$$\chi_{cn}(r) = \sum_{c'=1}^{\Gamma} V_{cc'}(r)\Phi_{c'n}(r) + \lambda A_c(r)\left[\int_0^{\infty} A_c(r')\Phi_{cn}(r')dr'\right]$$

Mass 13 bound states

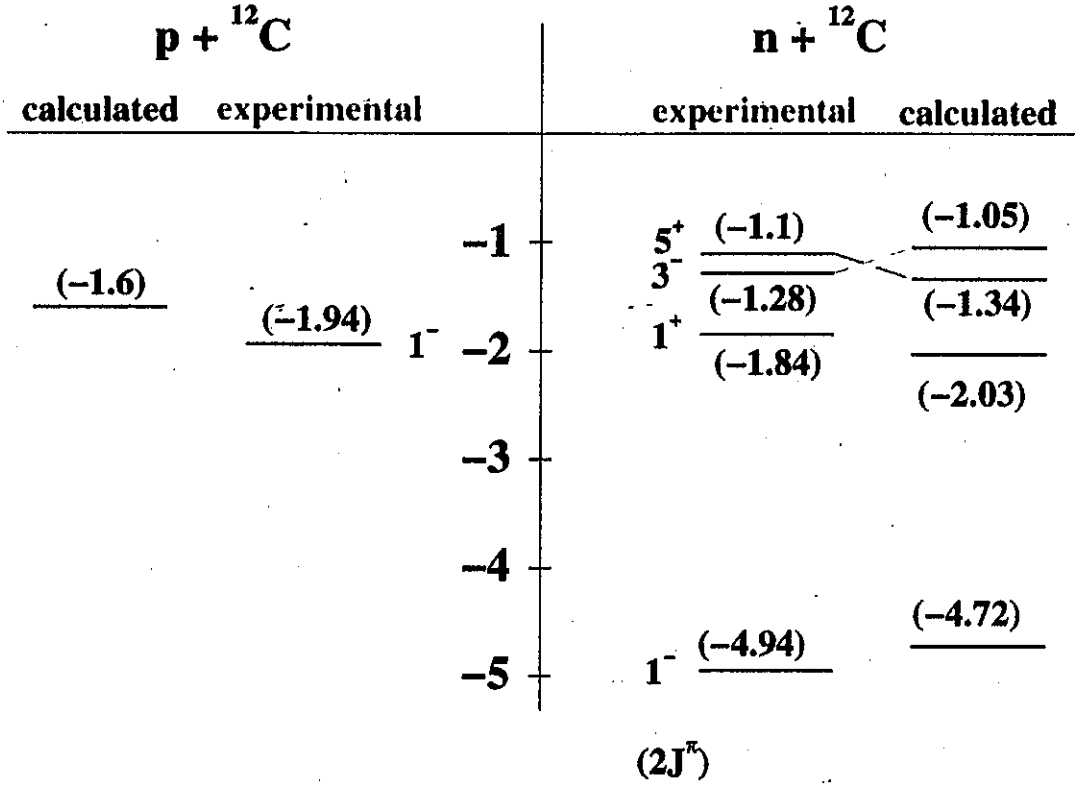

Energies in reference to p + ^{12}C and n + ^{12}C thresholds

n-^{12}C scattering results

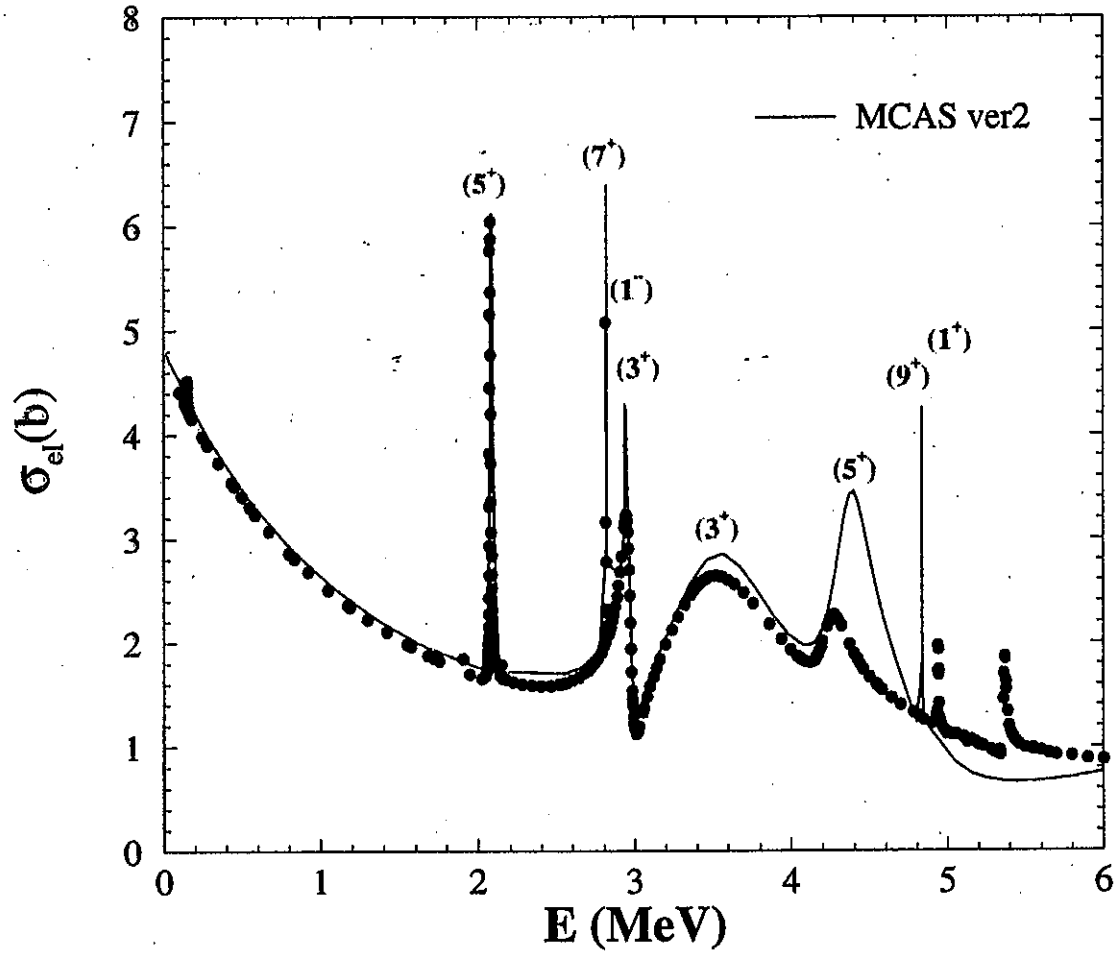

Total elastic cross section $(2J^{\pi})$

$n - {}^{12}$C scattering results ctnd.

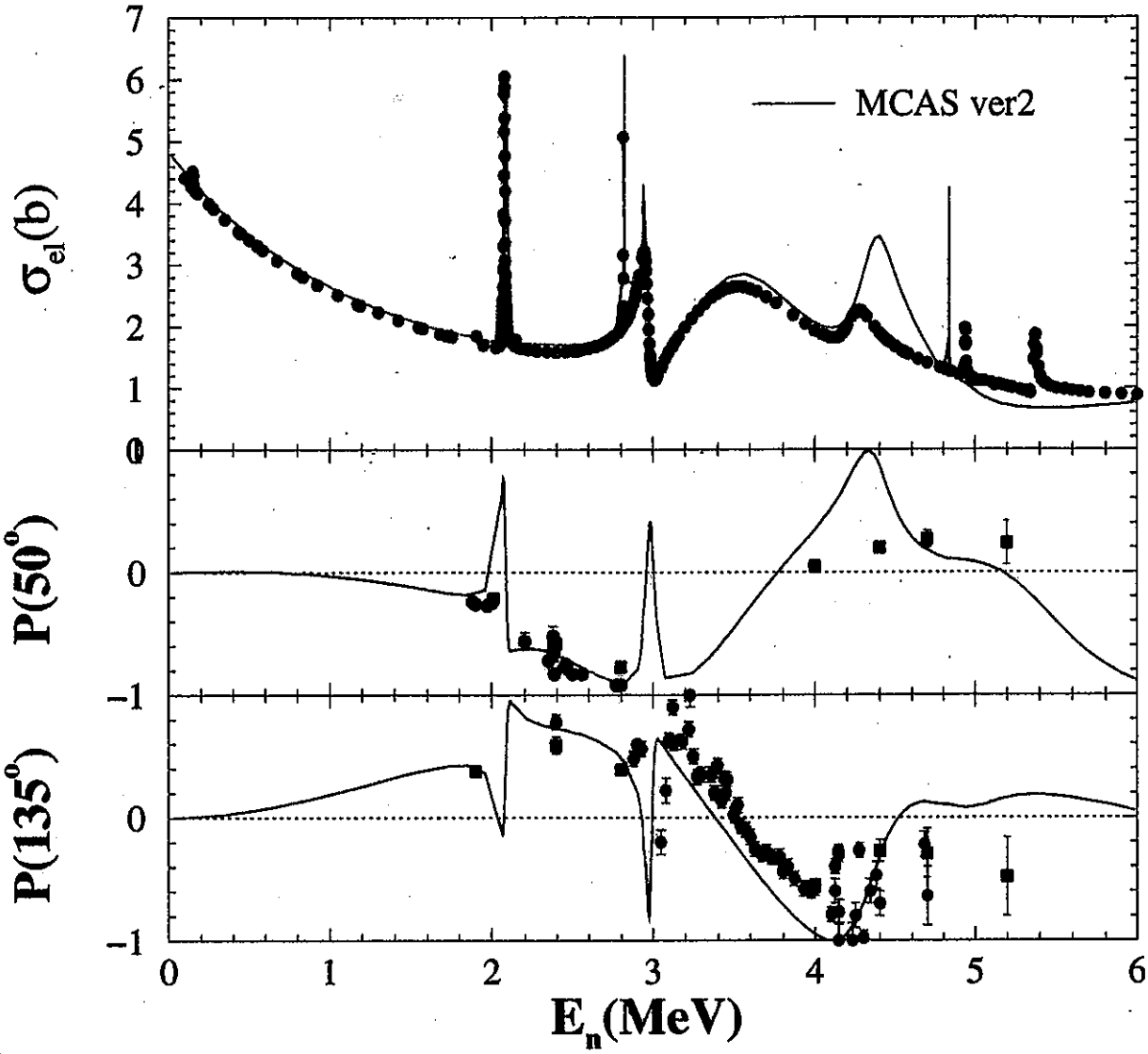

Total elastic cross section and polarizations at two scattering angles

p-^{12}C scattering results

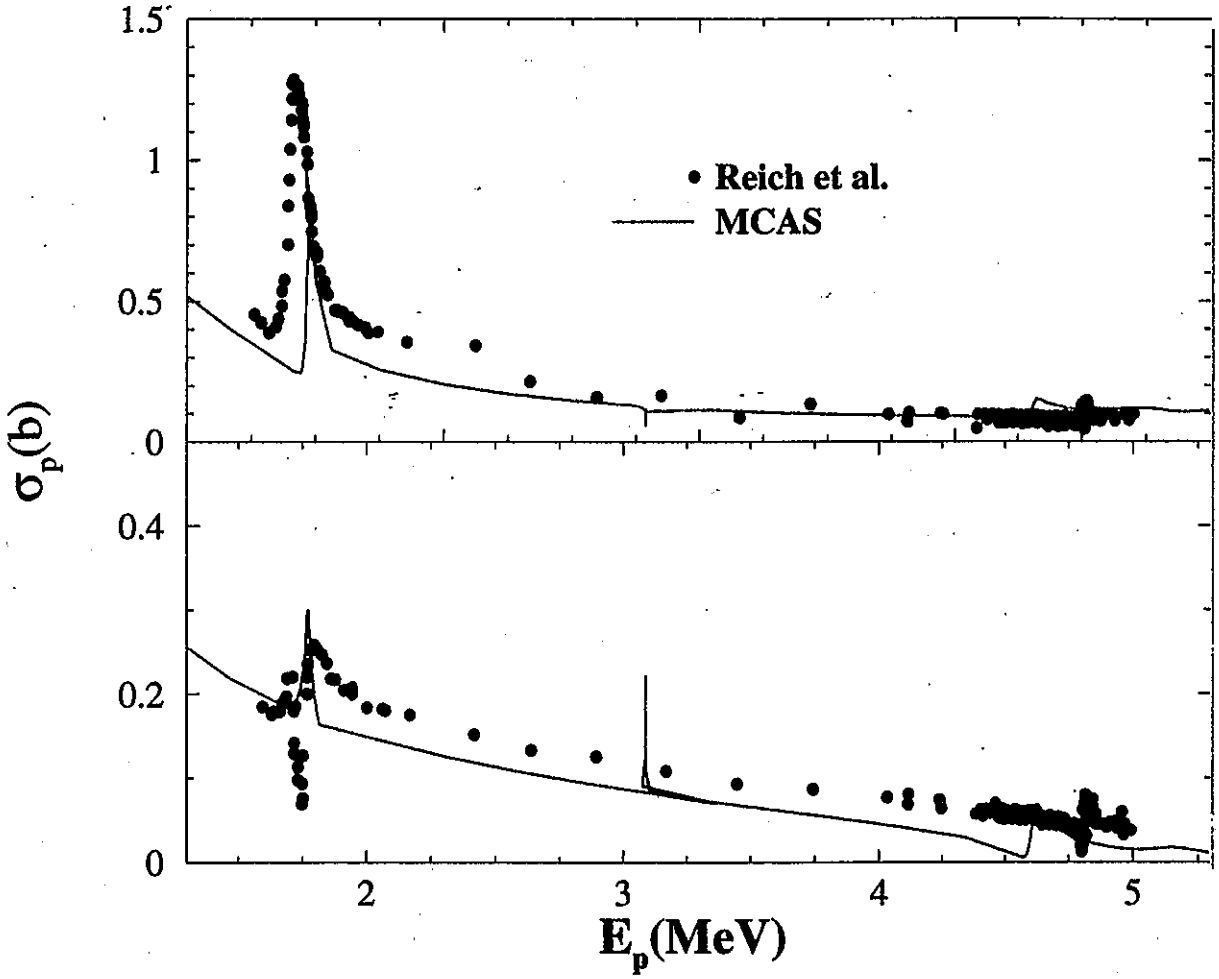

Cross sections at two scattering angles

54.7° (top) and 90° (bottom)

p-^{12}C scattering results ctnd.

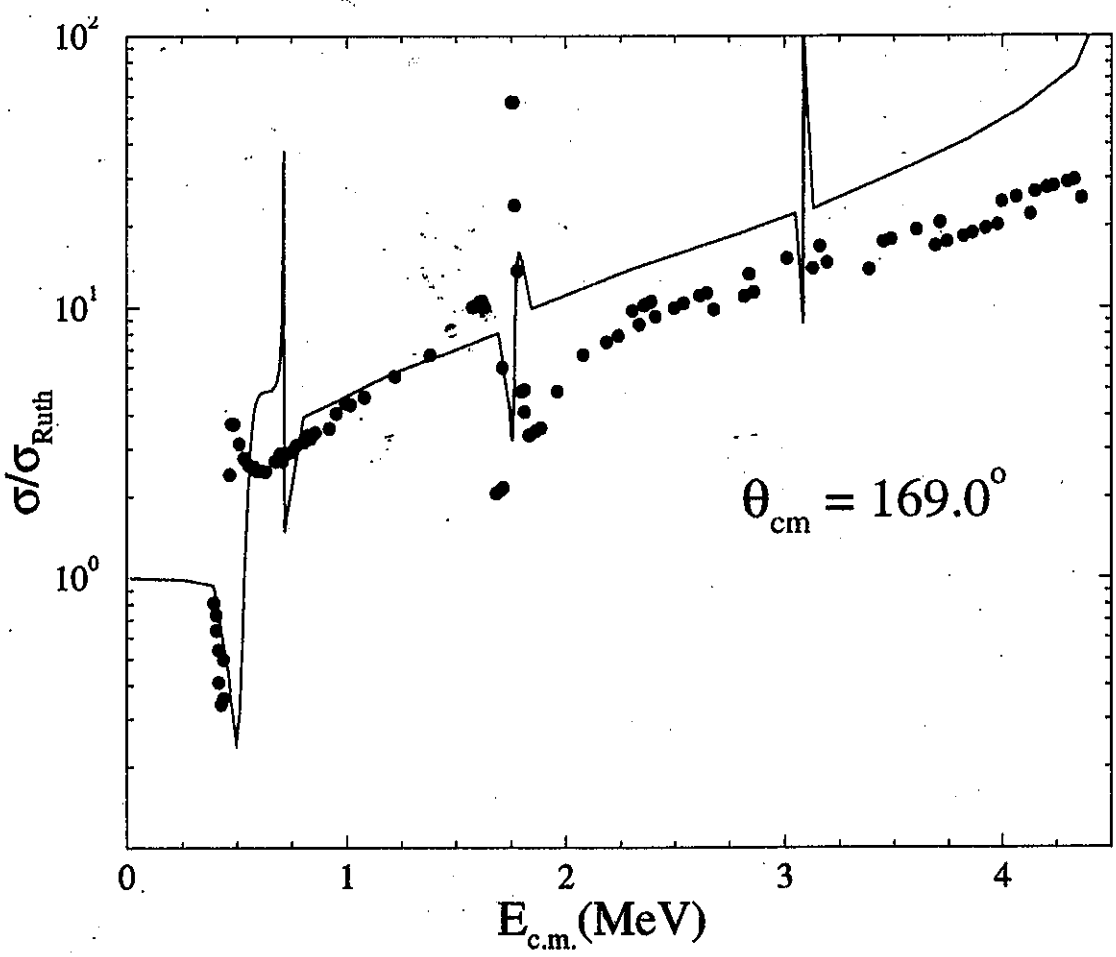

Ratio to Rutherford cross sections

• • • Jackson *et al.*

Phys. Rev. **89**, 369 (1953)

Mass 13 spectra with MCAS

^{13}N			^{13}C		
E_{calc}	J^π	E_{exp}	E_{exp}	J^π	E_{calc}
5.81	$\frac{1}{2}^-$		4.26	$\frac{1}{2}^-$	2.94
5.98	$\frac{3}{2}^+$	6.37	3.46	$\frac{3}{2}^+$	3.64
3.08	$\frac{5}{2}^-$	5.84	(2.84)	$\frac{3}{2}^+$	2.96
5.14	$\frac{7}{2}^+$	5.63	2.94	$\frac{5}{2}^-$	-0.05
5.22	$\frac{3}{2}^+$	5.37	2.82	$\frac{7}{2}^+$	2.82
4.61	$\frac{5}{2}^+$	4.81	2.08	$\frac{5}{2}^+$	2.09
0.71	$\frac{5}{2}^+$	1.73	-1.10	$\frac{5}{2}^+$	-1.87
1.77	$\frac{3}{2}^-$	1.69	-1.28	$\frac{3}{2}^-$	-1.46
0.57	$\frac{1}{2}^+$	0.46	-1.84	$\frac{1}{2}^+$	-1.99
-1.60	$\frac{1}{2}^-$	1.94	-4.94	$\frac{1}{2}^-$	-4.86

Energies relative to p(n)-^{12}C threshold

Conclusions

An algebraic multi-channel scattering theory has been developed and applied that is

- limited only by computational considerations (in number of channels that can be used)
- can accomodate Pauli exclusion effects (even for collective model $V_{cc'}(r)$)
- lends itself to a procedure to specify bound (subthreshold) states (the compound nucleus)
- can be used to locate all resonances and specify their characteristics $(E_j; \Gamma_j)$ (in the selected incident energy range whatever Γ_j)
- specify the complete T and S matrices off-shell and predict low energy cross sections ($\Rightarrow$ base info. for capture cross sections)
- ascertain inelastic scattering cross sections and all spin measureables (elastic and inelastic)

Future studies

⋆ Immediate future work

1. to use much larger number of channels and with larger J^π values and for energies to 20 MeV
2. to use different proton and neutron interactions (and so apply to analyses of scattering with "exotic" nuclei near the drip lines)
3. extend application to non-zero spin targets

⋆ Not so immediate future work (manpower shortage)

1. use shell model and low energy NN force information to specify the $V_{cc'}(r)$
2. use S matrices to evaluate proton capture rates
3. formulate and apply an MCAS for α scattering (and then evaluate α capture rates) + ^3He, t
4. Specify low energy optical potentials (non-local and complex)

+ include charge exchange channels (p,n) (^3He,t)

Nucleus–hydrogen scattering

Energies 25 to 250 MeV

g-folding optical potentials and the DWA

collaborators:–

P. K. Deb, Ohio University, U.S.A.

B. A. Brown, N.C.S.L., Michigan, U.S.A.

H. V. von Geramb, Hamburg University, Germany

S. Karataglidis, CEA/DIF/DPTA/SPN, Bruyeres-le-Chatel, France

B. Giraud, CEA-Saclay, France

J. Dobaczewski, Warsaw University, Poland

plus a host of experimentalists

Motivation in Nuclear Physics

- Predictive theory
  - A "parameter free" prescription
  - For $A = 1$ recovers free NN scattering
  - Semi-consistent treatment of medium effects

- Direct probe of matter densities
  - Complements electron scattering as a probe (of charge and current densities)
  - Proton (neutron) scattering most sensitive to neutron (proton) distributions
  - Accounts explicitly for non-local effects (exchange (knock-out) amplitudes)

- Optical potentials/reaction cross sections
  - elemental inputs in many other fields of study

Review:–

K. Amos, P. J. Dortmans, H. V. von Geramb, S. Karataglidis, and J. Raynal, Adv. in Nucl. Phys. **25**, 275 (2000)

Tests of nuclear structure ctnd.

- Nuclear structure — light mass nuclei:

  Large space no-core shell model calculations

  —— one must diagonalise a Hamiltonian

$$H^{(\omega)} = \sum_{i=1}^{A} \frac{p_i^2}{2m} + \sum_{i<j}^{A} V(ij) + \frac{1}{2} A m \omega^2 R^2$$

  ⋆ Single particle basis – HO with energy $\hbar\omega$

  ⋆ Model space – complete $N\hbar\omega$

  (relative to unperturbed ground)

  ⋆ Specific cases

A = 3, 4	N = 6, 8, $\cdots$ 32
A = 5, 6	N = 6, 8
A = 7	N = 6
A = 8 – 12	N = 4

  ⋆ Interactions

  NN G-matrices – Zheng *et al.*

  Fitted potentials – e.g. MK3W, WBP, WBT

Tests of nuclear structure ctnd.

- Shell model for ^{12}C:

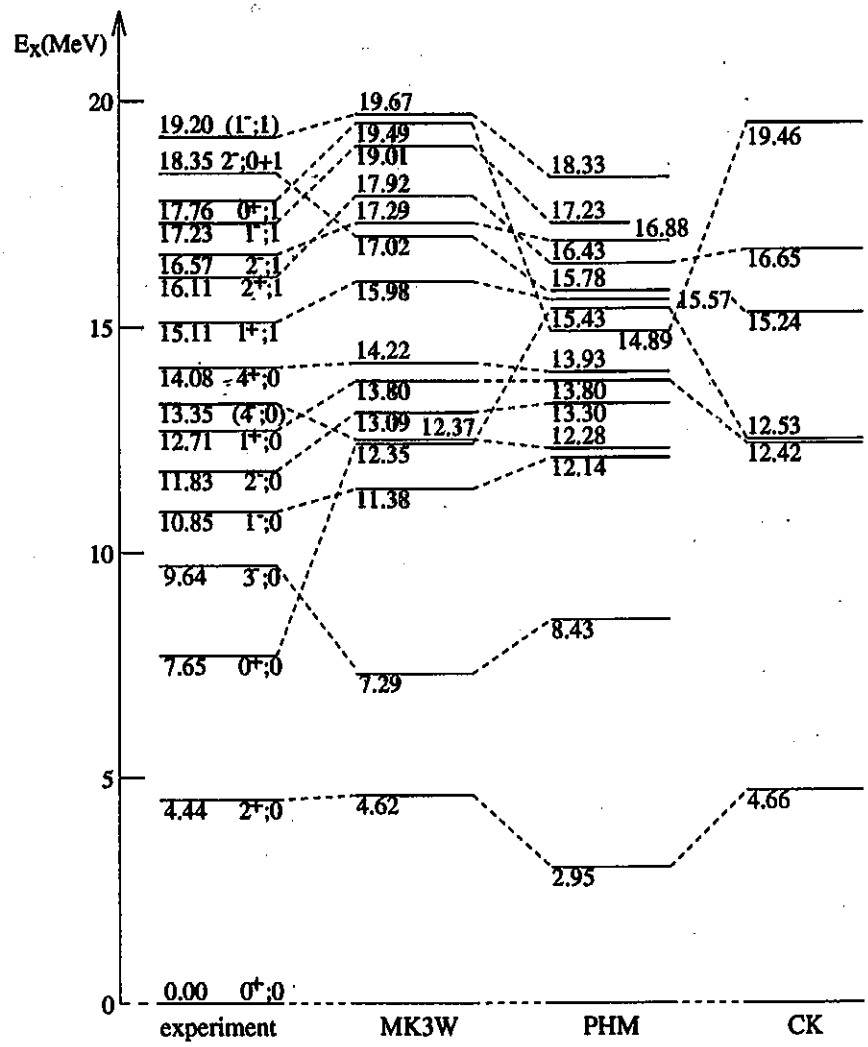

Energy level diagram for low-lying states in ^{12}C

Tests of nuclear structure ctnd.

- ^{12}C electron scattering:

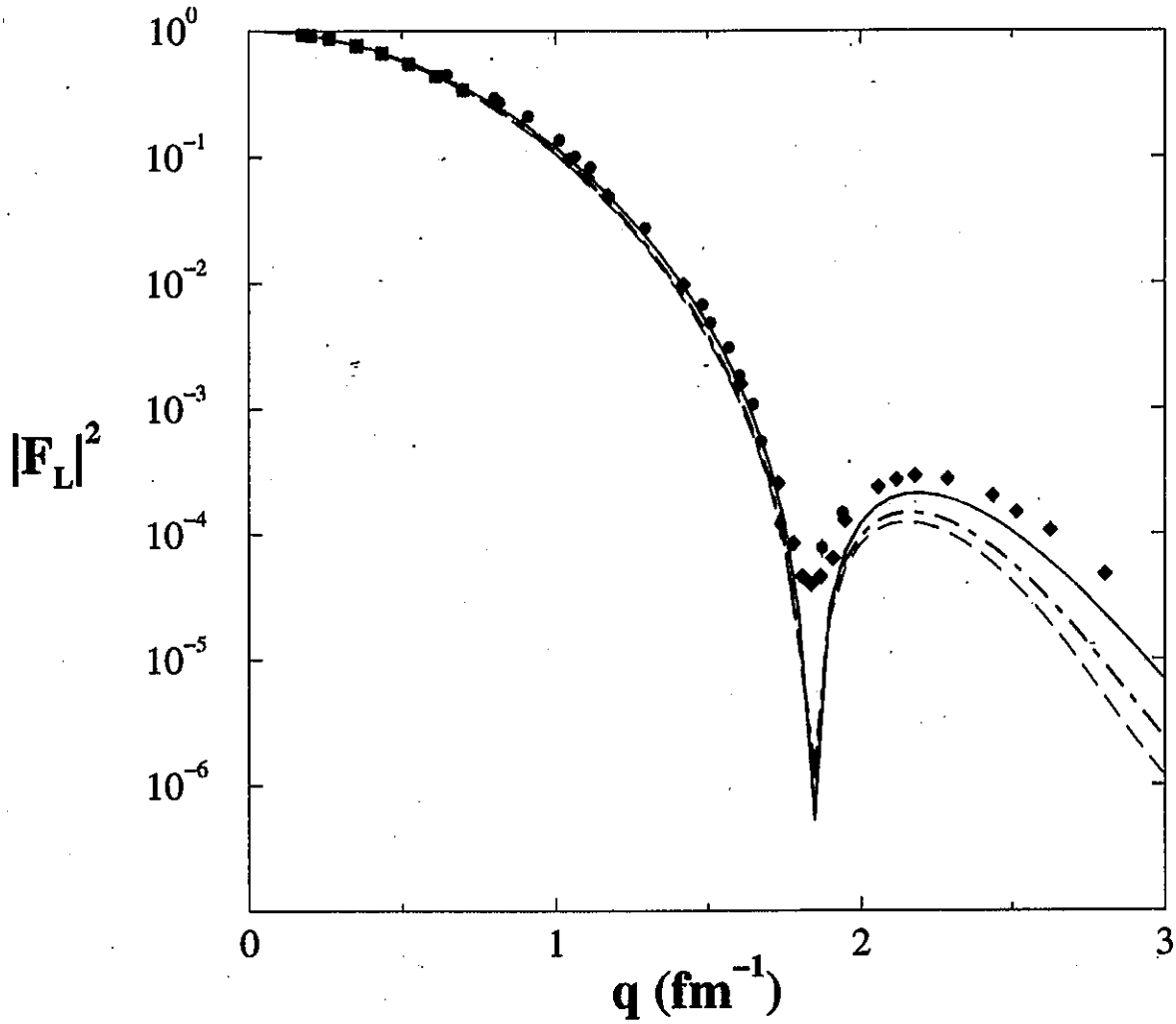

^{12}C longitudinal form factor

g-folding optical potential

- Formal theory: e.g. KFT formalism

$$U = U_{OM}(E) = \left\langle \Phi_{gs} \left| V + V G^{(+)}_{QQ} V \right| \Phi_{gs} \right\rangle$$
$$\equiv \sum_{i=1}^{A} \langle \Phi_{gs} | g_{0i}(\omega) | \Phi_{gs} \rangle$$

- Assumed g-matrix: – satifies a BBG equation

$$g_{01}(\omega) = V_{01} + V_{01} G_M(\omega) g_{01}(\omega)$$

- Convolution in momentum space:

$$U(\boldsymbol{k}', \boldsymbol{k}; E) = \int d\boldsymbol{p}\, d\boldsymbol{p}' \sum_{\alpha \le \epsilon_F} \Phi^{\dagger}_{\alpha}(\boldsymbol{p}', \epsilon_\alpha)$$
$$\times \langle \boldsymbol{k}', \boldsymbol{p}' | g(E + \epsilon_\alpha) | \boldsymbol{k}, \boldsymbol{p} \rangle_{\mathcal{A}} \Phi_\alpha(\boldsymbol{p}, \epsilon_\alpha)$$

- Convolution in coordinate space:

$$U(\boldsymbol{r}, \boldsymbol{r}'; E) = \delta(\boldsymbol{r} - \boldsymbol{r}') \sum_i n_i \int \varphi^*_i(\boldsymbol{s})\, g_D(\boldsymbol{r}, \boldsymbol{s}; E)\, \varphi_i(\boldsymbol{s})\, d\boldsymbol{s}$$
$$+ \sum_i n_i\, \varphi^*_i(\boldsymbol{r})\, g_E(\boldsymbol{r}, \boldsymbol{r}'; E)\, \varphi_i(\boldsymbol{r}')$$

Coordinate space Optical Potential

Assuming pairwise interactions ($\sum_{i=1}^{A} g_{0i} \Rightarrow A g_{01}$)

$$U_{NA} = A \left(\Psi \left(1 \ldots A \right) \left| g_{01} \right| \Psi \left(1 \ldots A \right) \right)$$

- Cofactor expansions:

$$\left| \Psi \left(1 \ldots A \right) \right\rangle = \frac{1}{\sqrt{A}} \sum_{jm\alpha} \left| \varphi_{jm\alpha}(1) \right\rangle a_{jm\alpha} \left| \Psi \left(1 \ldots A \right) \right\rangle$$

- Optical potential expansion:

$$U_{pA}(0,1) = \sum_{j'm'\alpha' jm\alpha} \left\langle \Psi \left| a^{\dagger}_{j'm'\alpha'} a_{jm\alpha} \right| \Psi \right\rangle \times \left(\varphi_{j'm'\alpha'}(1) \right| g_{10} \left\{ \left| \varphi_{jm\alpha}(1) \right\rangle - \left| \varphi_{jm\alpha}(0) \right) \right\}$$

- Three requirements:
  - a) Nuclear structure – SP states $\varphi_{jm\alpha}(\mathbf{r})$
  - b) Nuclear structure – density matrix elements
  - c) Effective NN interaction –

$$g_{01} \equiv g_{eff} \left(r, k_f(R); E(R) \right) \qquad r = |\mathbf{r_0} - \mathbf{r_1})| \qquad R = \tfrac{1}{2} \left(\mathbf{r_0} + \mathbf{r_1} \right))$$

Coordinate space OMP ctnd.

- One Body Density Matrix Elements (OBDME):

From the many body density matrix elements

$$\rho^{mm'M_iM_f}_{\alpha\alpha' J_i J_f} = \left\langle \Psi \left| a^\dagger_{j'm'\alpha'} a_{jm\alpha} \right| \Psi \right\rangle$$

$$= \sum_{I,N} \frac{(-1)^{j-m}}{\sqrt{2J_f+1}} \langle j\, m\, j'\, -m' | I\, -N \rangle \times \langle J_i\, M_i\, I\, N | J_f\, M_f \rangle\, S_{\alpha\alpha' I}$$

Then, with $\tilde{a}_{jm\alpha} = (-1)^{j-m} a_{j-m\alpha}$, the OBDME (singly reduced) are

$$S_{\alpha\alpha' I} = \left\langle \Psi_{J_f} \left\| \left[a^\dagger_{\alpha'} \times \tilde{a}_\alpha \right]^I \right\| \Psi_{J_i} \right\rangle$$

$$\rightarrow \left\langle \Psi_{J} \left\| \left[a^\dagger_{\alpha'} \times \tilde{a}_\alpha \right]^I \right\| \Psi_{J} \right\rangle \text{ (elastic)}$$

- Elastic and spin zero transfer case:

(and no non-Hartree-Fock terms)

$$S_{\alpha\alpha' I} \Rightarrow S_{\alpha\alpha 0} = \sum_m \left\langle \Psi \left| a^\dagger_{jm\alpha} a_{jm\alpha} \right| \Psi \right\rangle = n_{j(\alpha)}$$

the j-shell occupancies for nucleons type α

The NN t matrices

- NN Lippmann-Schwinger Equation:

$$t(\boldsymbol{q}',\boldsymbol{q};\omega) = V(\boldsymbol{q}',\boldsymbol{q}) + \frac{1}{(2\pi)^3}\int V(\boldsymbol{q}',\boldsymbol{k})\frac{1}{[\boldsymbol{k}_0^2-\boldsymbol{k}^2+i\varepsilon]}t(\boldsymbol{k},\boldsymbol{q};\omega)\,d\boldsymbol{k}$$

- Use partial wave expansions: (isospins $T = 0, 1$)

$$X(\boldsymbol{q}',\boldsymbol{q};\omega) = \frac{2}{\pi k}\sum_{JLL'ST}^{N}\mathcal{Y}^{N}_{JL'S}(\widehat{\boldsymbol{q}}')x^{JST}_{L'L}(q\,q;\omega)\mathcal{Y}^{N\dagger}_{JLS}(\widehat{\boldsymbol{q}})$$

J, L, S: total, orbital, spin, angular momenta

$\mathcal{Y}^{N}_{JLS}(\widehat{\boldsymbol{q}})$: tensor spherical harmonics

$$t^{JST}_{L'L}(q',q;\omega) = V^{JST}_{L'L}(q',q) + \frac{2}{\pi}\sum_{l}\lim_{\varepsilon\to 0}\int_0^\infty \frac{V^{JST}_{L'l}(q',k)}{[k_0^2-k^2+i\varepsilon]}\,t^{JST}_{lL}(k,q;\omega)\,k^2dk$$

These integral equations are solved numerically

The NN t matrices ctnd.

- Dirac relation:

$$\lim_{\epsilon \to 0} \frac{1}{[k_0^2 - k^2 \pm i\epsilon]} = \boldsymbol{P} \frac{1}{[k_0^2 - k^2]} \mp i\pi\delta(k_0^2 - k^2)$$

$\boldsymbol{P} \Rightarrow$ principal value of integral to be taken

- K matrix equations:
  (relate to t matrices by the Heitler equation)

$$t^{JST}_{L'L}(q', q; \omega) = K^{JST}_{L'L}(q', q; \omega) - ik_0 \sum_l K^{JST}_{L'l}(q', k_0; \omega) t^{JST}_{lL}(k_0, q; \omega)$$

satisfy Fredholm integral equations (2^{nd} kind)

$$K^{JST}_{L'L}(q', q; \omega) = V^{JST}_{L'L}(q', q; \omega) + \frac{2}{\pi} \sum_l \boldsymbol{P} \int_0^\infty \frac{V^{JST}_{L'l}(q', k)}{[k_0^2 - k^2]} K^{JST}_{lL}(k, q; \omega)\ k^2 dk$$

Solutions of NN LS equation

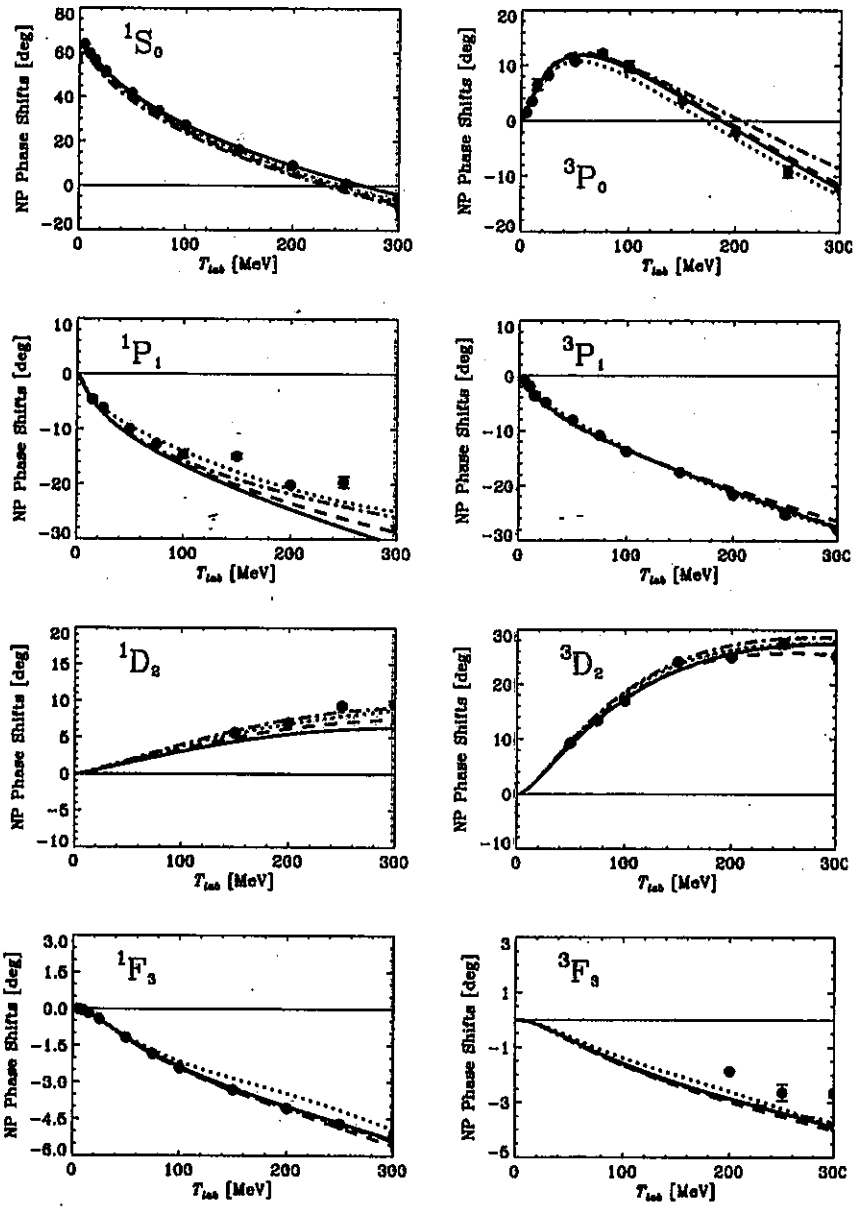

The single channel SM97 phase shift analysis and results found using the different forces

Solutions of NN LS equation ctnd.

Low-Energy np scattering + deuteron properties

Property	Bonn-B	Experiment
a_s (fm)	-23.7	-23.748 (10)
a_t (fm)	5.42	5.424 (4)
r_s (fm)	2.70	2.75 (5)
r_t (fm)	1.76	1.759 (5)
E_D (MeV)	2.2246	2.224589
μ_D (nm)	0.8514*	0.857406 (1)
Q_D (fm^2)	0.2783*	0.2859 (3)
P_D (%)	4.99	–
A_S	0.8862	0.8802 (20)
D/S	0.0264	0.0256 (4)
r_{rms} (fm)	1.9688	1.9627 (38)

* Meson exchange currents not included.

The t matrices off-shell

• Definition: $t^{JST}_{L'L}\left(q', q; \omega \propto k_0^2\right)$

t matrices are said to be *off-shell* when the variables q and q' differ from the on-shell momentum value k_0

The t matrix is "half-off-shell" if one of the two variables is fixed at the value of k_0

• The Noyes-Kowalski ratios ($f^{JST}_{L'L}$):

For half-off-shell conditions $(\omega \propto k_0^2)$

a) uncoupled channels $L' = L$

$$f^{JST}_{L}(q', k_0) = \frac{t^{JST}_{LL}(q', k_0; \omega)}{t^{JST}_{LL}(k_0, k_0; \omega)} \equiv \frac{K^{JST}_{LL}(q', k_0; \omega)}{K^{JST}_{LL}(k_0, k_0; \omega)}$$

(These ratios are purely real quantiies)

b) coupled states

$$f^{JST}_{L'L}(q', k_0) = \frac{K^{JST}_{L'L}(q', k_0; \omega)}{K^{JST}_{L'L}(k_0, k_0; \omega)}$$

(again ratios purely real quanties)

The t matrices off-shell ctnd.

Kowalski-Noyes ratios

Uncoupled channels case

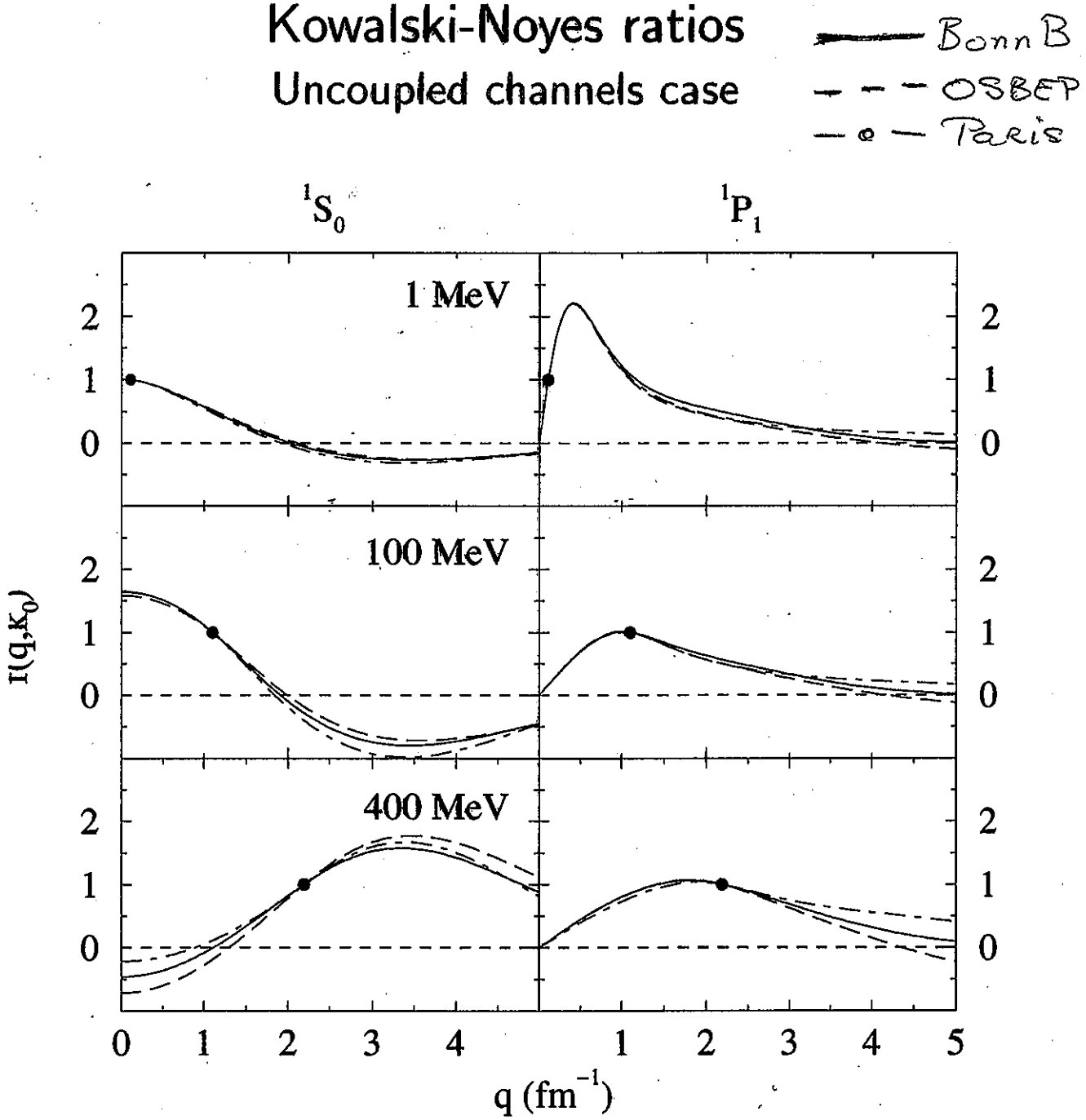

f-ratios for the $^1S_0$ (left) and $^1P_1$ (right) channels.
(The dots represent the on-shell values)

The t matrices off-shell ctnd.

Kowalski-Noyes ratios

Coupled channels case

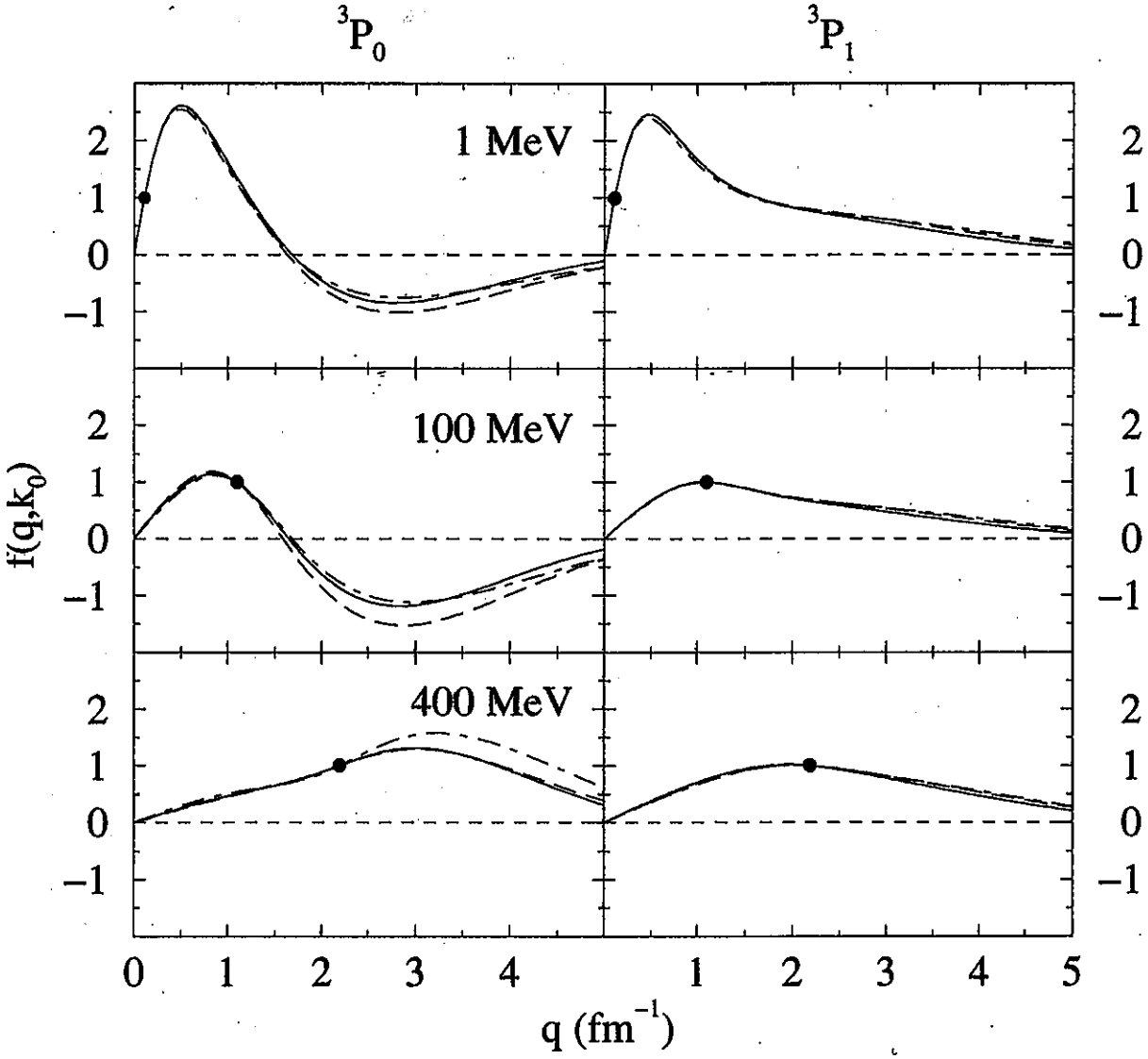

f-ratios for the $^3S_1$ (left) and $^3D_1$ (right) channels.
(The dots represent the on-shell values)

Two nucleon g matrices

- NN Lippmann-Schwinger equation:

  With $V = V_{NN}^{(\mathrm{Bonn})}$, LS gives NN t matrices
  (one nucleon bound – must treat medium)
  Medium effects (Mass operator, Pauli blocking)

- Form NN g matrices in infinite matter:

  Solutions of Brueckner-Bethe-Goldstone Eqns.

$$g(\boldsymbol{q}', \boldsymbol{q}; \boldsymbol{K}) = V(\boldsymbol{q}', \boldsymbol{q}) + \int V(\boldsymbol{q}', \boldsymbol{k}') \frac{Q(\boldsymbol{k}', \boldsymbol{K}; k_f)}{[E(\boldsymbol{k}, \boldsymbol{K}) - E(\boldsymbol{k}', \boldsymbol{K})]} g(\boldsymbol{k}', \boldsymbol{q}; \boldsymbol{K})\, d\boldsymbol{k}'$$

- Momenta:

  $\boldsymbol{p}_0,\ \boldsymbol{p}_1$ Projectile and Bound state nucleon
  $\boldsymbol{k} = \frac{1}{2}(\boldsymbol{p}_0 - \boldsymbol{p}_1)$ NN relative
  $\boldsymbol{K} = \frac{1}{2}(\boldsymbol{p}_0 + \boldsymbol{p}_1)$ NN C.M. momenta
  $\boldsymbol{k_f}$ Fermi momentum

- Pauli operator:

$$Q(\boldsymbol{k}', \boldsymbol{K}; k_f) = \begin{cases} 1 & \text{if } \left|\boldsymbol{k}' \pm \boldsymbol{K}\right| > k_f \\ 0 & \text{otherwise} \end{cases}$$

Two nucleon g matrices ctnd.

- Energy denominator:

$$E(\boldsymbol{k},\boldsymbol{K}) = \frac{\hbar^2}{m}\left(k^2+K^2\right) + U\left(|\boldsymbol{k}+\boldsymbol{K}|\right) + U\left(|\boldsymbol{k}-\boldsymbol{K}|\right)$$

- Auxiliary potentials: $U\left(|\boldsymbol{k}+\boldsymbol{K}|\right) \equiv U(\boldsymbol{p}_0)$

  These are actually formed by a semi-consistent folding of g matrices
  (details in review – Adv. Nucl. Phys. **25**)

- Brueckner angle averages:

$$|\boldsymbol{k}\pm\boldsymbol{K}|^2 \approx K^2+k^2 \pm \left(\frac{2}{\sqrt{3}}\right) kK\overline{Q}^{\frac{3}{2}}(k,K;k_f)$$

where

$$\overline{Q}(k,K;k_f) = \begin{cases} 1 & \text{if } k \geq k_f + K \\ 0 & \text{if } k \leq \sqrt{k_f^2 - K^2} \\ \frac{k^2+K^2-k_f^2}{2kK} & \text{otherwise.} \end{cases}$$

Two nucleon g matrices ctnd.

- Partial wave g matrices:

$$g^{(\alpha)}_{LL'}(q',q;K) = V^{(\alpha)}_{LL'}(q',q) + \frac{2}{\pi}\sum_l \int_0^\infty V^{(\alpha)}_{Ll}(q',k')\,\{\Omega\}\,g^{(\alpha)}_{lL'}(k',q;K)\,k'^2\,dk'$$

$$\Omega(k,k',K;k_f) = \frac{\overline{Q}(k',K;k_f)}{\left[\overline{E}(k,K) - \overline{E}(k',K)\right]}$$

- C.M. momentum average: Use $K \to \overline{K}$

$$\overline{K} = \begin{cases} \sqrt{k^2+p^2-\frac{1}{4}\Xi(k,k_f)} & \text{if } k_f - p \le 2k \le k_f + p \\ \sqrt{k^2+p^2} & \text{if } 0 \le 2k \le k_f - p\,. \end{cases}$$

$$\text{with } \Xi(k,k_f) = \left[(2k+p)^2 - k_f^2\right]$$

Common approximation for single particle energies

$$\epsilon(q_i) = \frac{\hbar^2 q_i^2}{2m^\star} + U_i$$

$$\overline{E}(k,K) = \frac{\hbar^2}{m^\star}\left(k^2+K^2\right) + U_o + U_1$$

identifies the effective mass $m^\star$

Two nucleon g matrices ctnd.

Auxiliary potentials

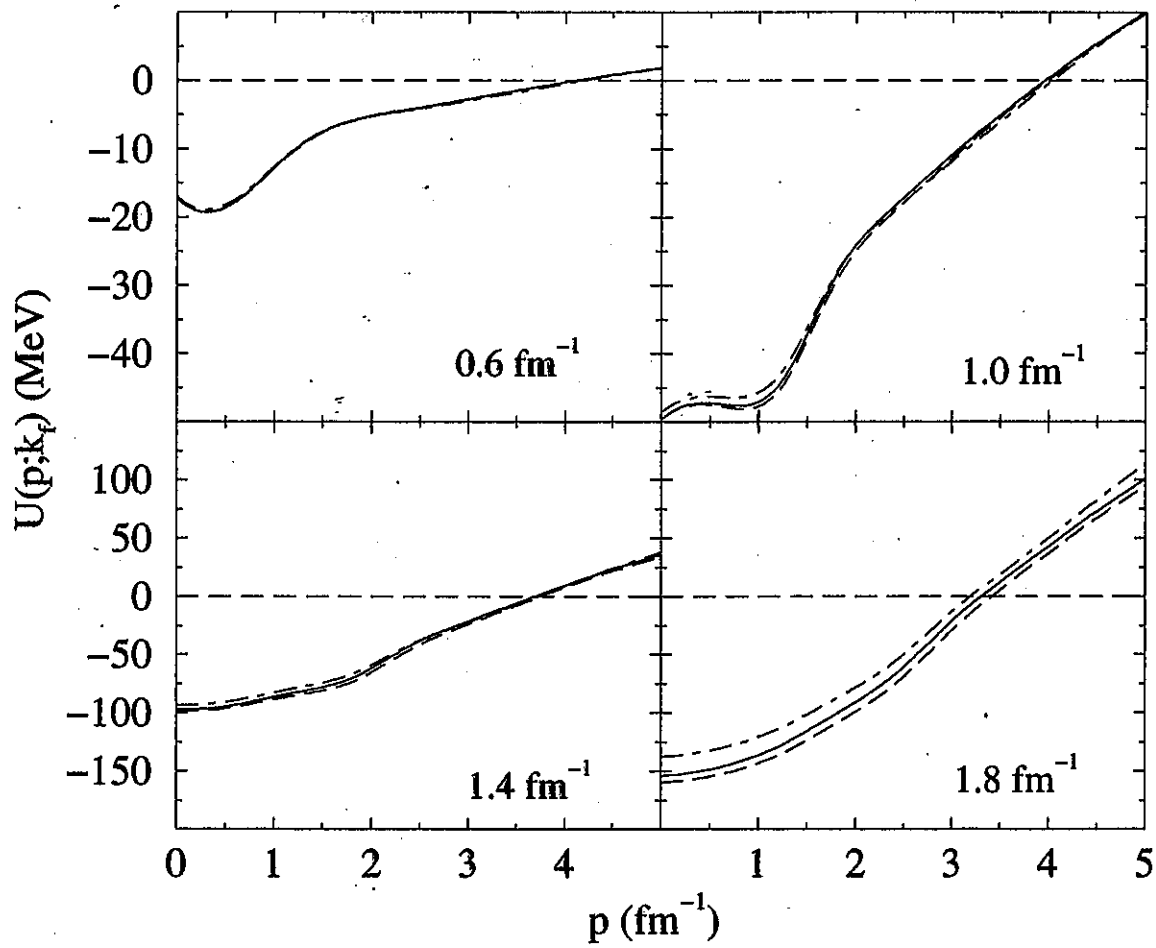

The auxiliary potentials found using various NN interactions and for various values of k_f

——— Bonn B
— — — OSBEP
— ∘ — Paris

Two nucleon g matrices ctnd.

Table of on-shell Bonn-B $K^{(\alpha)}$ matrices

channel	ID	65 MeV	200 MeV
$^1S_0$	free	-0.789	-0.064
	PB	-0.799	-0.073
	PB+SCP	-0.741	−0.042
$^1P_1$	free	0.259	0.280
	PB	0.296	0.282
	PB+SCP	0.308	0.312
$^3P_0$	free	-0.244	0.011
	PB	-0.237	0.017
	PB+SCP	-0.228	0.034
$^3S_1$	free	-1.605	-0.222
	PB	-1.257	-0.260
	PB+SCP	-1.020	-0.209
$^3S_1 \leftrightarrow {}^3D_1$	free	-0.072	-0.038
	PB	-0.341	-0.100
	PB+SCP	-0.346	-0.136

Two nucleon g matrices ctnd.

Kowalski-Noyes ratios

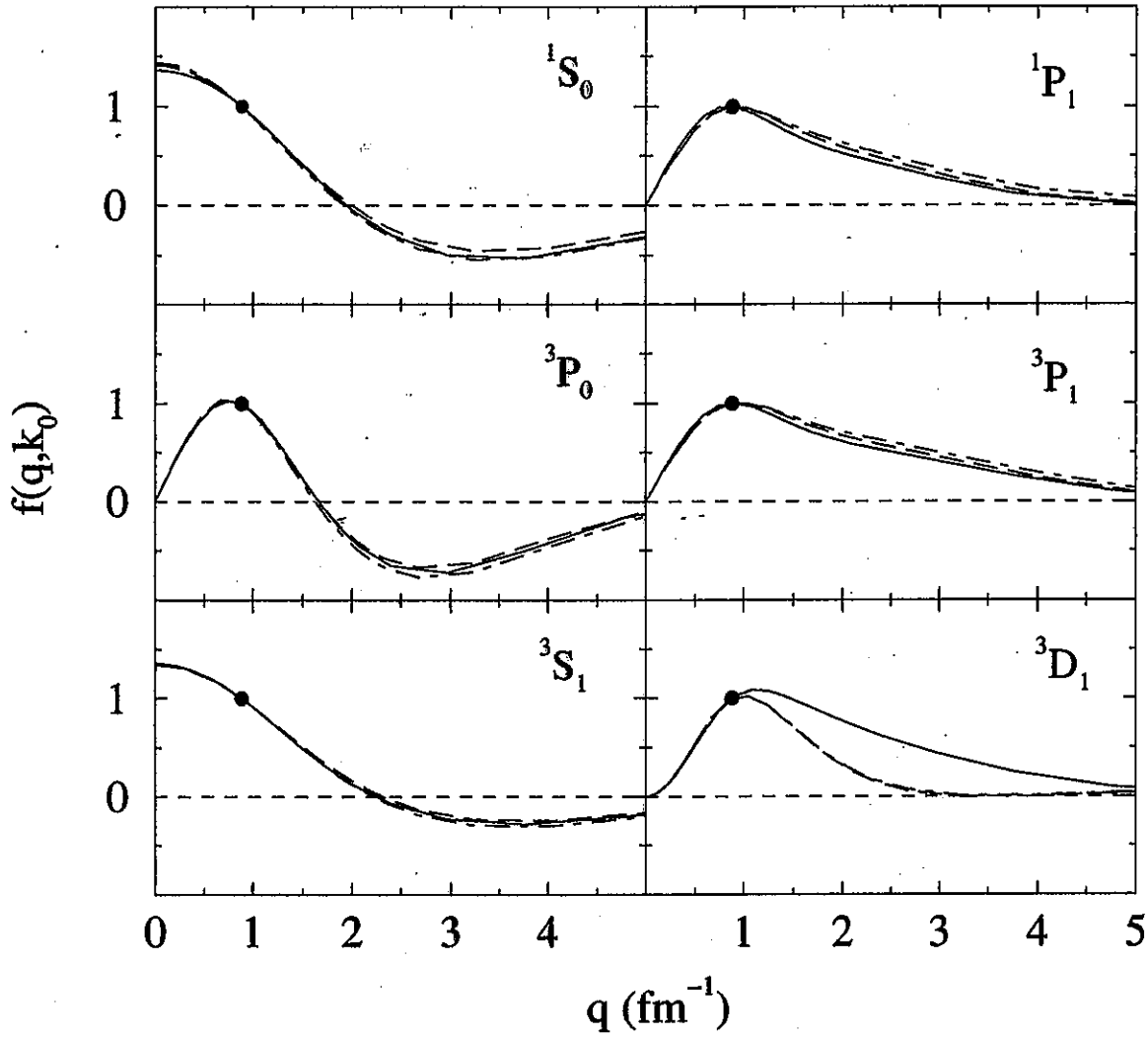

Ratios found at 65 MeV for the Bonn-B interaction.

The solid, dashed and dot-dashed lines refer to the free, PB, and PB+SCP calculations respectively. The dots again identify the on-shell values.

g_{eff} – Coordinate space

- Require a mapping:

$$g(\boldsymbol{p}', \boldsymbol{p}; E, k_f) \longrightarrow g(\boldsymbol{r}, E, \rho\{k_f(r)\})$$

where $\boldsymbol{r} \to |\boldsymbol{r}_0 - \boldsymbol{r}_1| = r$

- Operator forms for effective g matrices:

$$g_{\text{eff}}^{ST}(\boldsymbol{r}, E; k_f) = \sum_i g_{\text{eff}}^{(i)ST}(r, E; k_f)\Theta_i$$

$$g_{\text{eff}}^{(i)ST}(r, E; k_f) = \sum_{j=1}^{n_i} S_j^{(i)}(E; k_f)\frac{e^{-\mu_j^{(i)}r}}{r}$$

  - Θ_i — characteristic operators:
    - $i = 1$: central forces:
      $$\{1, (\boldsymbol{\sigma}\cdot\boldsymbol{\sigma}), (\boldsymbol{\tau}\cdot\boldsymbol{\tau}), (\boldsymbol{\sigma}\cdot\boldsymbol{\sigma}\boldsymbol{\tau}\cdot\boldsymbol{\tau})\}$$
    - $i = 2$: tensor force: $\{\boldsymbol{S_{12}}\}$
    - $i = 3$: two-body spin-orbit force: $\{\boldsymbol{L}\cdot\boldsymbol{S}\}$
  - $S_j^{(i)}(E; k_f)$ — complex, E-dependent strengths

g_{eff} in coordinate space ctnd.

- g^{eff} momentum space: (double Bessel transform)

$$g^{JST}_{\text{eff};LL'}(q',q;\omega)$$

$$= \sum_i \langle\theta_i\rangle \int_0^\infty r^{2+\lambda} j_L(q'r) g^{(i)ST}_{\text{eff}}(r,\omega) j_{L'}(qr)\, dr$$

$$= \sum_{ij} \langle\theta_i\rangle\, S^{(i)}_j(\omega) \int_0^\infty r^{2+\lambda} j_L(q'r) \frac{e^{-\mu^{(i)}_j r}}{r} j_{L'}(qr)\, dr$$

$$= \sum_{ij} \langle\theta_i\rangle\, S^{(i)}_j(\omega) \tau^\alpha(q',q;\mu^{(i)}_j)$$

($\alpha : \{LL'JST\}$ and $\lambda = 2$ for the tensor force)

- Optimal set of ranges and strengths satisfy:

$$\min := \left\| g^{JST}_{LL'}(q',q;\omega) - g^{JST}_{\text{eff}\,LL'}(q',q;\omega) \right\|$$

- Setting the ranges:

  Because off-shell variations (f-ratios) of t- and g-matrices are similar (≤ 1 fm^{-1}),

Ranges taken INDEPENDENT of energy and density

Elastic scattering (general)

- Tests of the effective interactions:

Mass and energy variations

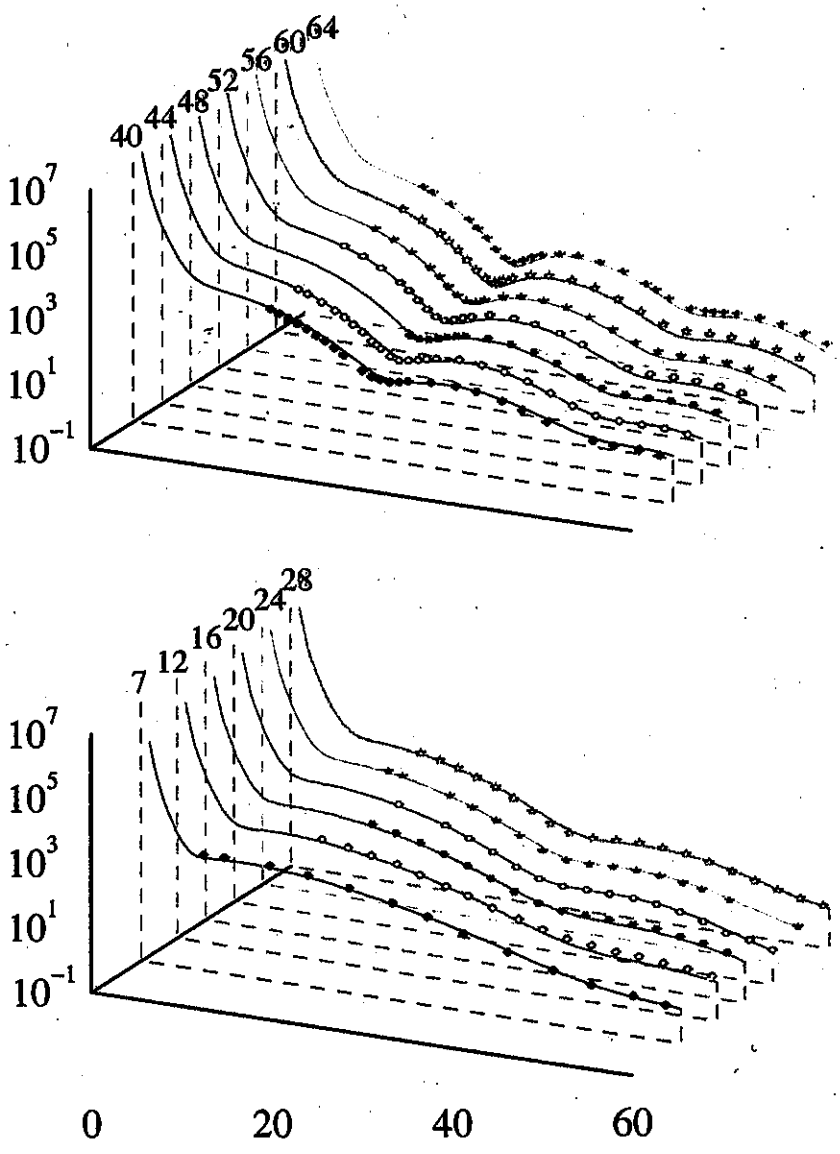

Cross sections for 65 MeV proton scattering

Elastic scattering (general) ctnd.

- Tests of the effective interactions:

Mass and energy variations

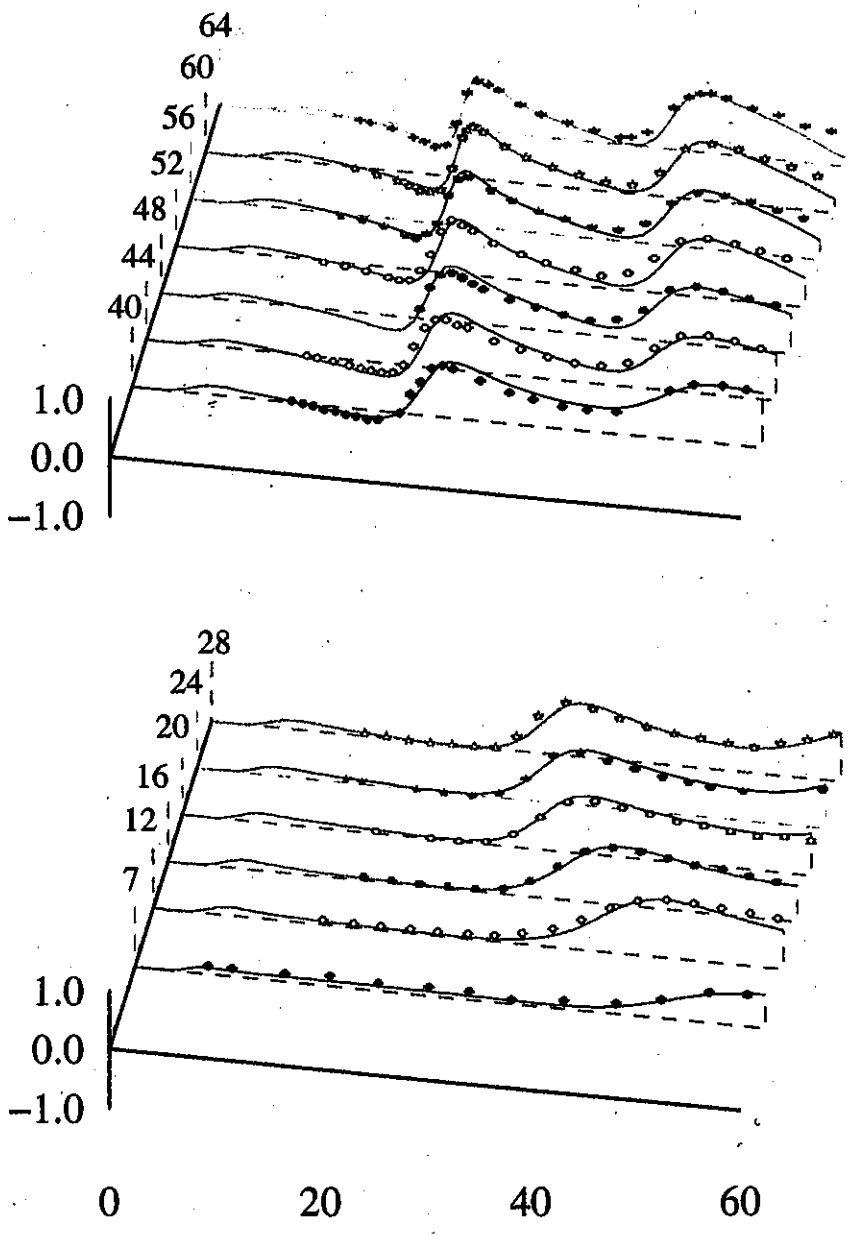

Analyzing powers for 65 MeV proton scattering

Elastic scattering (general) ctnd.

- Tests of the effective interactions:

Mass and energy variations

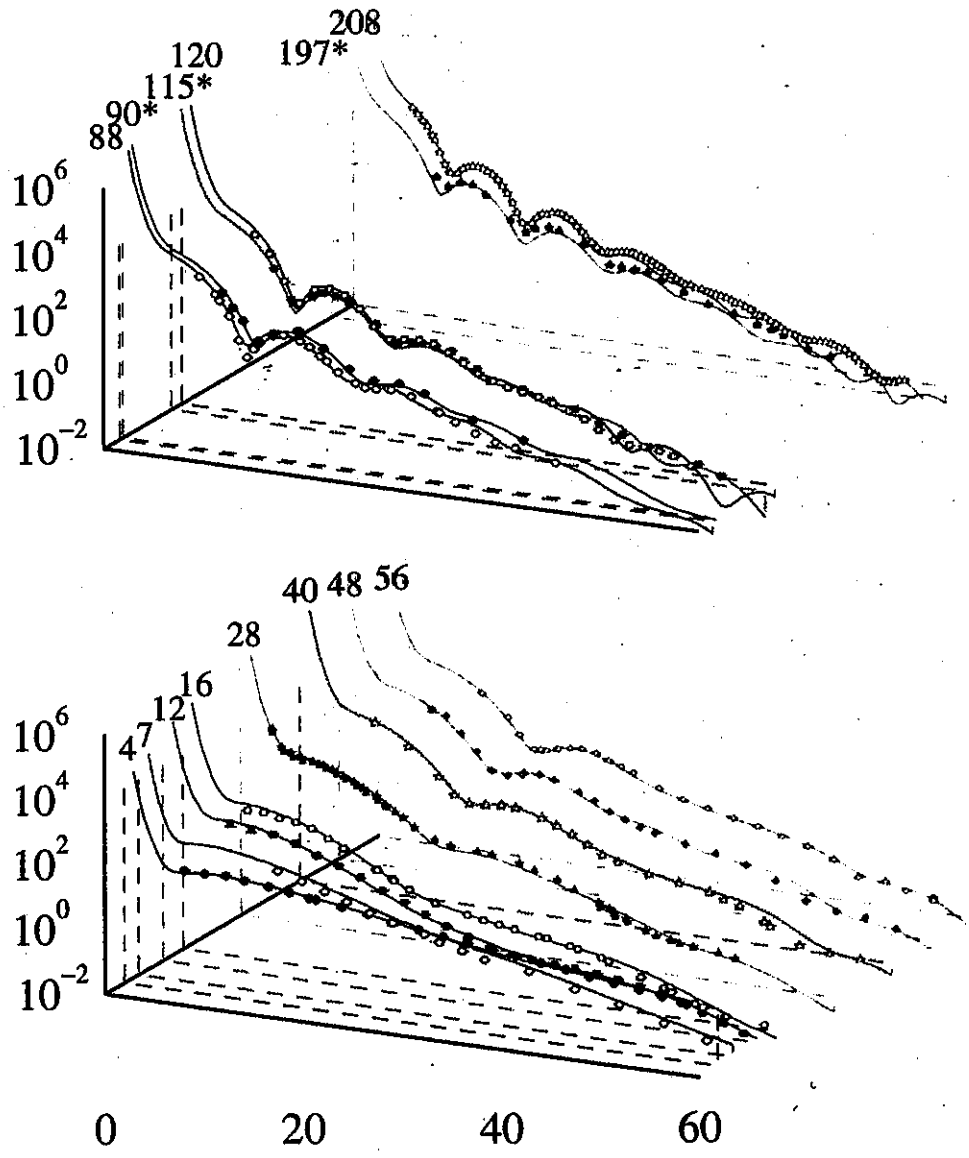

Cross sections for 200 MeV proton scattering

Elastic scattering (general) ctnd.

- Tests of the effective interactions:

Mass and energy variations

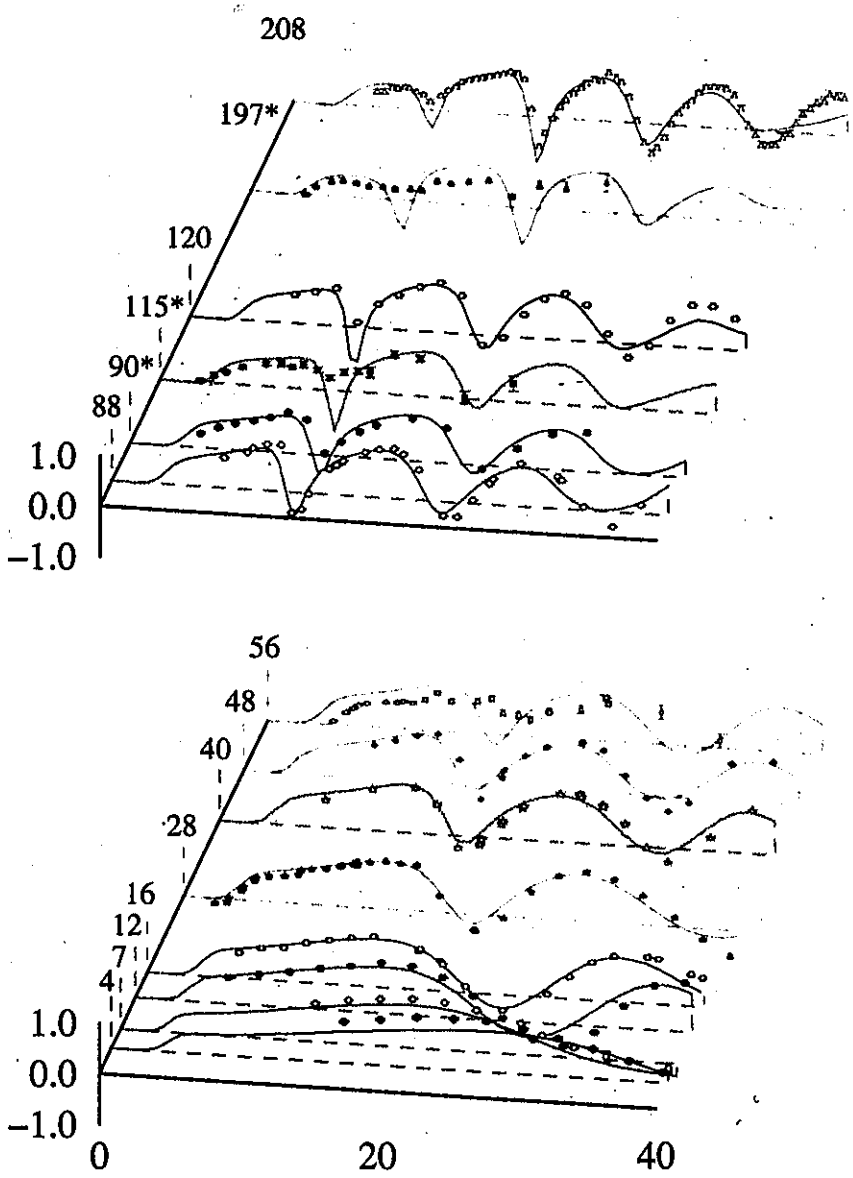

Analyzing powers for 200 MeV proton scattering

Elastic scattering (general) ctnd.

- Tests of the effective interactions:

Mass and energy variations

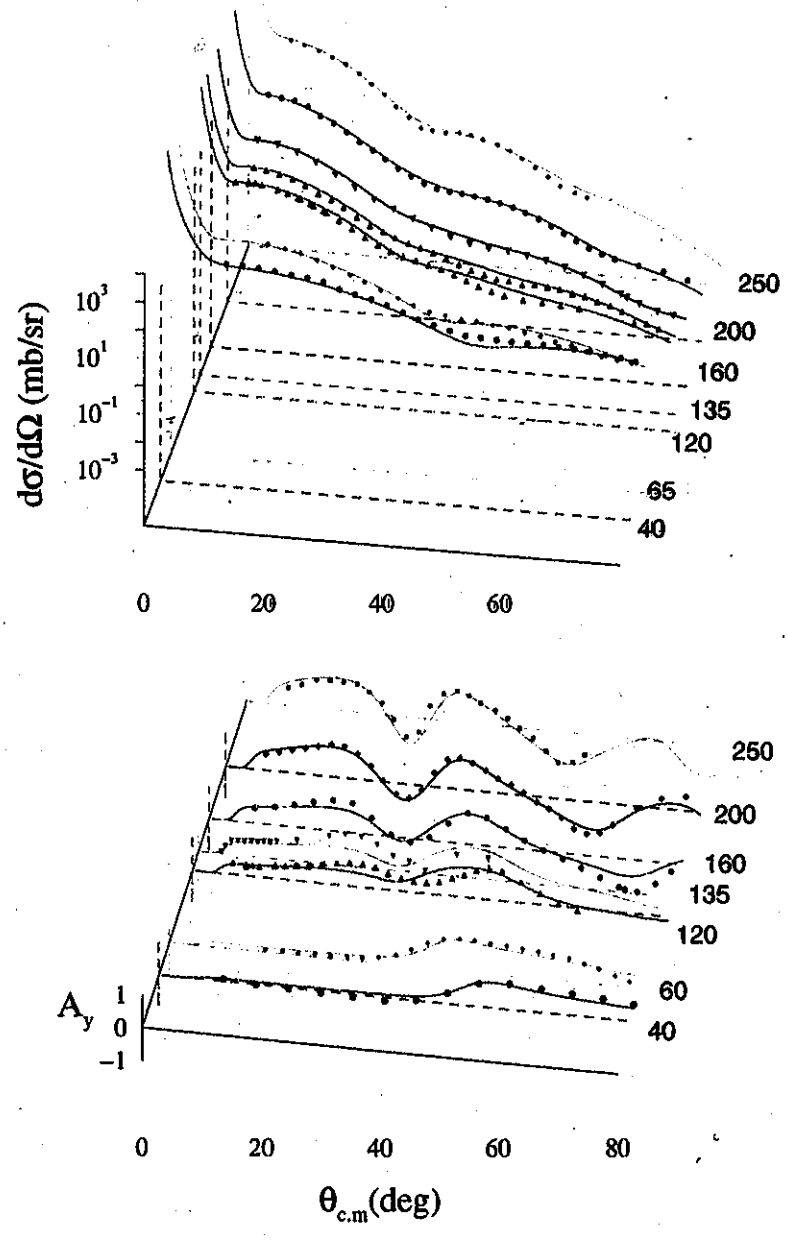

Results for proton scattering from ^{12}C

Elastic scattering (general) ctnd.

neutron-^{12}C scattering

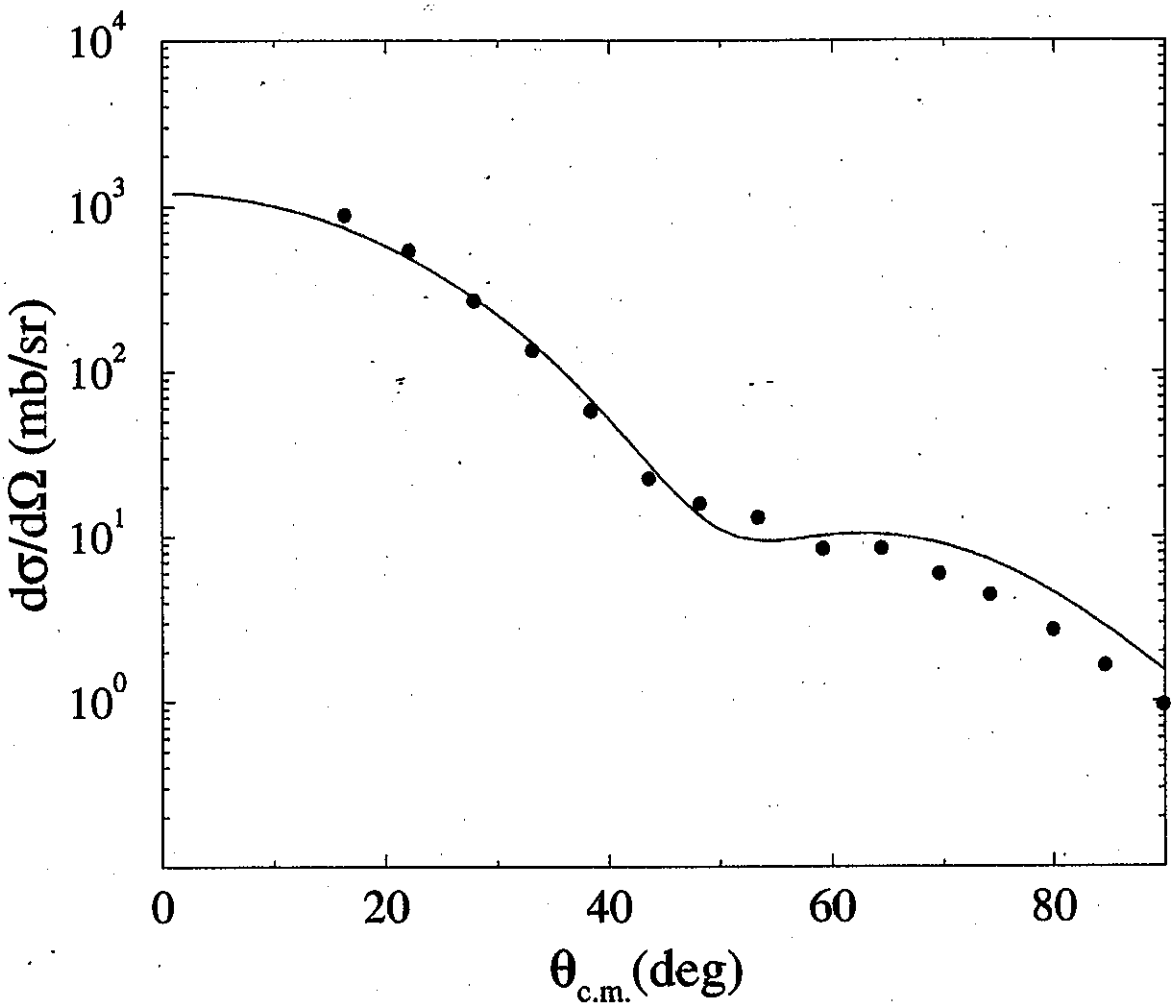

40 MeV predictions compared with data

$\sigma_R = 397$mb (expt. 383 mb)

Elastic scattering (general) ctnd.

- Effect of nonlocality: Recall

$$U(\boldsymbol{r},\boldsymbol{r}';E) = \delta(\boldsymbol{r}-\boldsymbol{r}')\sum_i n_i \int \varphi_i^*(\boldsymbol{s}) g_D(\boldsymbol{r},\boldsymbol{s};E)\varphi_i(\boldsymbol{s})\, d\boldsymbol{s}$$

$$+\sum_i n_i\, \varphi_i^*(\boldsymbol{r})\, g_E(\boldsymbol{r},\boldsymbol{r}';E)\, \varphi_i(\boldsymbol{r}')$$

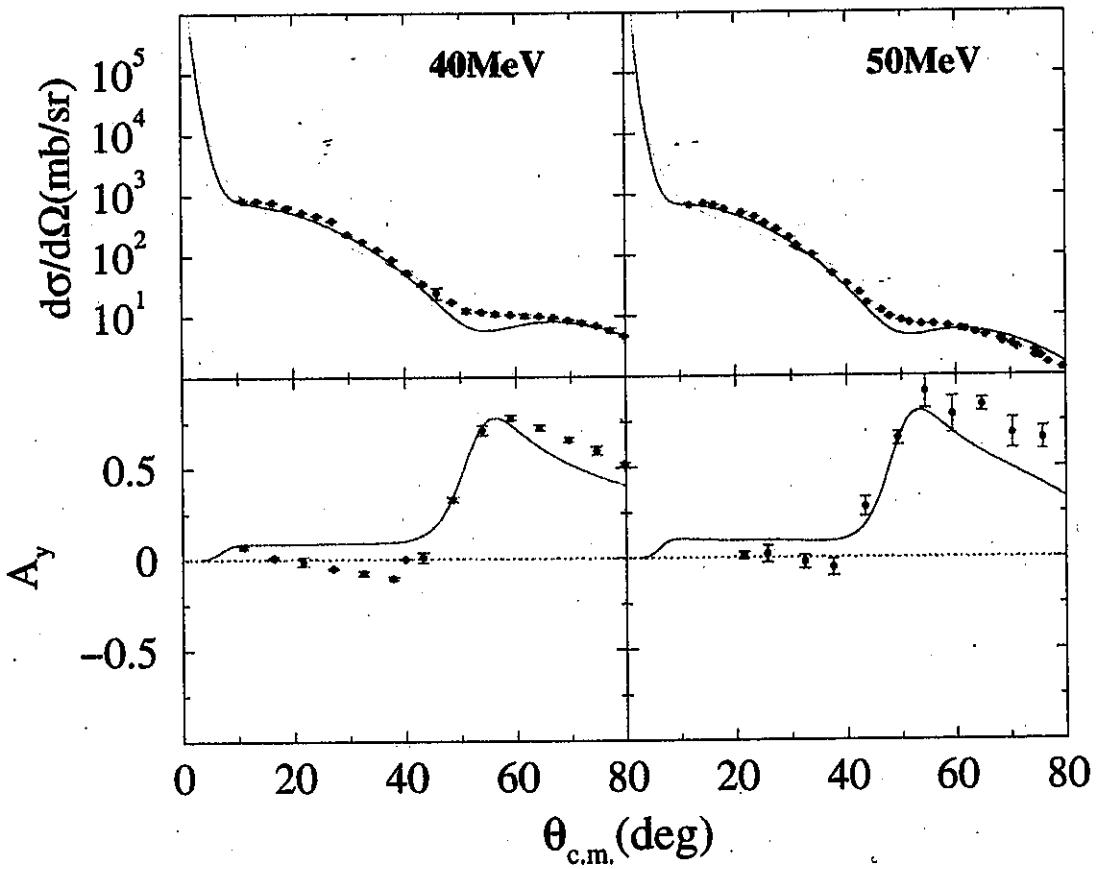

Cross sections and analysing powers
for the scattering of protons from ^{12}C.

Elastic scattering (general) ctnd.

- Medium effects in NN $g_{eff}(r)$:

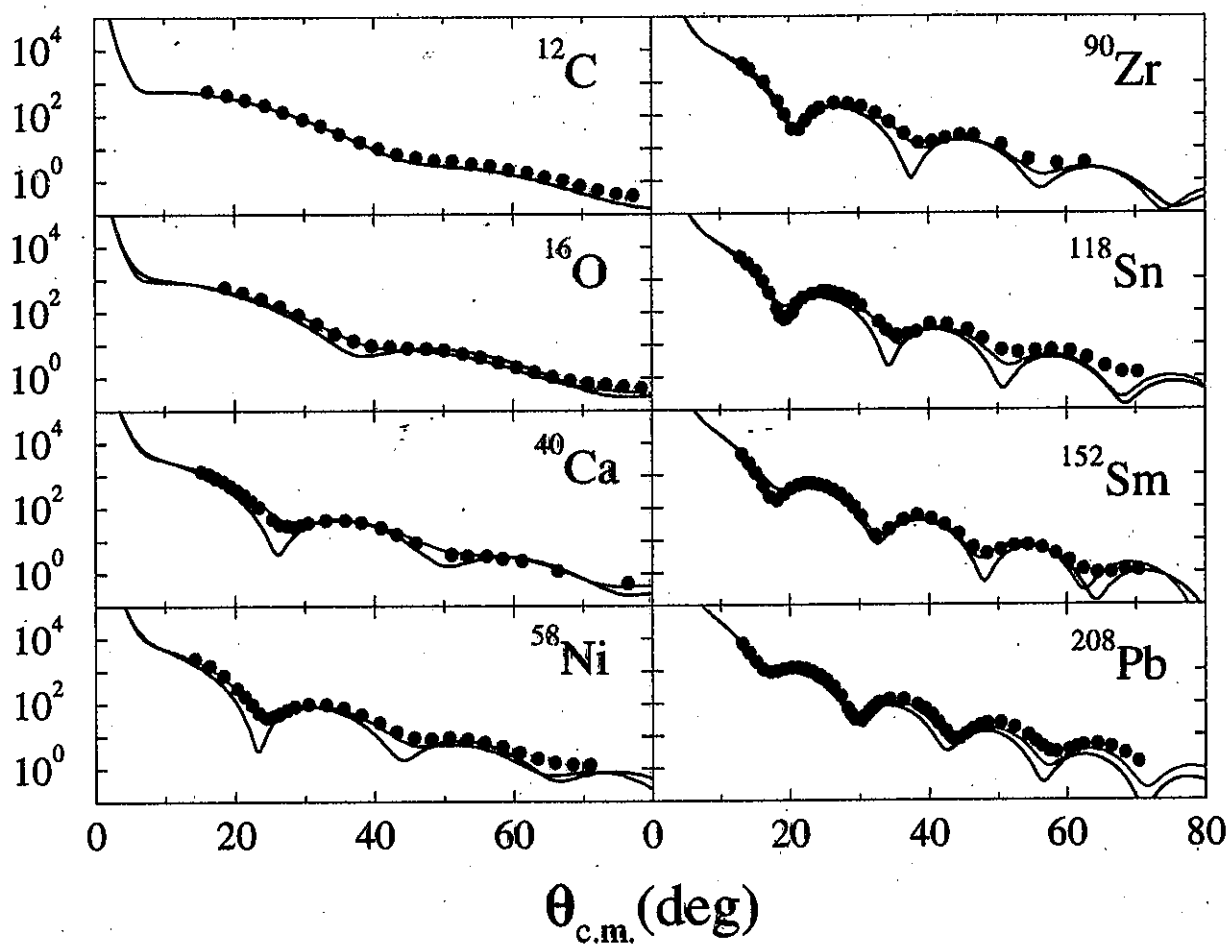

65 MeV cross section predictions compared with data

—— g matrix

—— t matrix

Elastic scattering (general) ctnd.

- Medium effects in NN $g_{eff}(r)$:

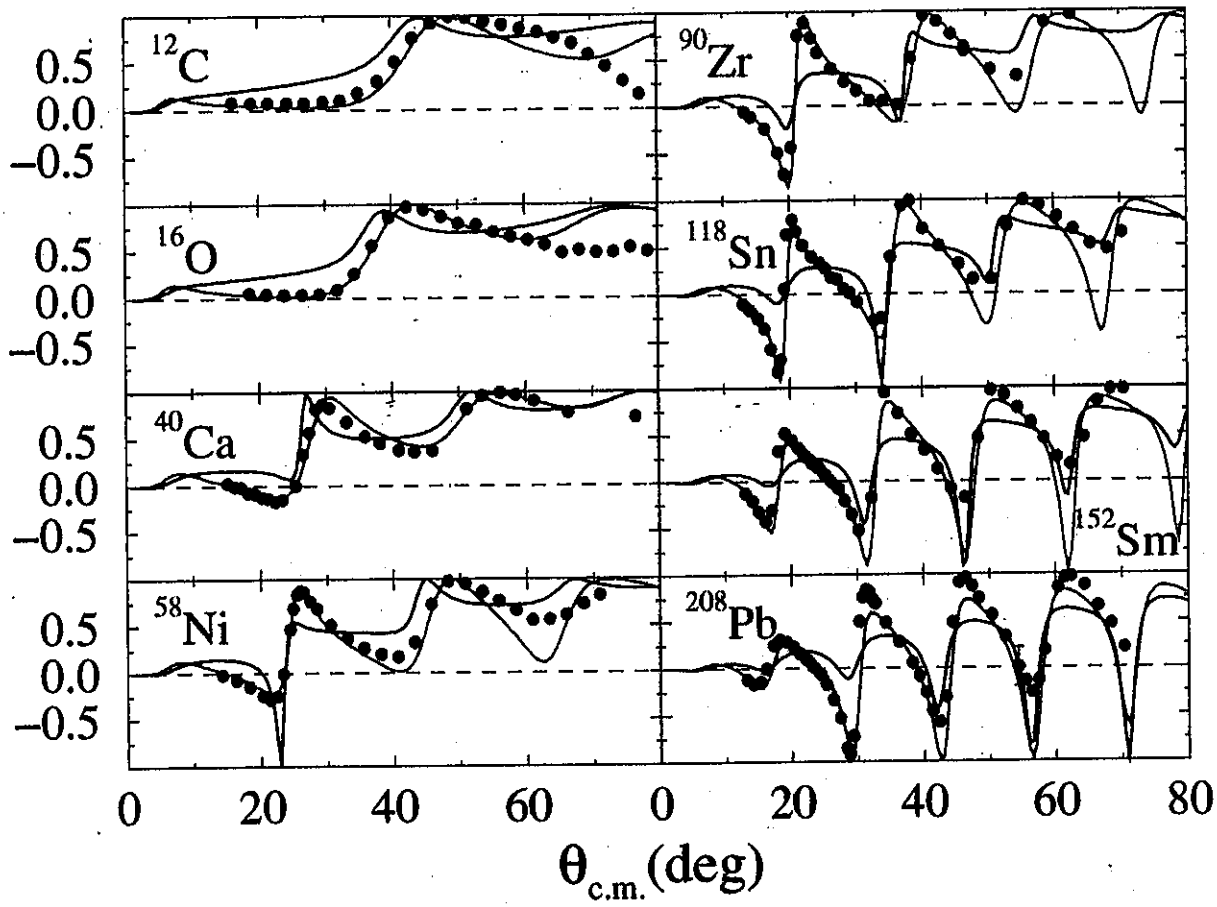

65 MeV analyzing power predictions compared with data

—— g matrix

—— t matrix

Elastic scattering (general) ctnd.

- Medium effects in NN $g_{eff}(r)$:

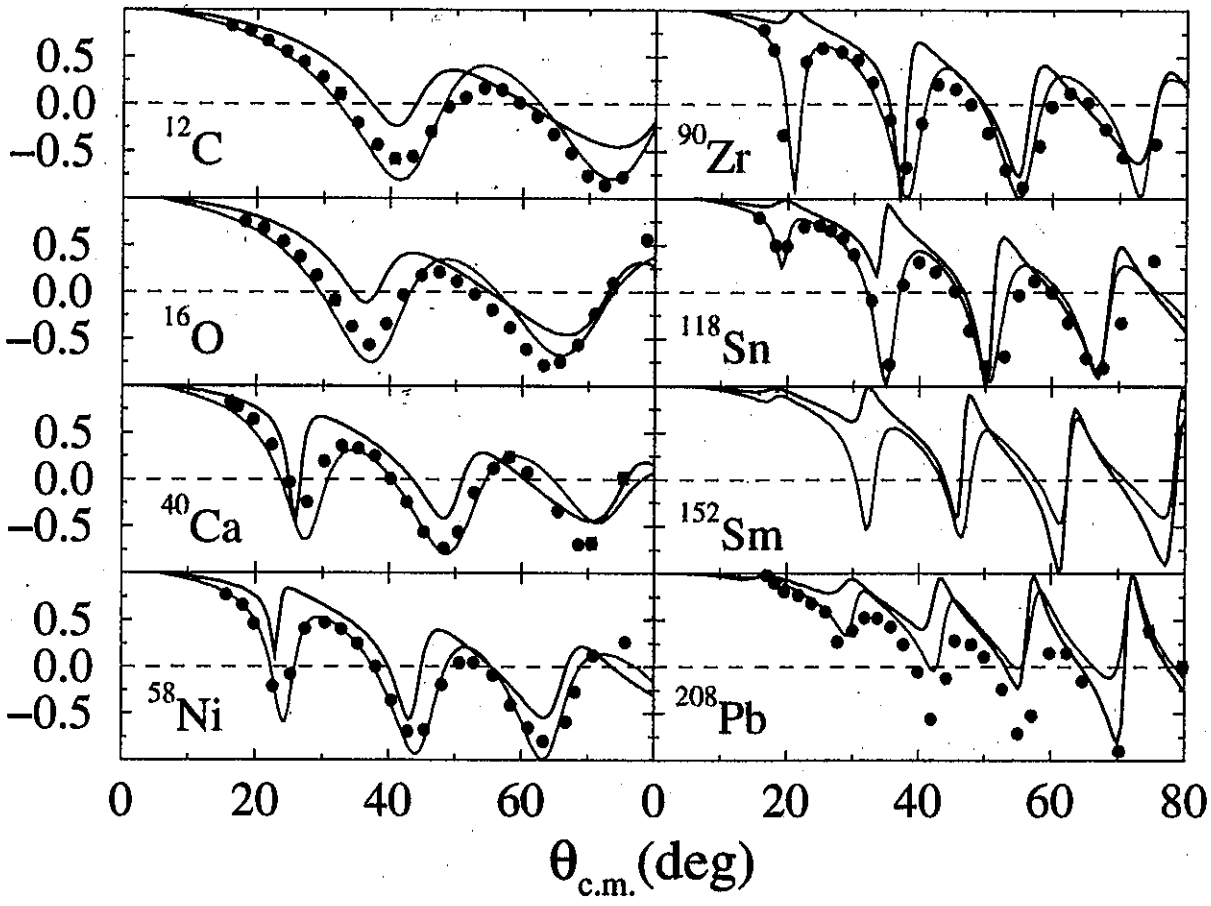

65 MeV spin rotation predictions compared with data

—— g matrix

—— t matrix

Different forces

156 MeV p-^{12}C scattering

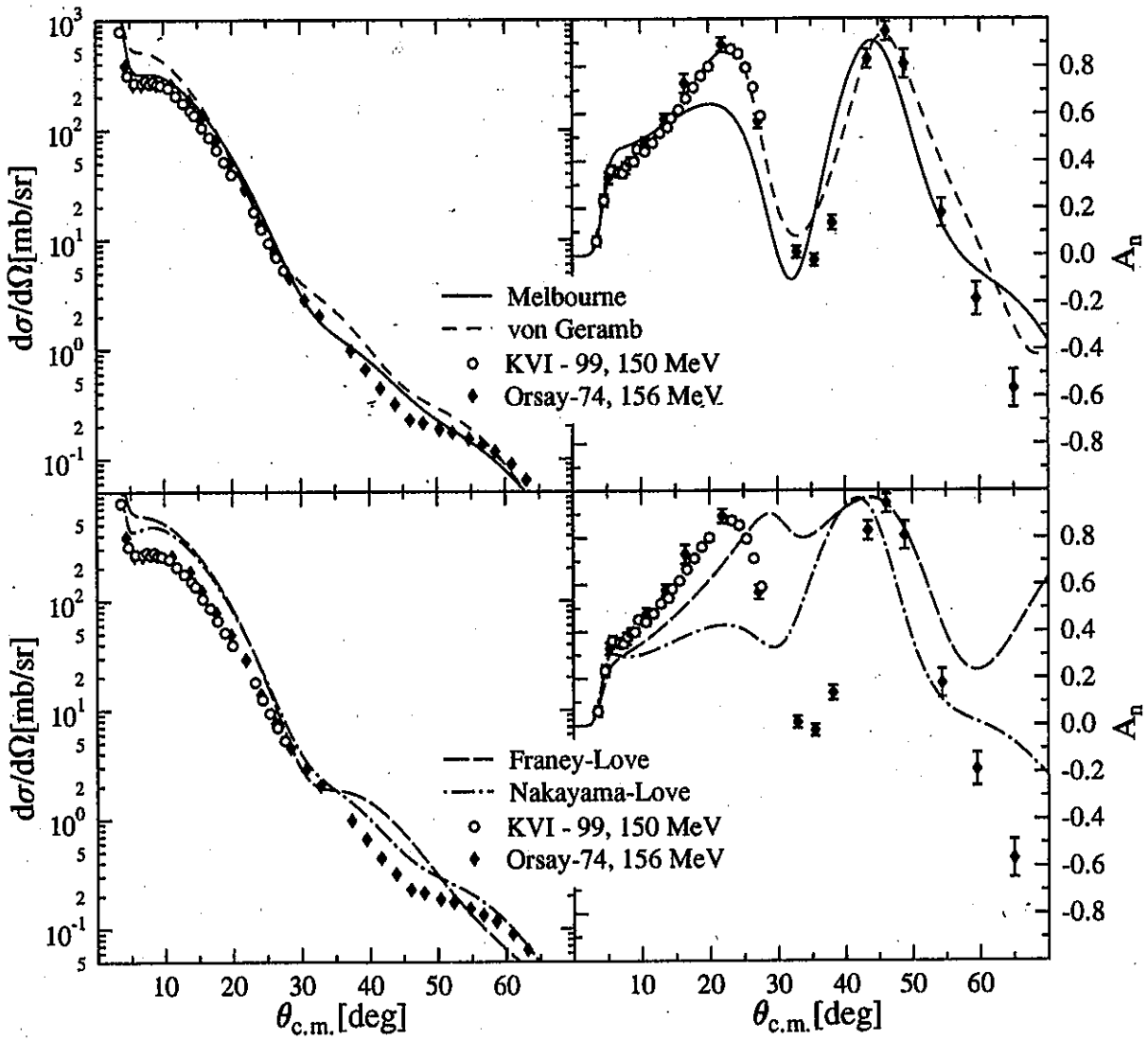

Predictions compared with data

(Shell Model – $(0+2)\hbar\omega$)

Analyses of Ca isotopes

Matter densities in ^{40,44,48}Ca

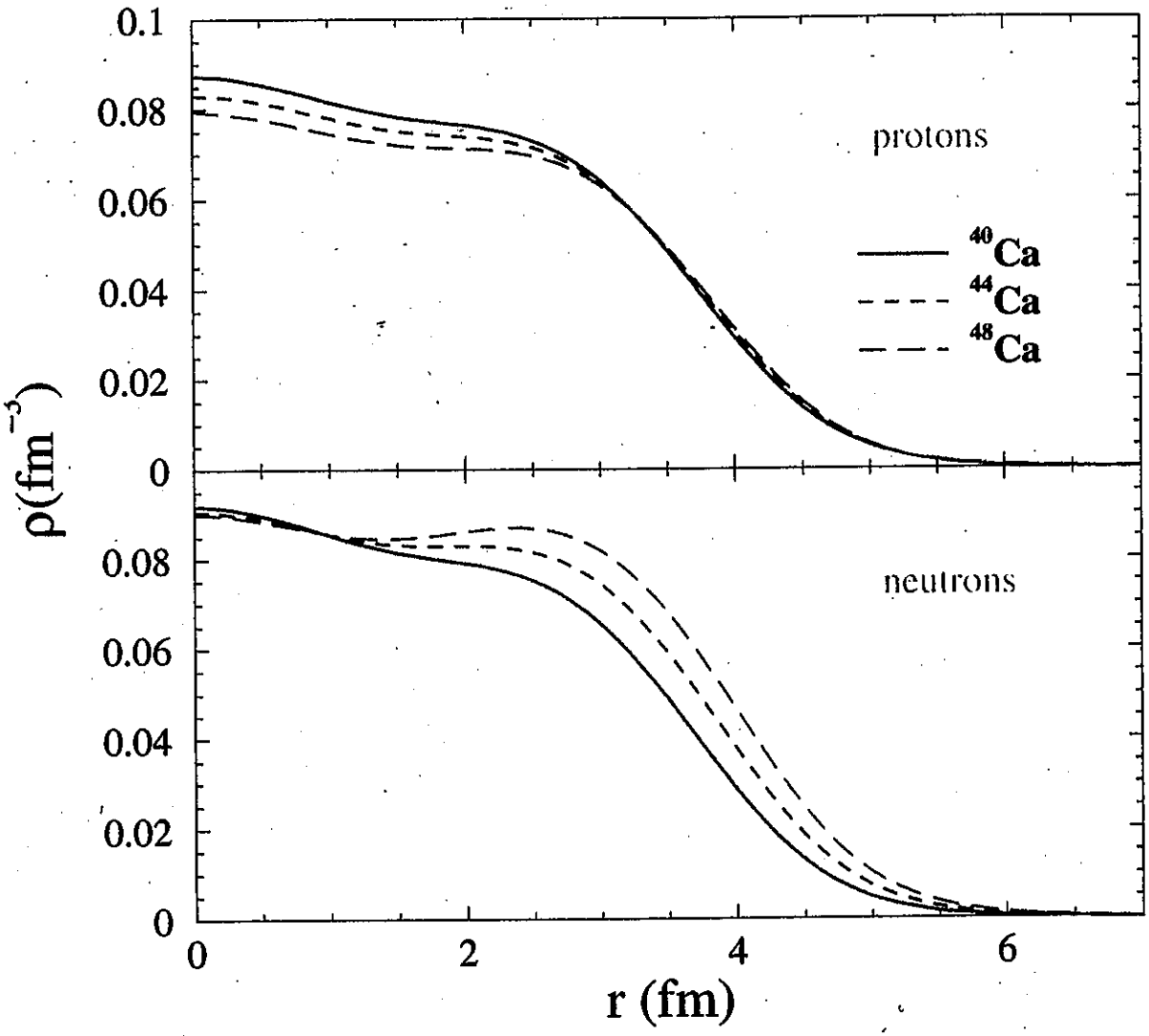

SHF model densities

Analyses of Ca isotopes ctnd.

Proton-^{40}Ca scattering

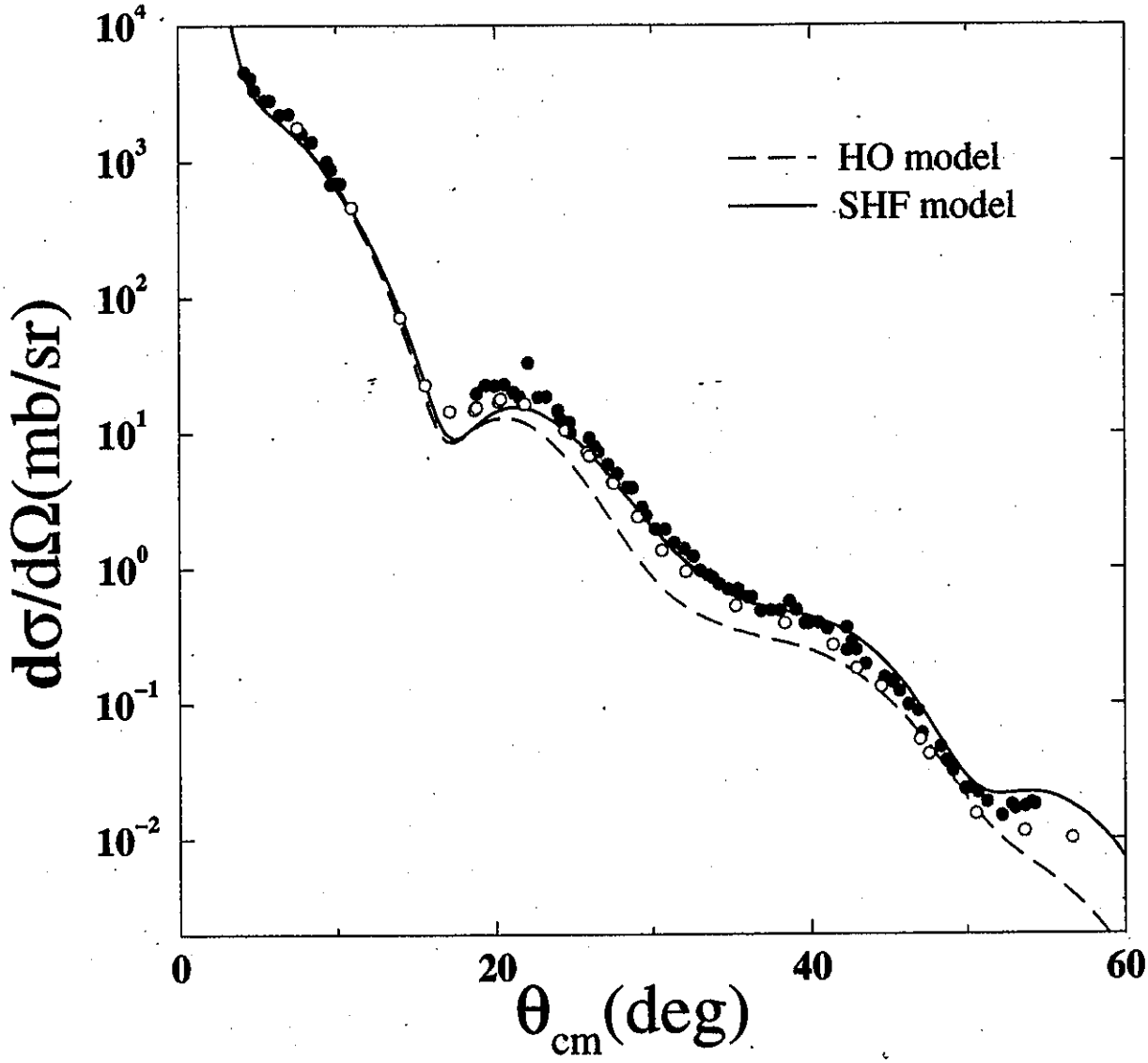

Data and predictions for 200 MeV proton scattering

Analyses of Ca isotopes ctnd.
Total reaction cross sections

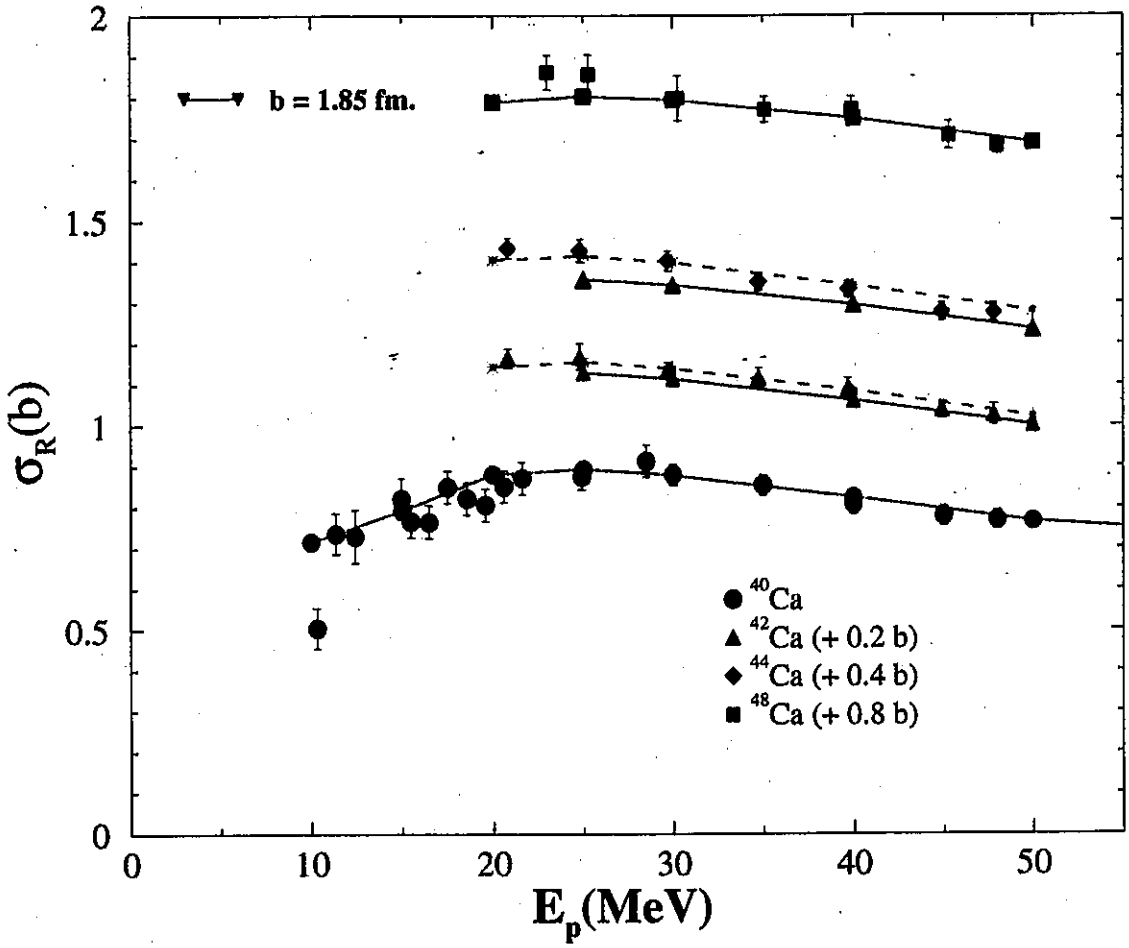

Proton-^{40,42,44,48}Ca scattering

Predictions compared with "shifted" data

Analyses of ^{208}Pb

Shell and SHF model densities

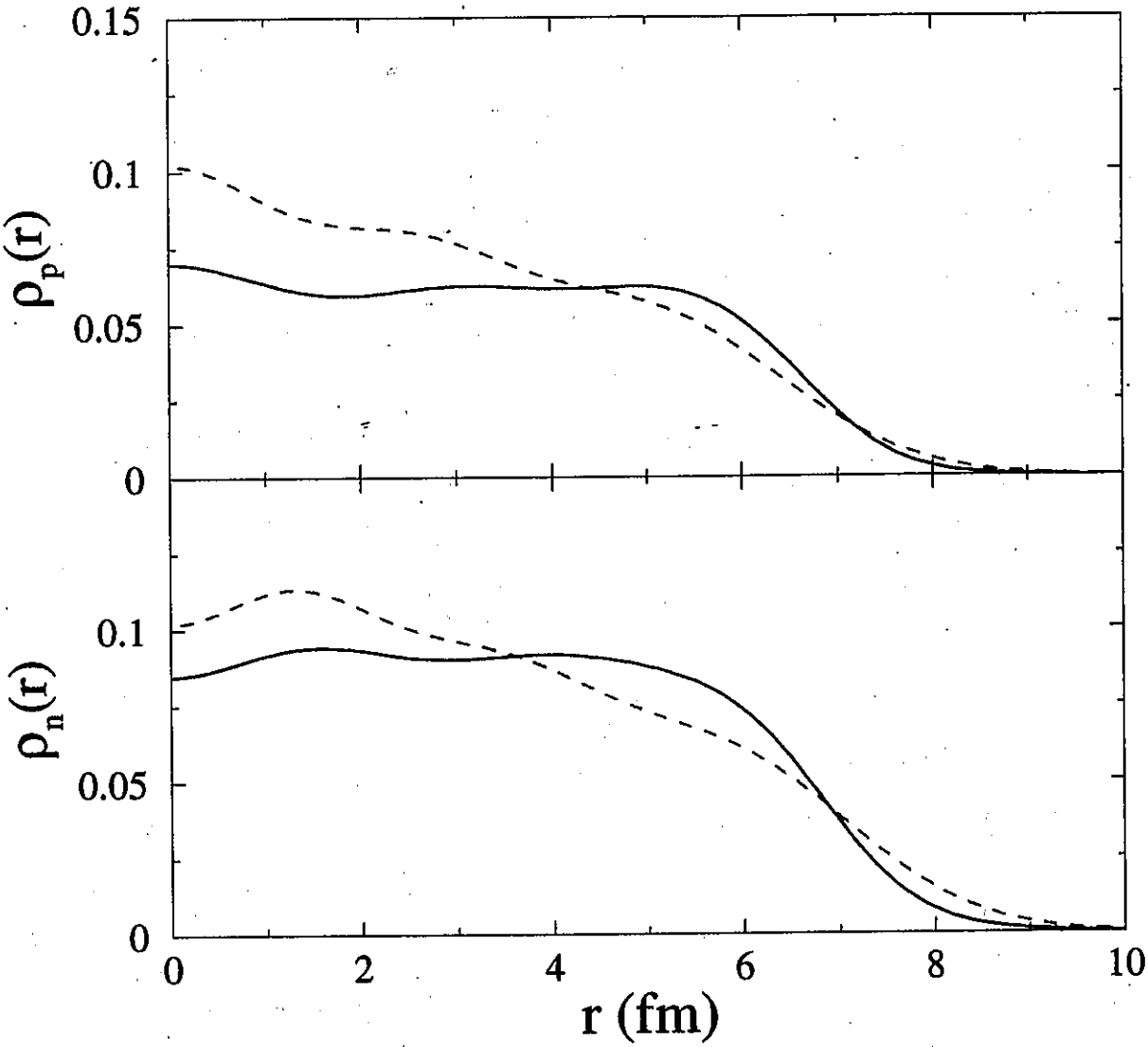

SHF and HO densities with same rms radii

- - - $0\hbar\omega$

—— SHF

Analyses of ^{208}Pb ctnd.

Diverse SHF model densities

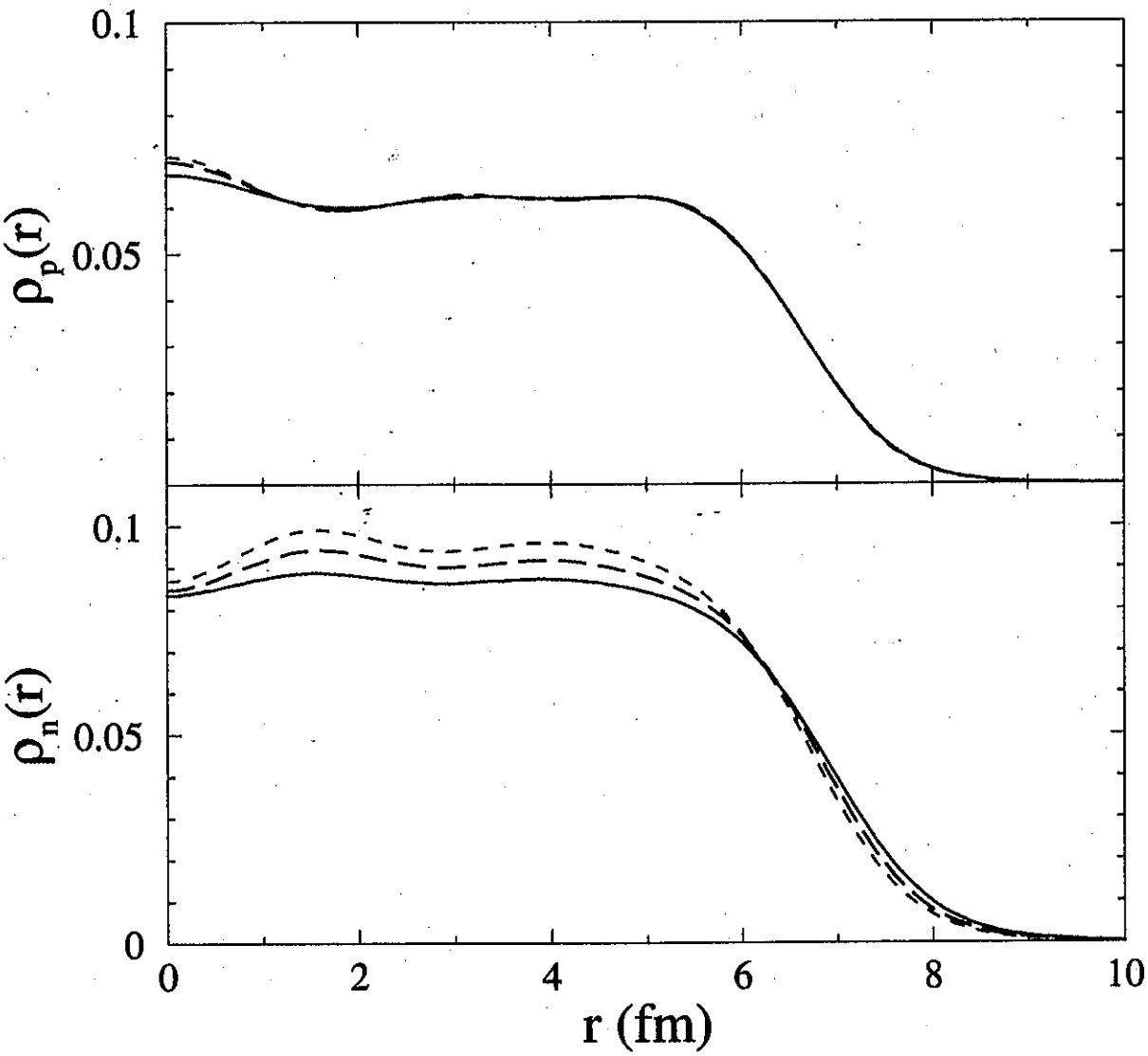

Proton (top) and neutron (bottom) densities

- - - - SHF1 model

– – – SHF2 model

—— SHF3 model

Analyses of ^{208}Pb ctnd.

^{208}Pb electron form factor

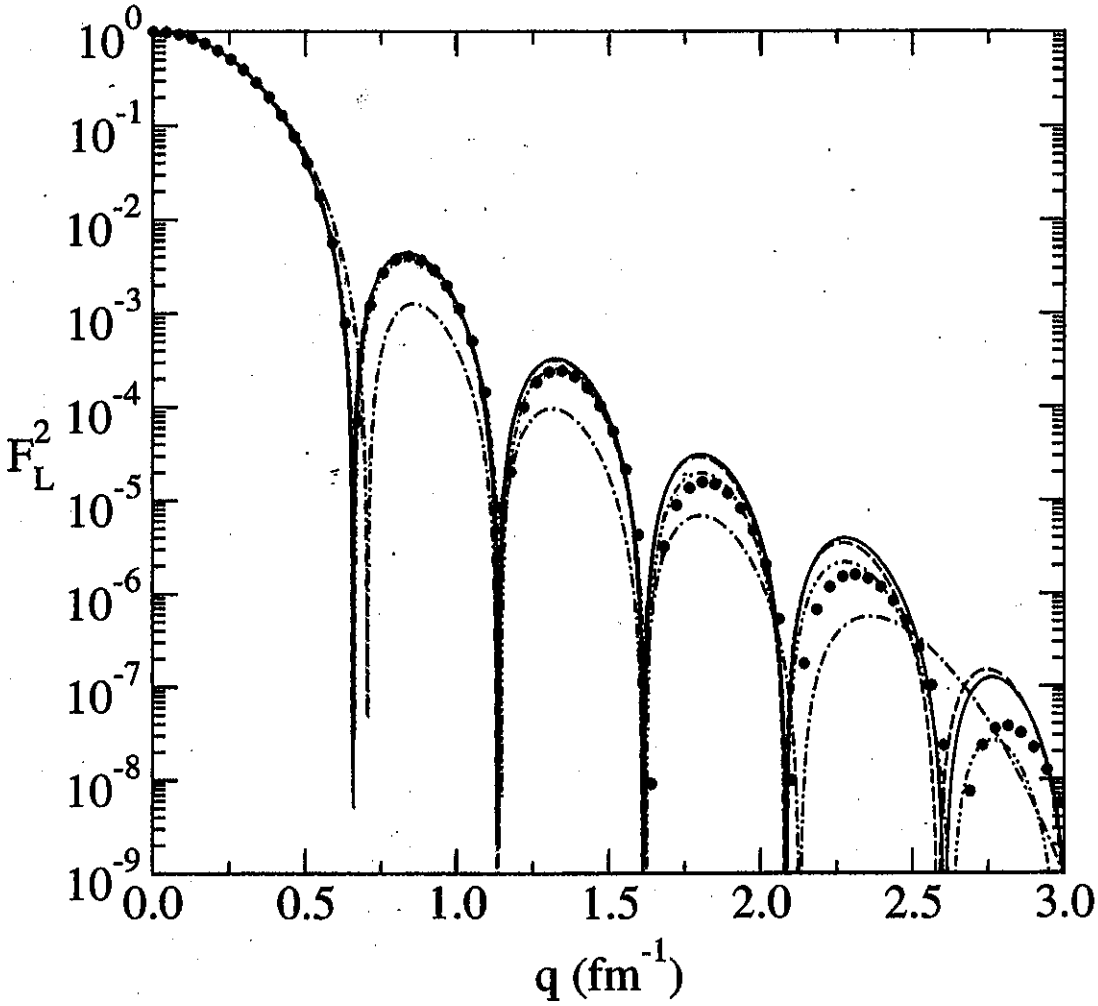

—— SHF1 model

– – – SHF2 model

– · · – SHF3 model

– · – · HO model

Analyses of ^{208}Pb ctnd.

^{208}Pb — 65 MeV scattering

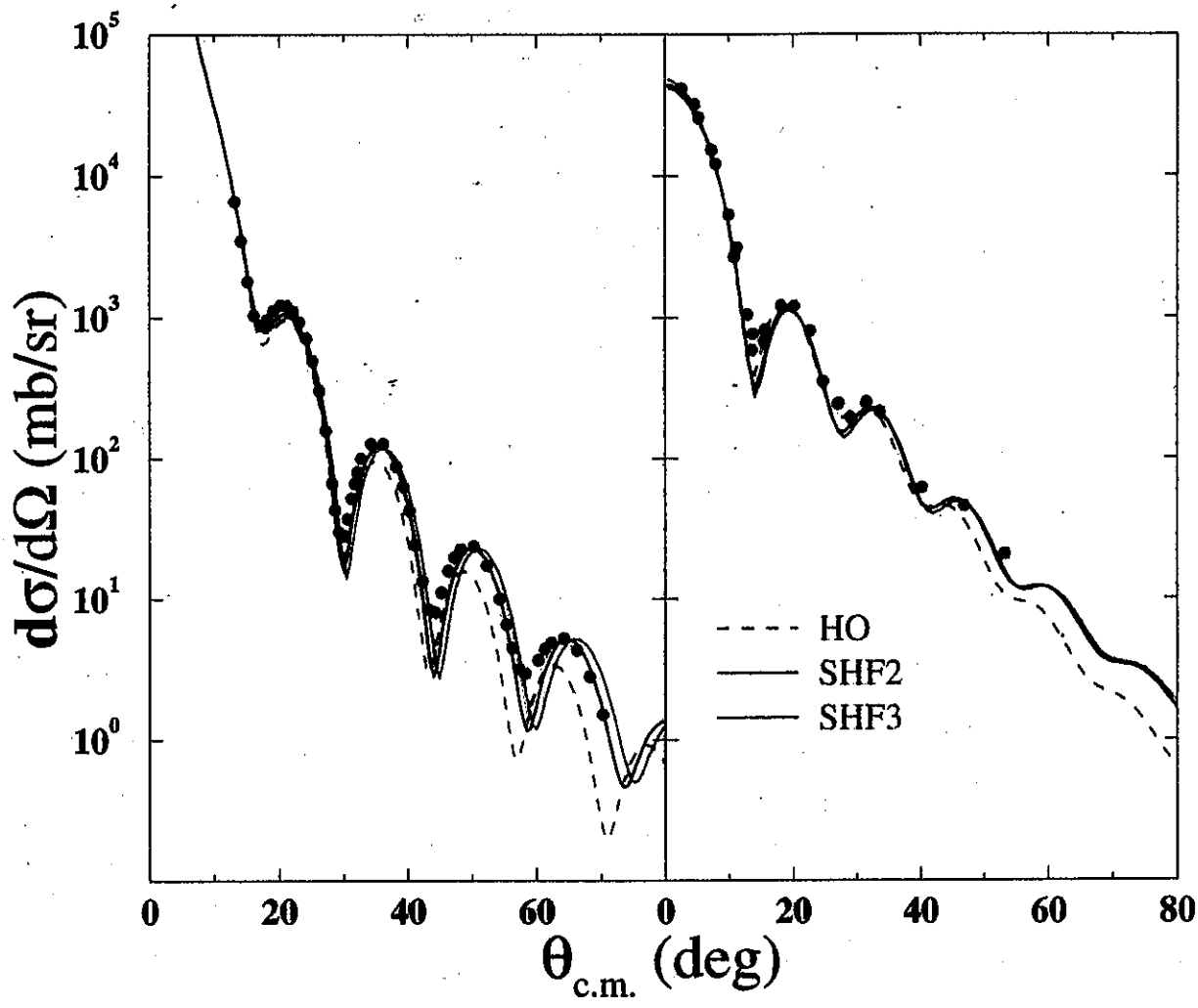

Proton (left) and neutron (right) cross sections

Analyses of ^{208}Pb ctnd.

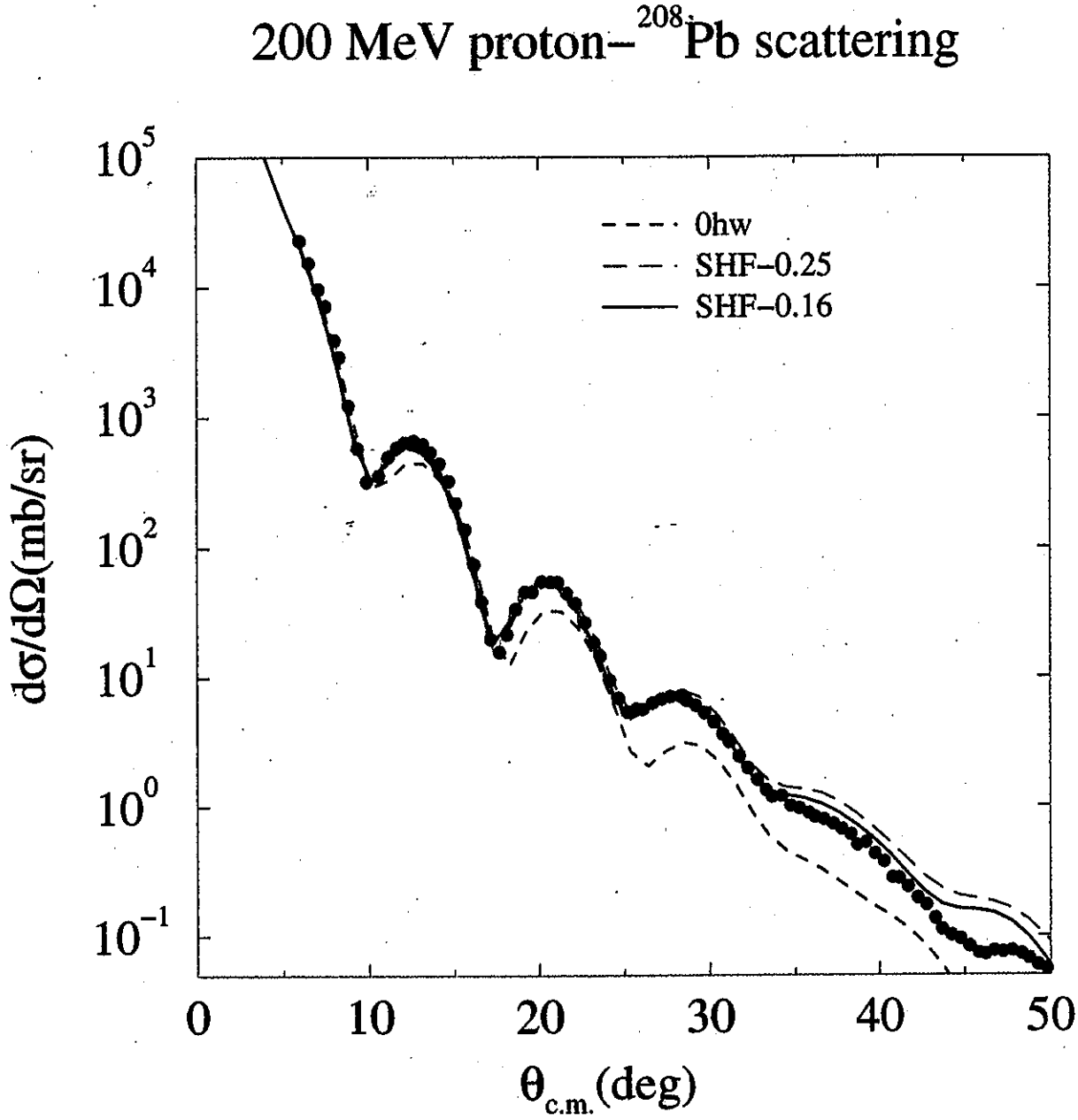

Predictions compared with cross-section data

label is skin thickness; $0\hbar\omega$ model = 0.16 fm

Analyses of ^{208}Pb ctnd.

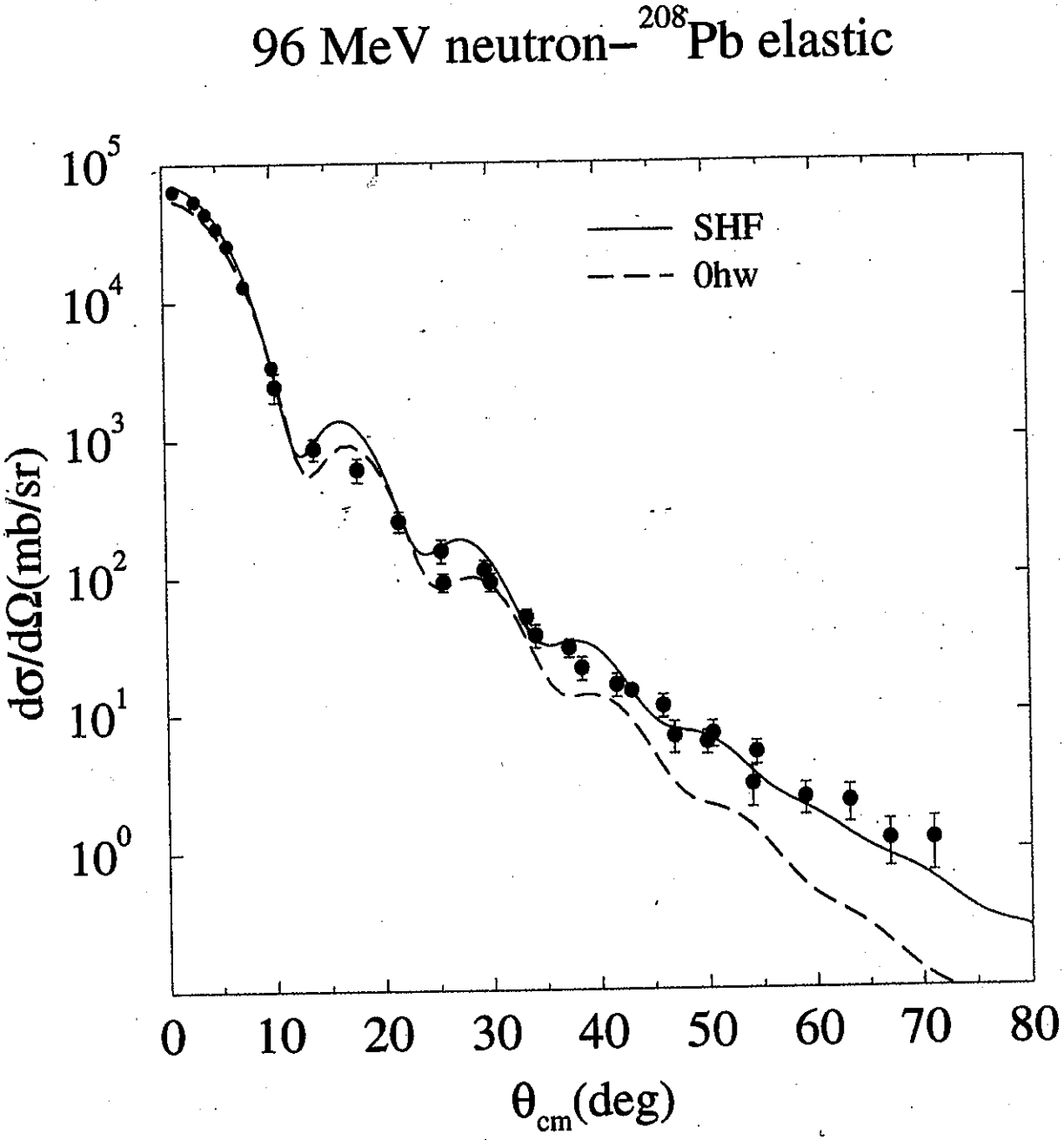

Predictions compared with cross-section data

• • — Data, (preliminary) from Upsalla

Analyses of ^{208}Pb ctnd.

RMS radii - ^{208}Pb neutron skins

Model	r_p	r_n	$(r_p - r_n)$
$0\hbar\omega$	5.45	5.61	0.16
SHF1	5.45	5.61	0.16
SHF2	5.45	5.70	0.25
SHF3	5.45	5.62	0.17

Total cross sections (barn)

Energy	SHF model	Expt.
40 MeV	4.73	4.39
65 MeV	4.67	4.63
200 MeV	2.95	2.99

Analyses of ^{208}Pb ctnd.

Integral observables

neutron scattering

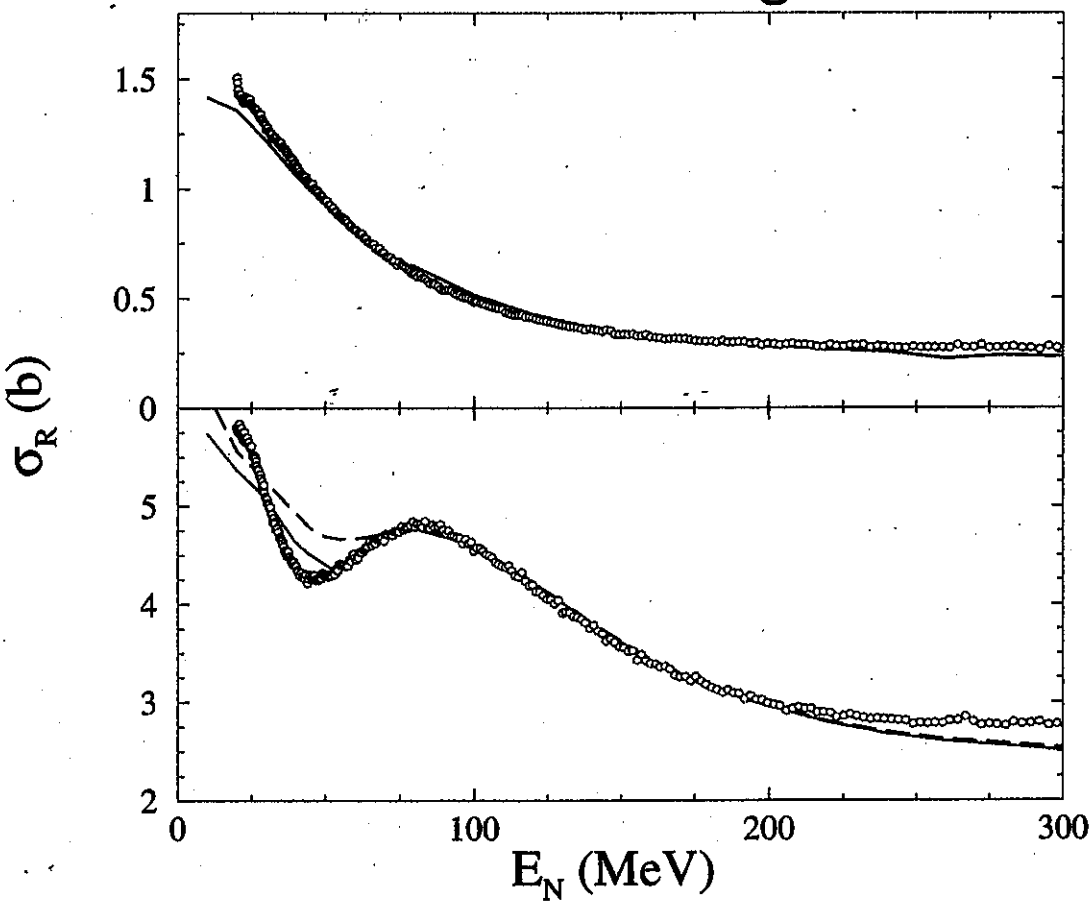

Total neutron scattering cross sections
from ^{12}C (top) and ^{208}Pb (bottom)

—— SHF3 model

– – – $0\hbar\omega$ model

Analyses of Sn isotopes

$^{100-170}$Sn densties

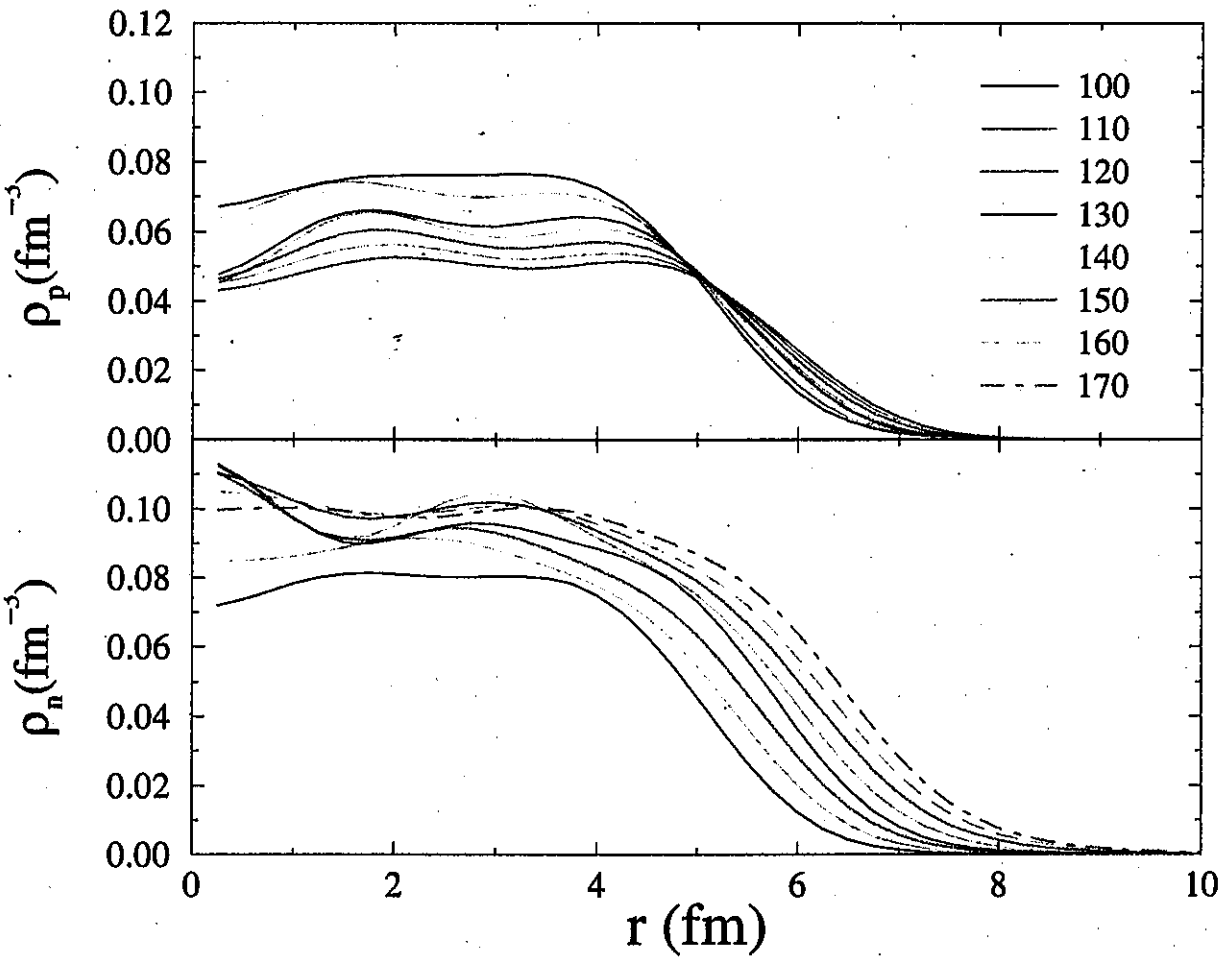

Proton (top) and neutron (bottom) densities
(using SKF model structures)

Analyses of Sn isotopes ctnd.

65 MeV proton-^{118}Sn scattering

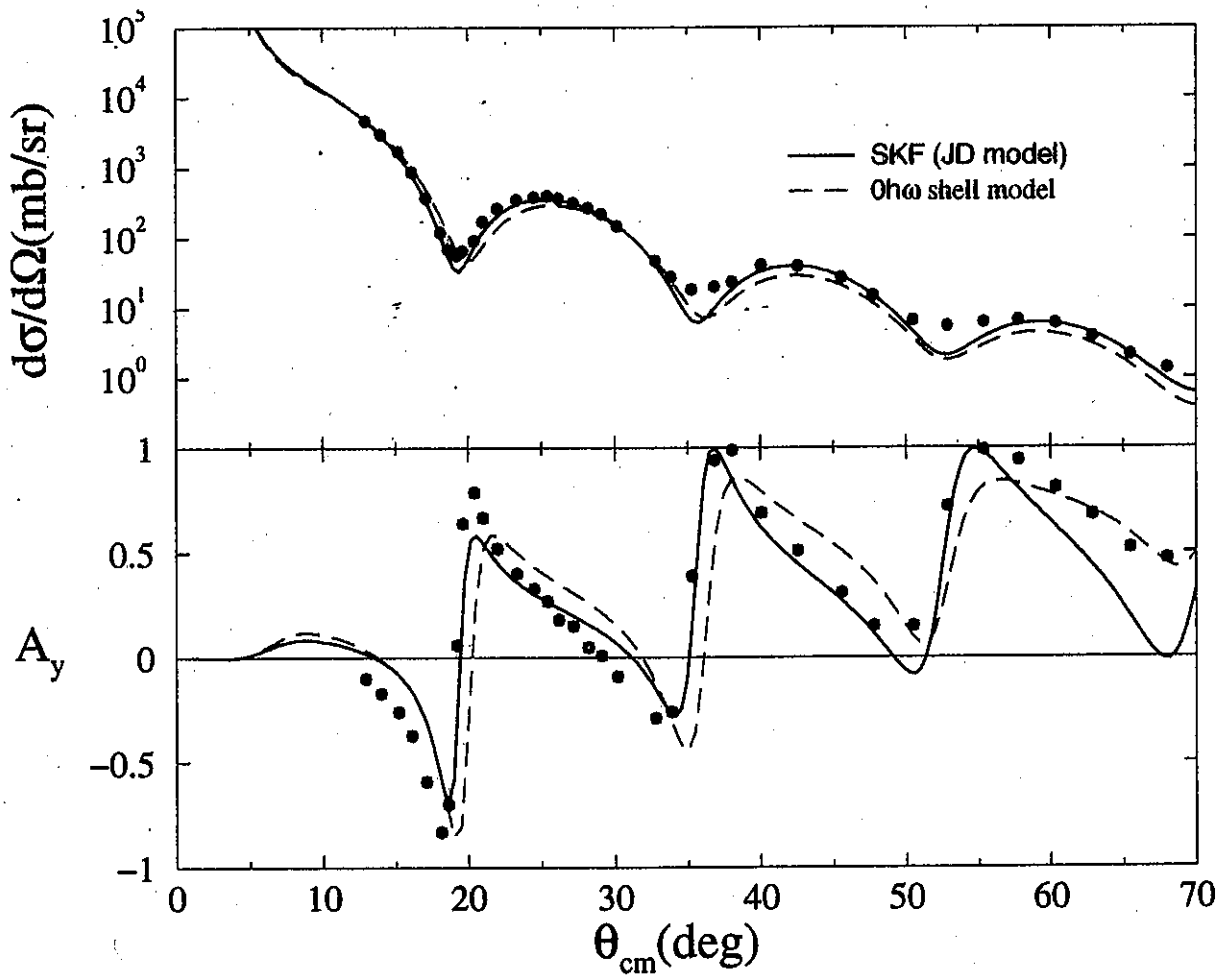

Proton scattering cross sections

Exotic nuclei

- Structure of exotic nuclei:

  (Shell model of halo/neutron skin nuclei)

  Application regime $\rho_n >$ 10-15% central value

  For larger radii — cluster models etc.

General properties of (light mass) halo nuclei

1. Usually 1 or 2 nucleons loosely bound to a core
2. Those particles (protons or neutrons) can exist some distance outside the core (makes the halo)
3. Halo particles orbit with low angular momentum (centrifugal barrier causes confinement)

   Halo states formed by orbits with $\ell \leq 1$
4. Two halo particles — the interaction between them binds the system

   Often system is "Borromean" $\Rightarrow$ clustering

RIB studies – new forms of matter
Light mass exotic nuclei

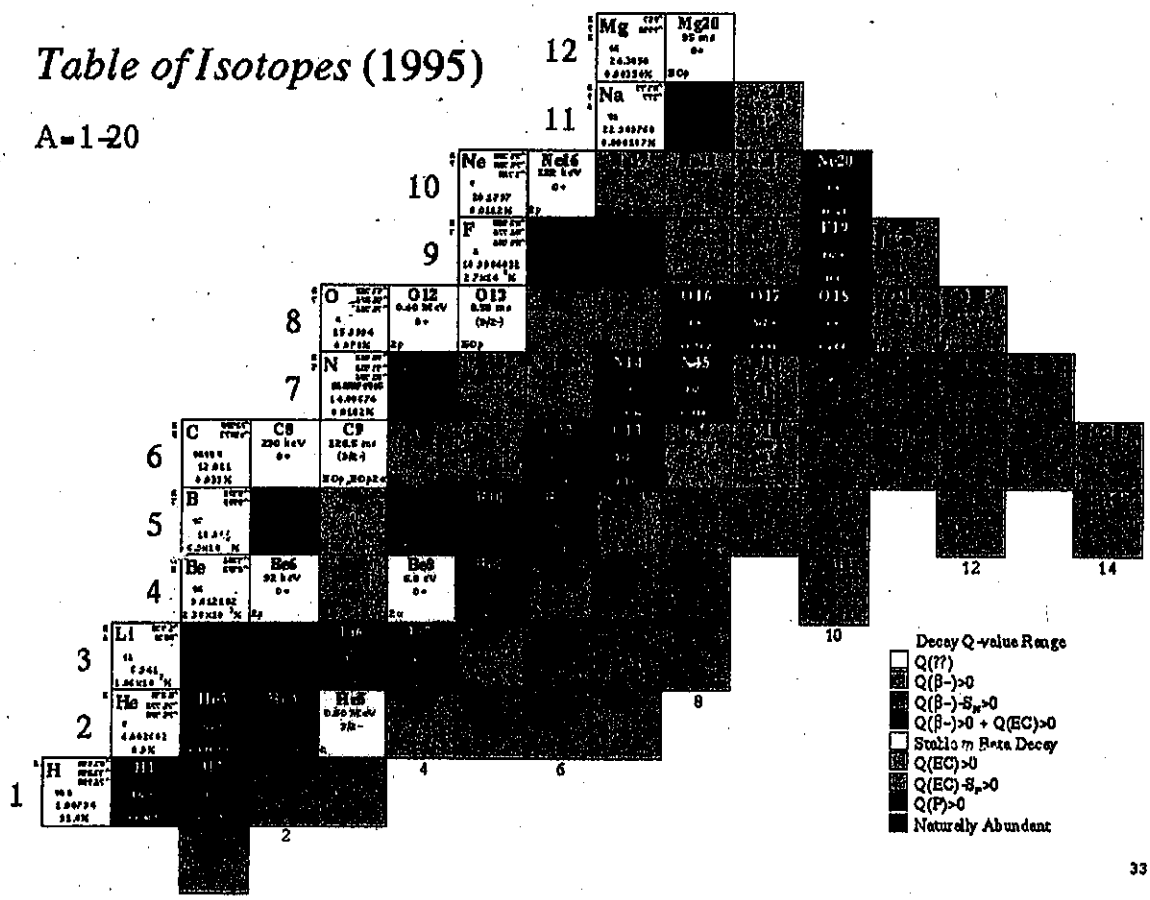

Chart of the (light) nuclides.

Exotic nuclei – structure ctnd.

- specific cases: ^{6,8}He, ^{9,11}Li

  ⋆ Ground state of ^{6}He: (in $\hbar\omega$ decomposition)

$$|\Psi(^{6}\mathrm{He})\rangle =$$

$$77.95\%\,|0\hbar\omega\rangle + 11.01\%\,|2\hbar\omega\rangle + 11.04\%\,|4\hbar\omega\rangle$$

⋆ Ground state of ^{11}Li: (in $\hbar\omega$ decomposition)

$$|\Psi(^{11}\mathrm{Li})\rangle = 62.71\%\,|0\hbar\omega\rangle + 37.29\%\,|2\hbar\omega\rangle$$

Its $2\hbar\omega$ components

$(0d)^2$ configurations — 19.62%

$(1s)^2$ configurations — 10.02%

To make the 'halo' conditions:–

Use Woods Saxon functions that fit electron scattering form factors of ^{6}Li; ^{9}Be

(but see later with Local Scale Transforms)

^{6,8}He – $0p$ states 2 MeV; higher 0.5 MeV

^{9,11}Li – $0p_{\frac{1}{2}}$ + higher states – 0.5 MeV

Exotic nuclei – structure ctnd.

Spectra of ^{6,8}He and ^{9,11}Li

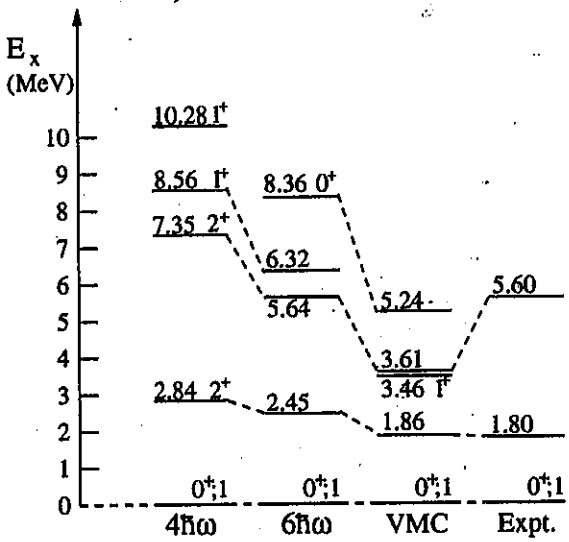

^{6}He spectrum

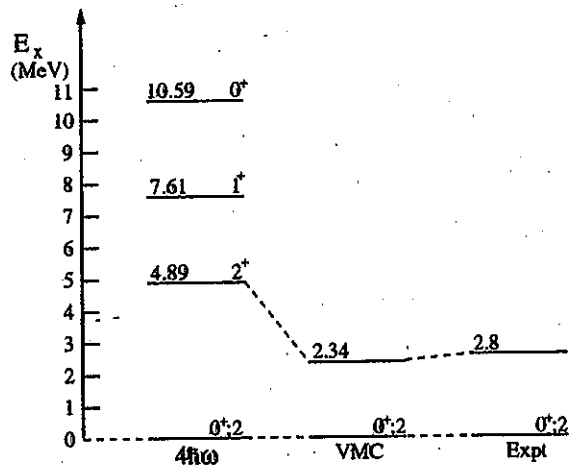

^{8}He spectrum

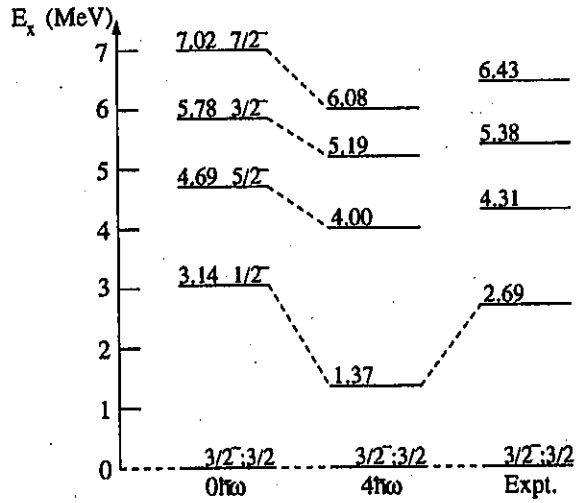

^{9}Li spectrum

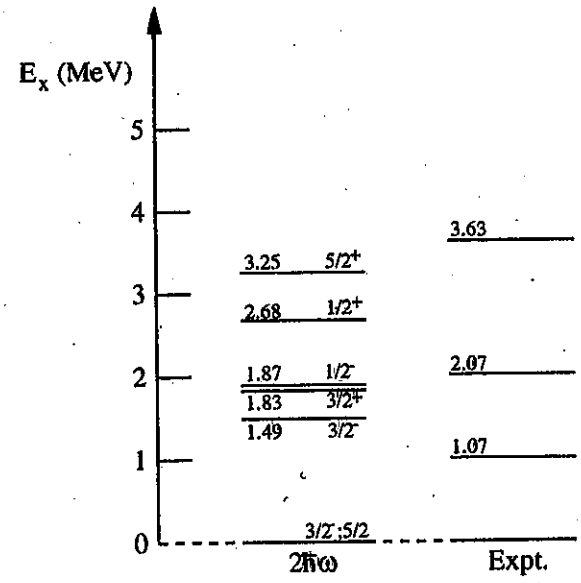

^{11}Li spectrum

Exotic nuclei – structure ctnd.

Nucleon occupancies in ^{11}Li ground state

Orbit	Protons	Neutrons	Total
$0s_{\frac{1}{2}}$	1.9874	1.9988	3.9862
$0p_{\frac{3}{2}}$	0.9352	3.7738	4.7090
$0p_{\frac{1}{2}}$	0.0343	1.5446	1.5789
$0d_{\frac{5}{2}}$	0.0162	0.3568	0.3730
$0d_{\frac{3}{2}}$	0.0196	0.0617	0.0813
$1s_{\frac{1}{2}}$	0.0057	0.2597	0.2654
$0f_{\frac{7}{2}}$	0.0000	0.0001	0.0001
$0f_{\frac{5}{2}}$	0.0000	0.0002	0.0002
$1p_{\frac{3}{2}}$	0.0016	0.0031	0.0046
$1p_{\frac{1}{2}}$	0.0000	0.0012	0.0012

Exotic nuclei – structure ctnd.

- **Shell model densities:** ^{6,8}He, ^{9,11}Li

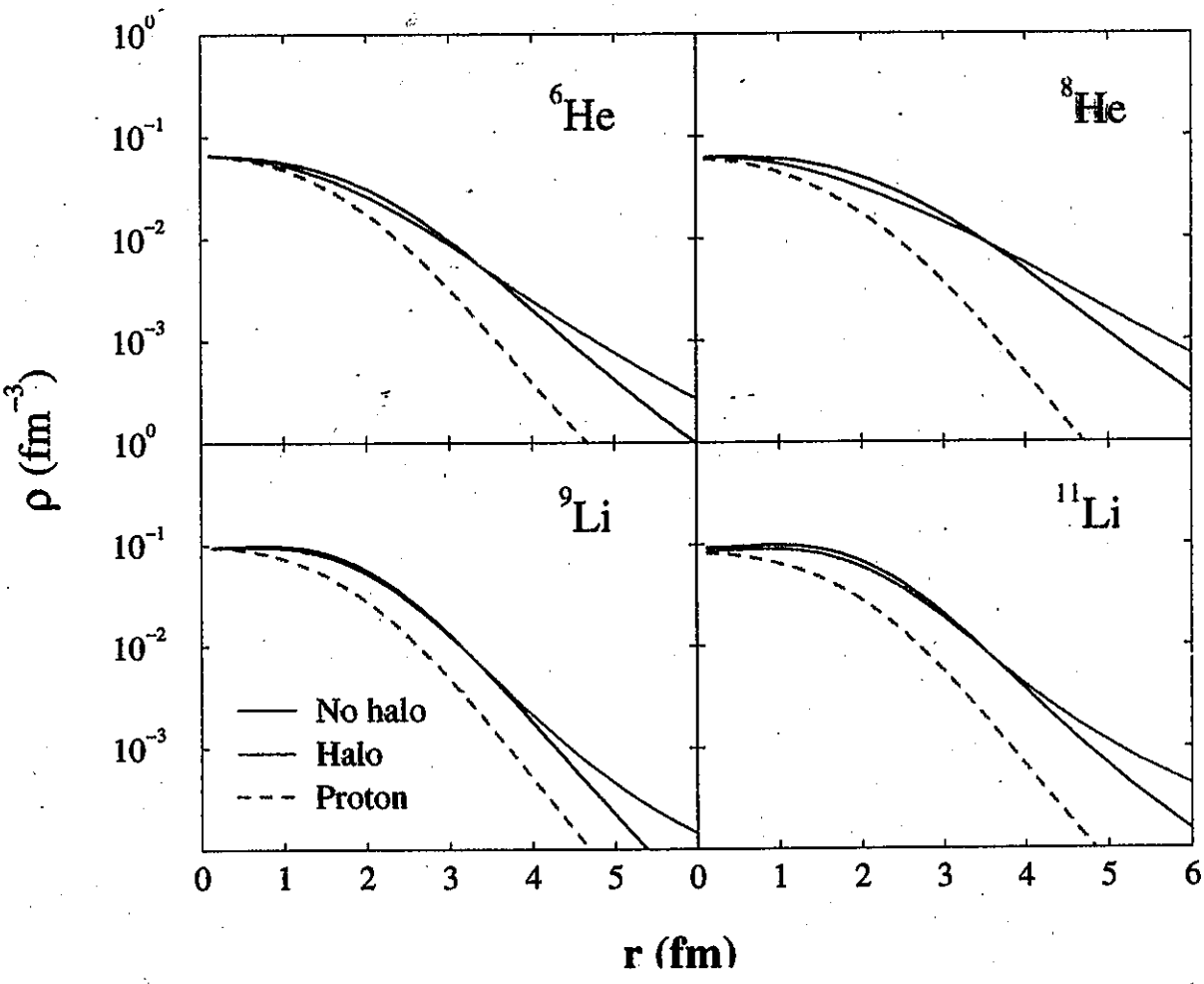

Note that the creation of a halo – extended neutron distribution – comes at the expense of the neutron density at, and inside of, the nuclear radius

Scattering of exotic nuclei

^{6,8}He, ^{9,11}Li scattering from Hydrogen

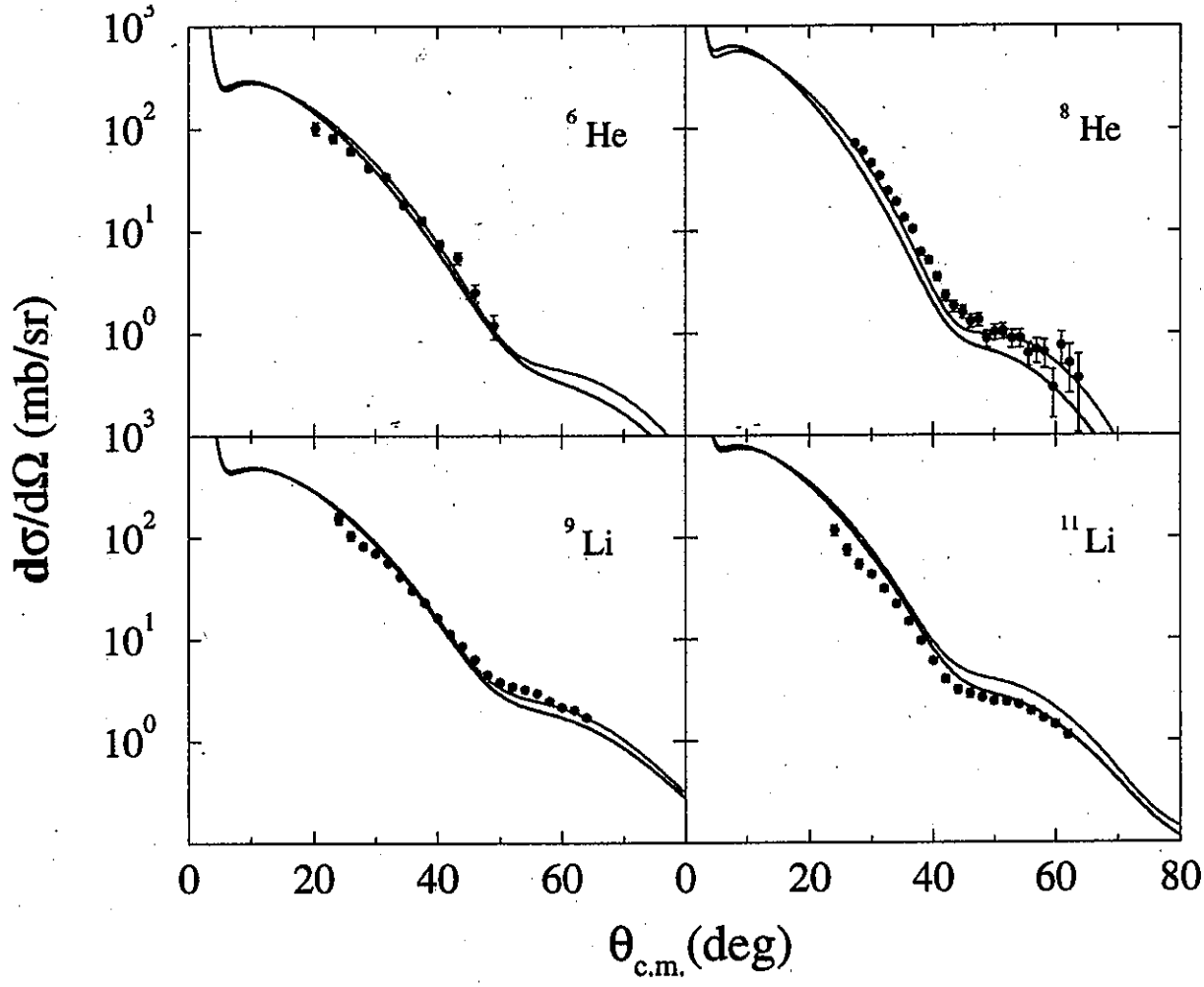

Elastic scattering predictions, E = 60-72A MeV

— No halo

— Halo

Scattering of exotic nuclei ctnd.

25A MeV ^{6}He scattering from Hydrogen

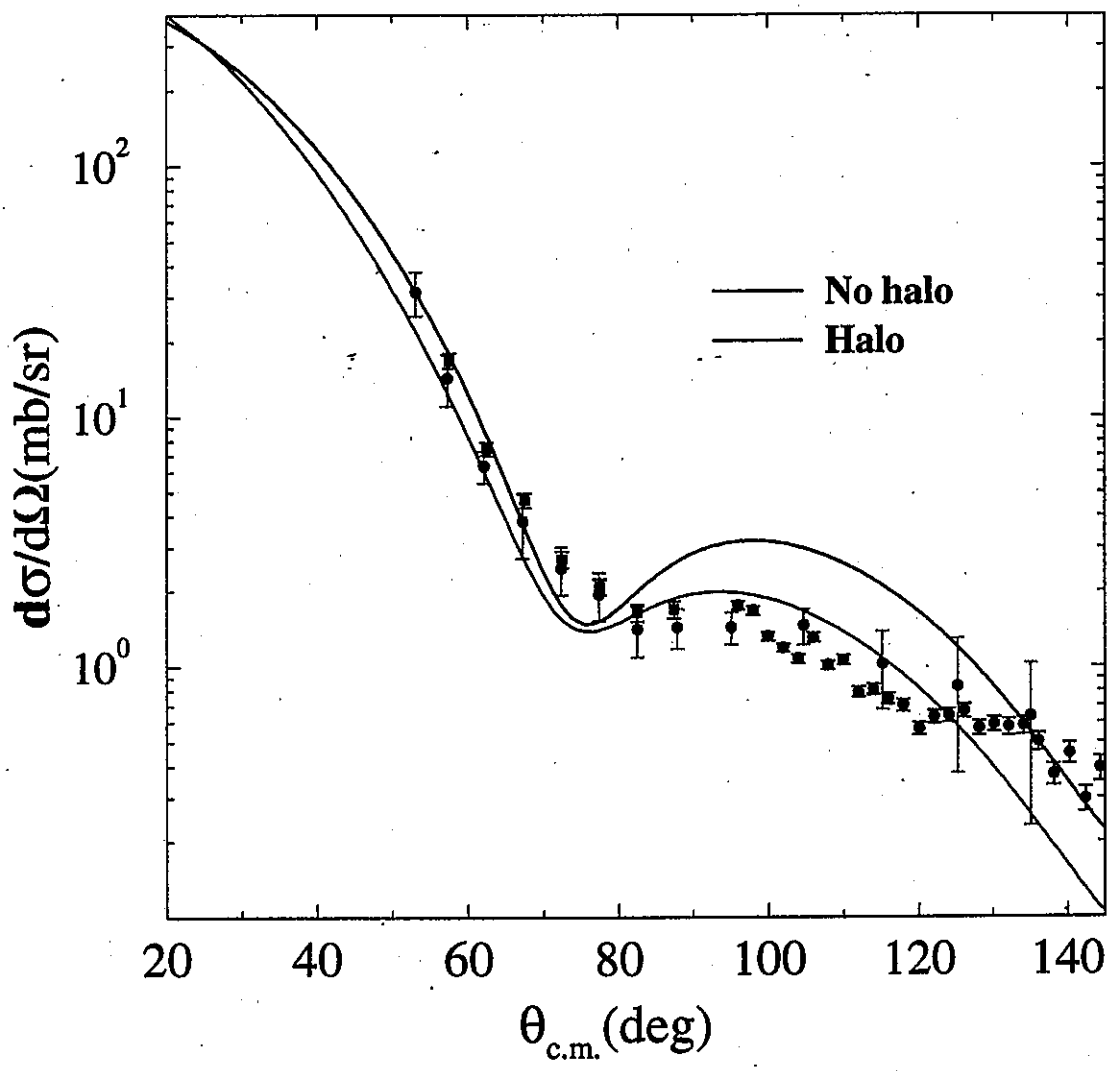

Predictions compared with data

Scattering of exotic nuclei
^{6}He scattering from Hydrogen

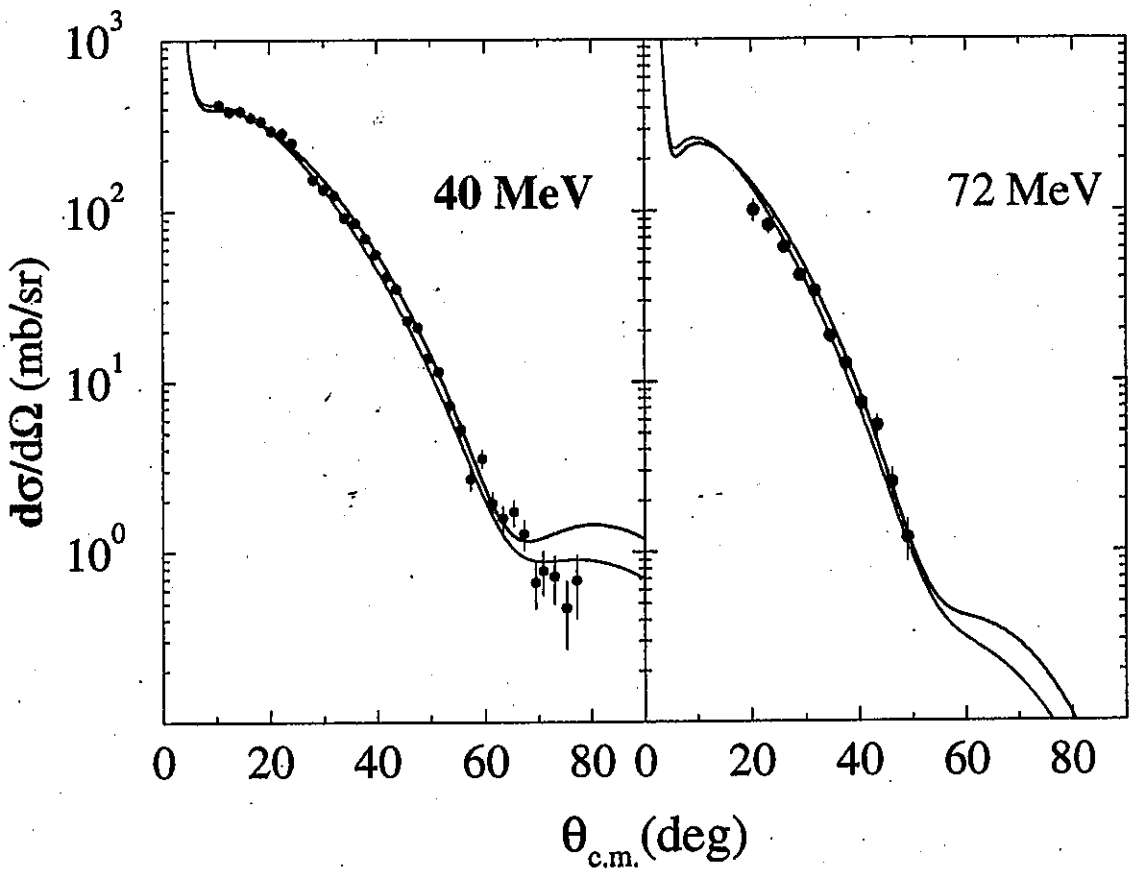

Predictions compared with data

40.9A MeV ^{6}He-p reaction cross section:–

$\sigma^{expt.} = 415 \pm 5\%$ mb

$\sigma^{calc} \sim 350$ No halo cases

$\sigma^{calc} = 406 - 440$ Halo cases

$\{4\hbar\omega - 8\hbar\omega\}$

Scattering of exotic nuclei
^{6}He scattering from hydrogen

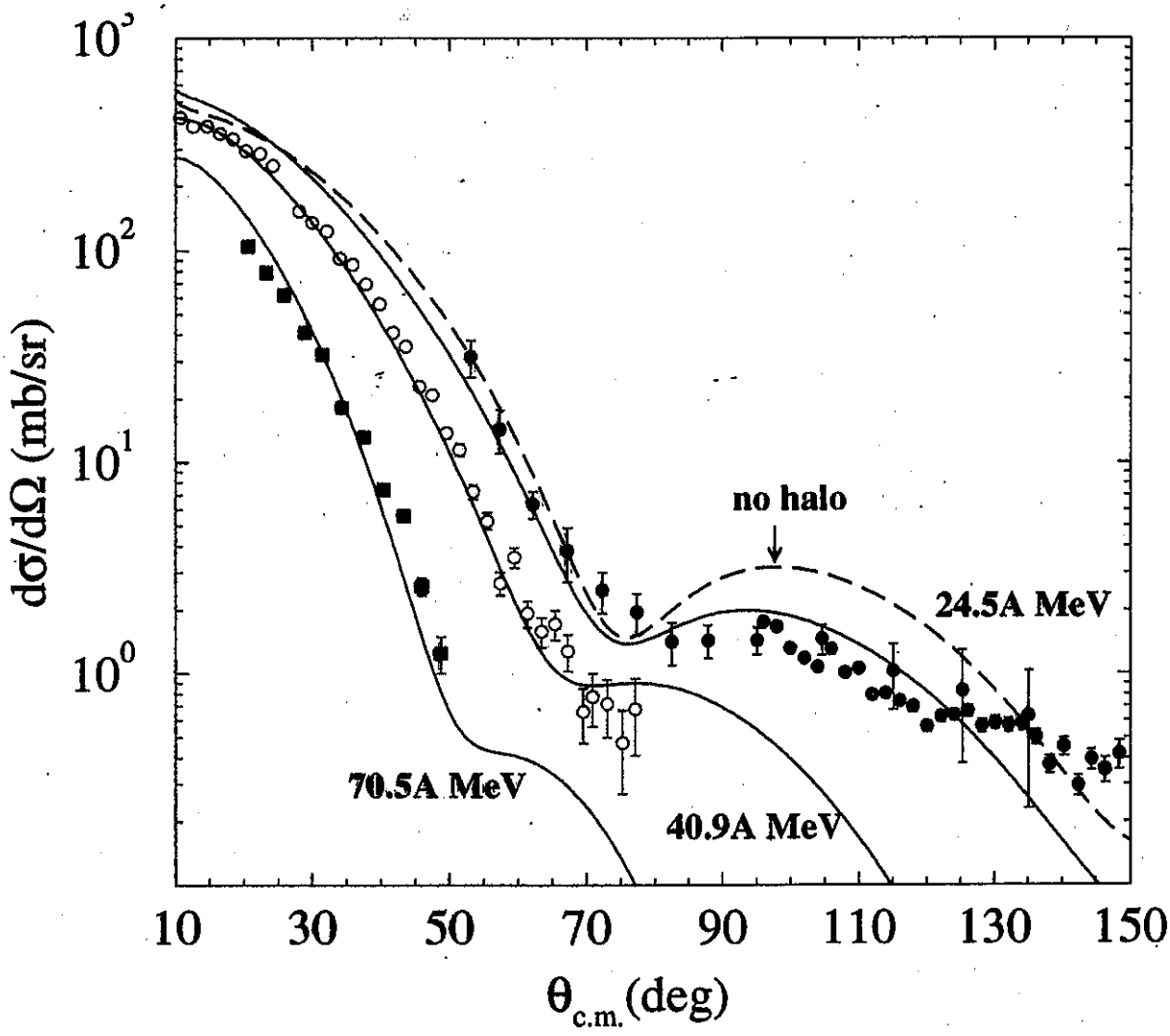

Predictions if ^{6}He has a neutron halo

Local Scale Transforms (LST)

• Purpose:

To vary the long range properties of HO states (usual SM wave functions) to have exponential long range forms and which are

(a) consistent with specific single nucleon B.E.s

(b) make a minimal change of structure in nucleus

• Methodology:

Consider a starting wave function, $u(r)$, where

$$\int_0^\infty u^2(r) r^2 \, dr = 1$$

Under LST with $r \to f(r)$

$$u(r) \longrightarrow v(r) = \frac{1}{r} f(r) \sqrt{\frac{df(r)}{dr}} u[f(r)]$$

H. O. character changed by

$$e^{-\frac{1}{2b^2} r^2} \longrightarrow e^{-\sqrt{\frac{2\mu\epsilon}{\hbar^2}} r}$$

Local Scale Transforms (LST) ctnd.

- LST properties: With $r \to 0,\ f(r) \to r$

$$r \to \infty: \ f(r) \to \gamma\sqrt{r} \quad \text{so } \gamma = b\left[\frac{8\mu\epsilon}{\hbar^2}\right]^{\frac{1}{4}}$$

- Useful form: Harmonic mean (rank m)

$$f(r) = \left[\left(\frac{1}{r}\right)^m + \left(\frac{1}{\gamma\sqrt{r}}\right)^m\right]^{-\frac{1}{m}}$$

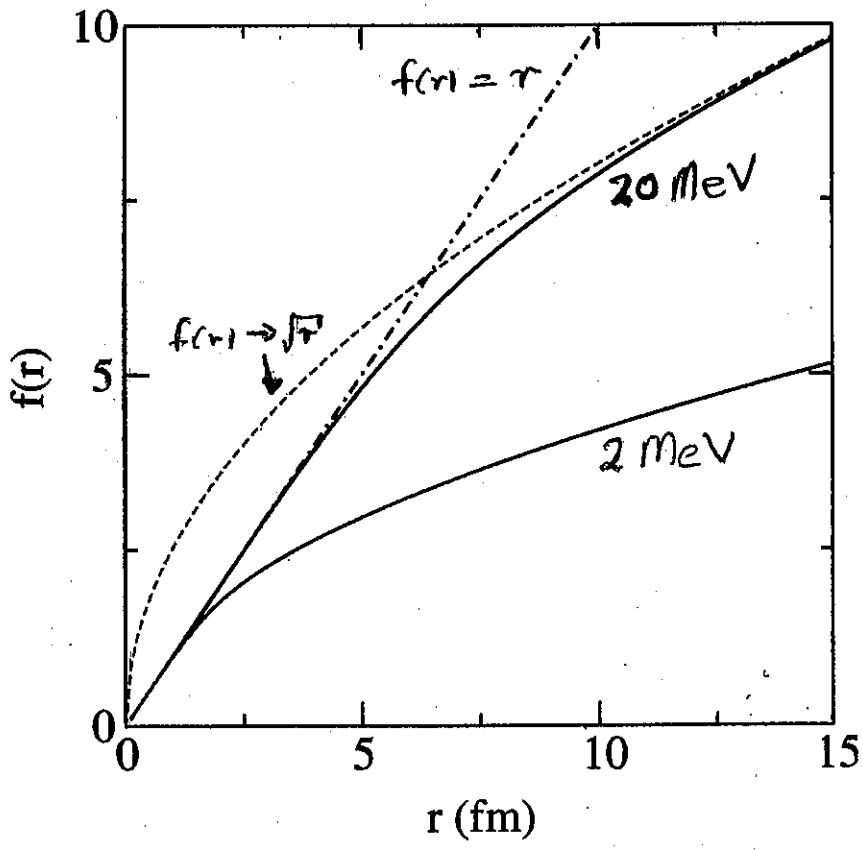

Local Scale Transforms (LST) ctnd.

^{6}He – $0p$ functions

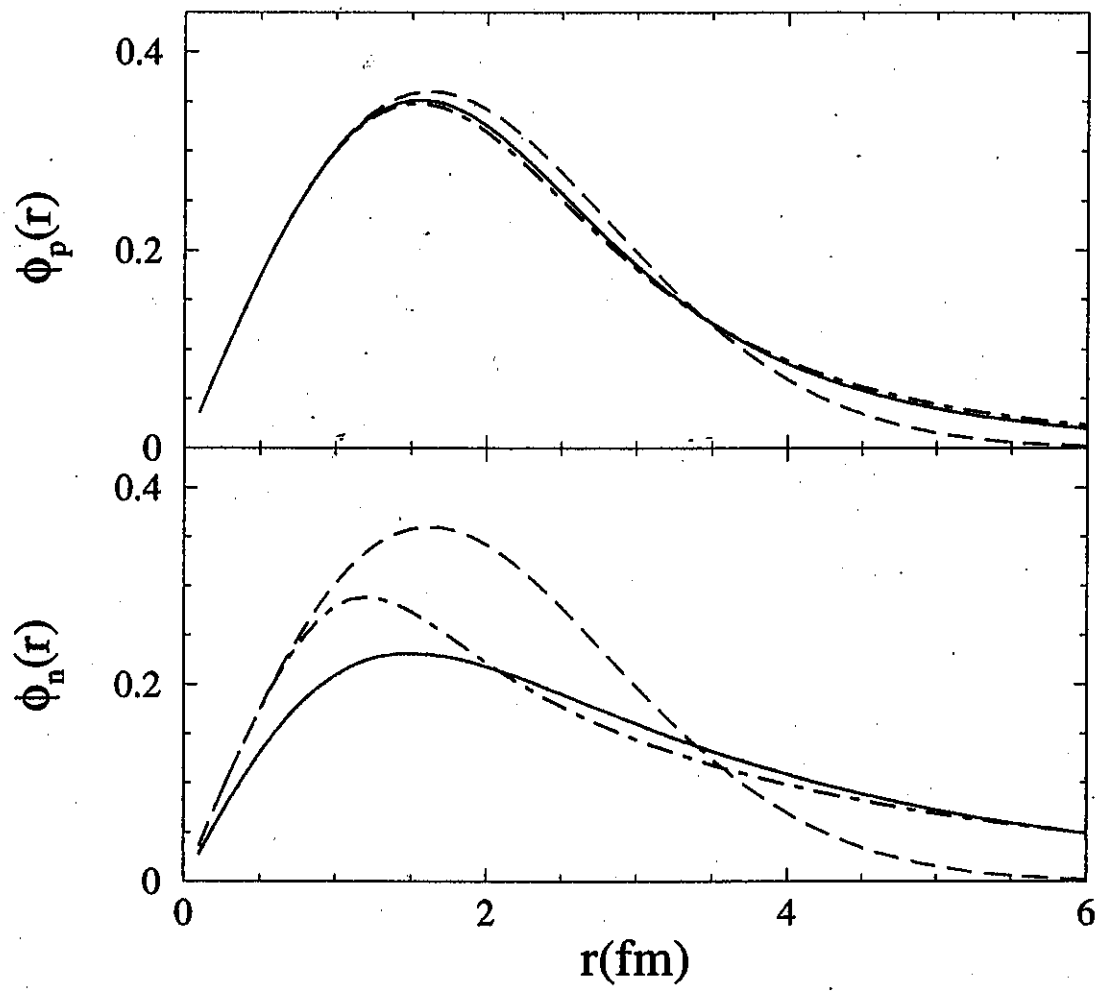

Proton (top) and neutron (bottom) functions

– · – LST ($j = \frac{3}{2}$) B.E.:– 7.76 (p); 2.5 (n)

—— LST ($j = \frac{1}{2}$) B.E.:– 6.53 (p); 1.8 (n)

– – – HO functions

Local Scale Transforms (LST) ctnd.

^{6}He densities

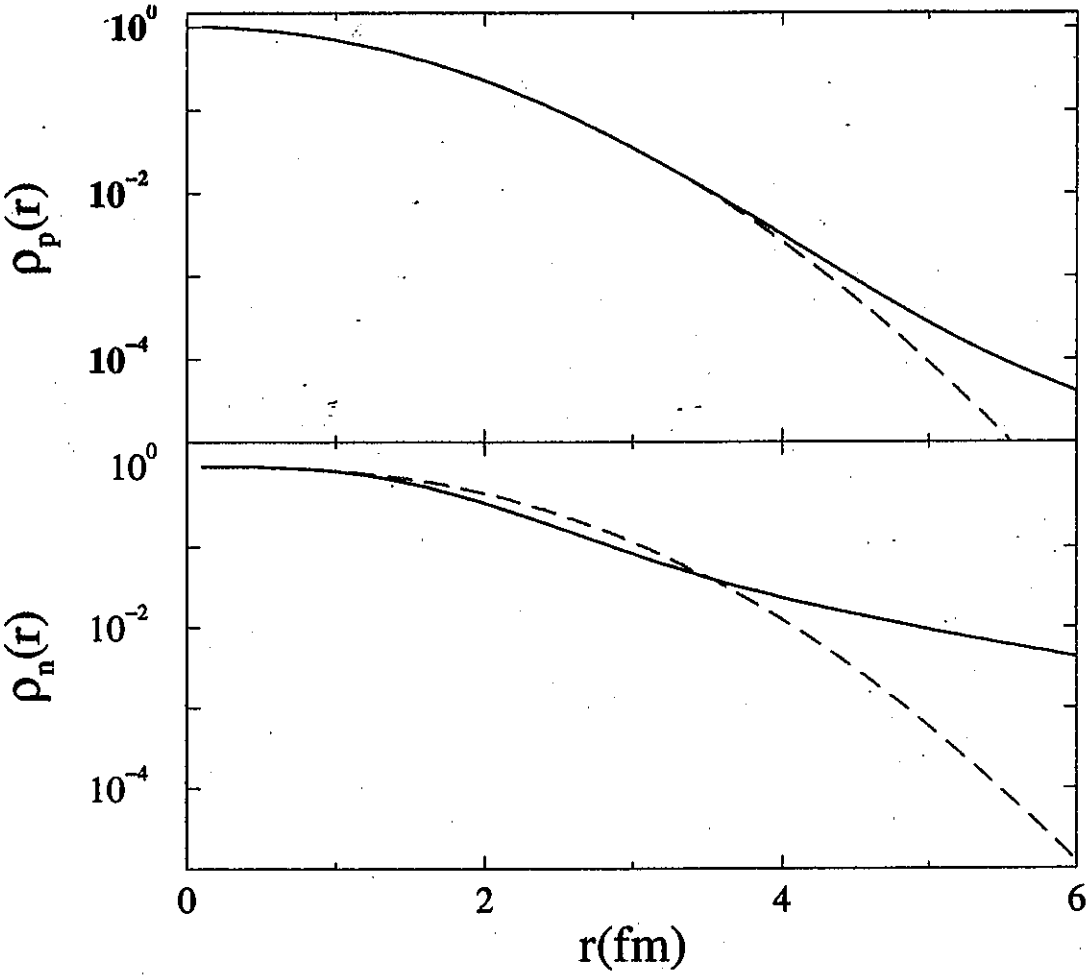

Proton (top) and neutron (bottom) densities

—— LST defined

– – – HO functions

Local Scale Transforms (LST) ctnd.

^{6}He-p scattering

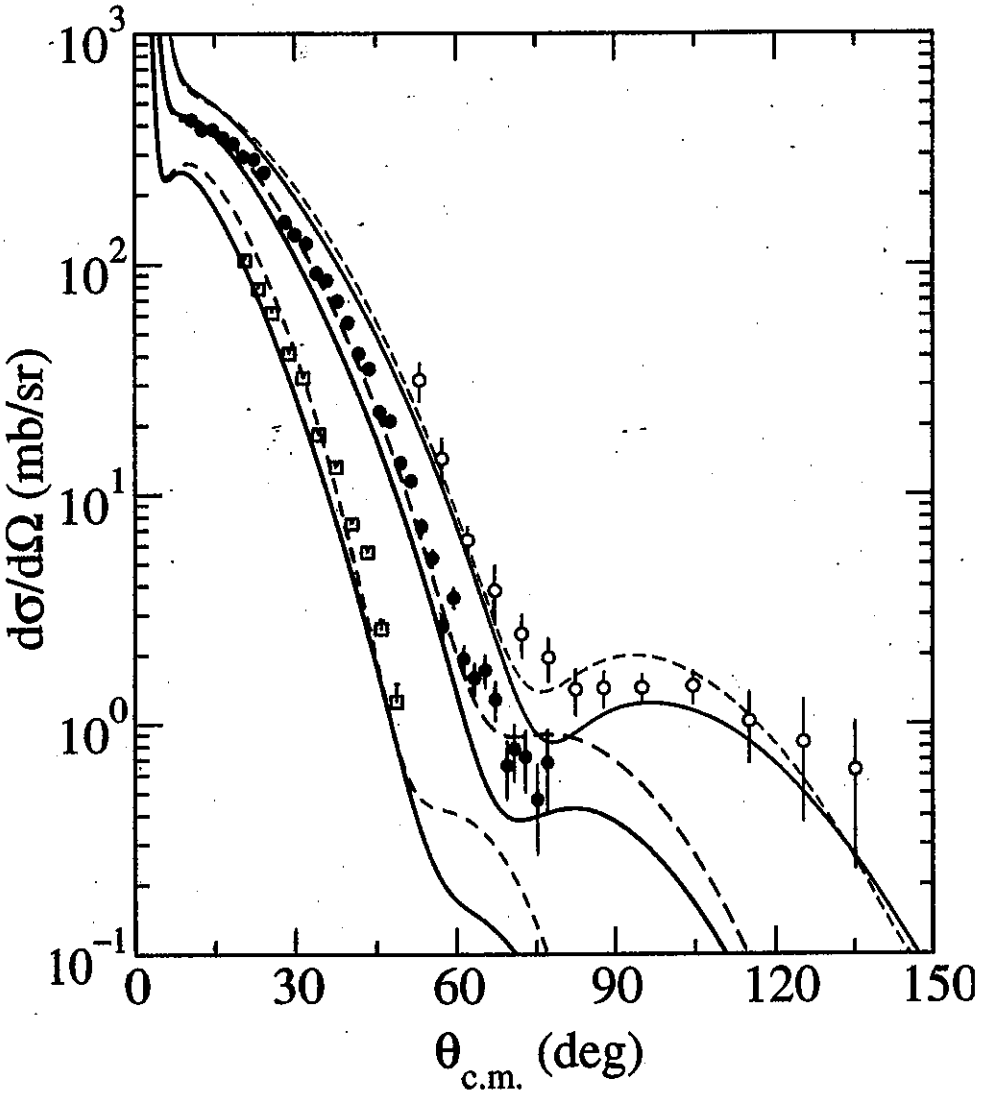

Predictions for halo structure models
24.5A, 40.9A and 70.5A MeV elastic

—— LST defined ; – – – WS functions

Integral observables

The S matrix, defined in terms of phase shifts:

$$S_l^{\pm} \equiv S_l^{\pm}(k) = e^{2i\delta_l^{\pm}(k)} = \eta_l^{\pm}(k) e^{2i\Re\left[\delta_l^{\pm}(k)\right]}$$

where

$$\eta_l^{\pm} \equiv \eta_l^{\pm}(k) = \left|S_l^{\pm}(k)\right| = e^{-2\Im\left[\delta_l^{\pm}(k)\right]} .$$

With $E \propto k^2$

$$\sigma_{el}(E) = \frac{\pi}{k^2} \sum_{l=0}^{\infty} \left\{ (l+1) \left|S_l^{+} - 1\right|^2 + l \left|S_l^{-} - 1\right|^2 \right\}$$

$$\sigma_R(E) = \frac{\pi}{k^2} \sum_{l=0}^{\infty} \left\{ (l+1) \left[1 - \left(\eta_l^{+}\right)^2\right] + l \left[1 - \left(\eta_l^{-}\right)^2\right] \right\}$$

$$= \frac{\pi}{k^2} \sum_{l=0}^{\infty} \sigma_R^{(l)}(E) \Longrightarrow \frac{\pi}{k^2} \int_0^{\infty} \sigma_R(E, \lambda)\, d\lambda$$

from which

$$\sigma_{\text{TOT}}(E) = \sigma_{el}(E) + \sigma_R(E)$$

Integral observables ctnd.

Reaction cross sections

100 MeV proton scattering

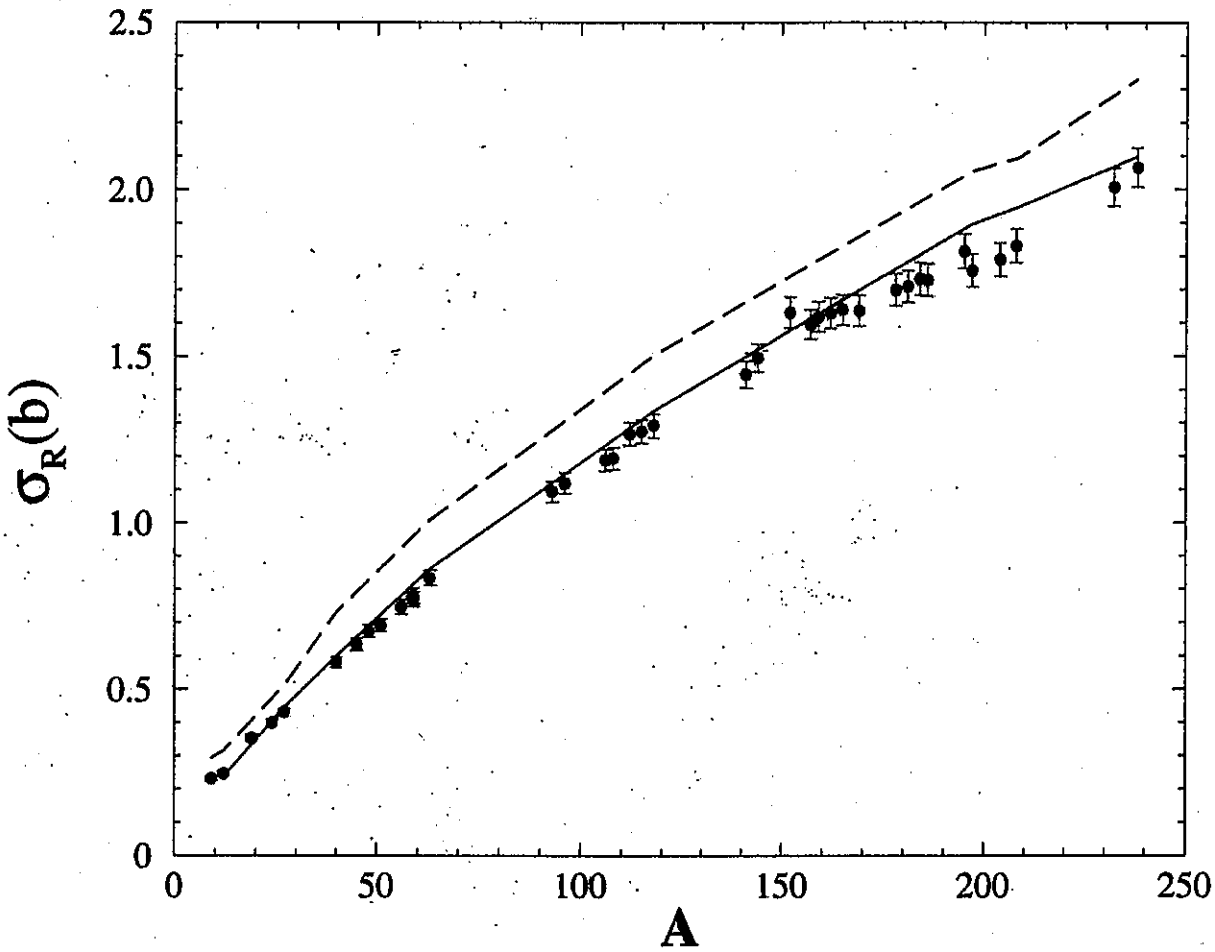

Total reaction cross section vs mass

—— g-folding

– – – t-folding

Integral observables ctnd.

Reaction cross sections

protons scattering from ^{40}Ca

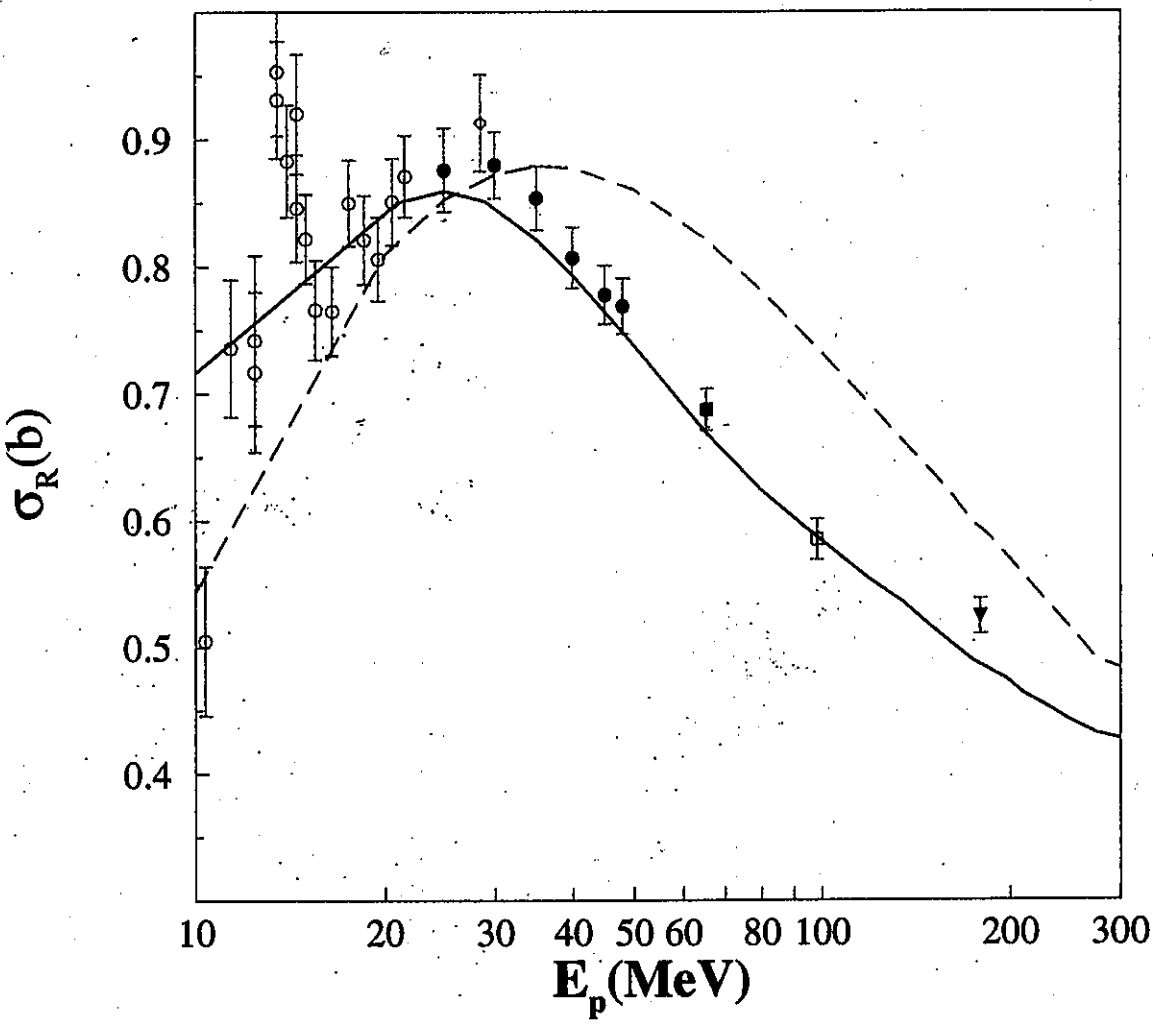

Total reaction cross section vs energy.

—— g-folding

- - - t-folding

Integral observables ctnd.

Matching energies

(equal reaction cross sections)

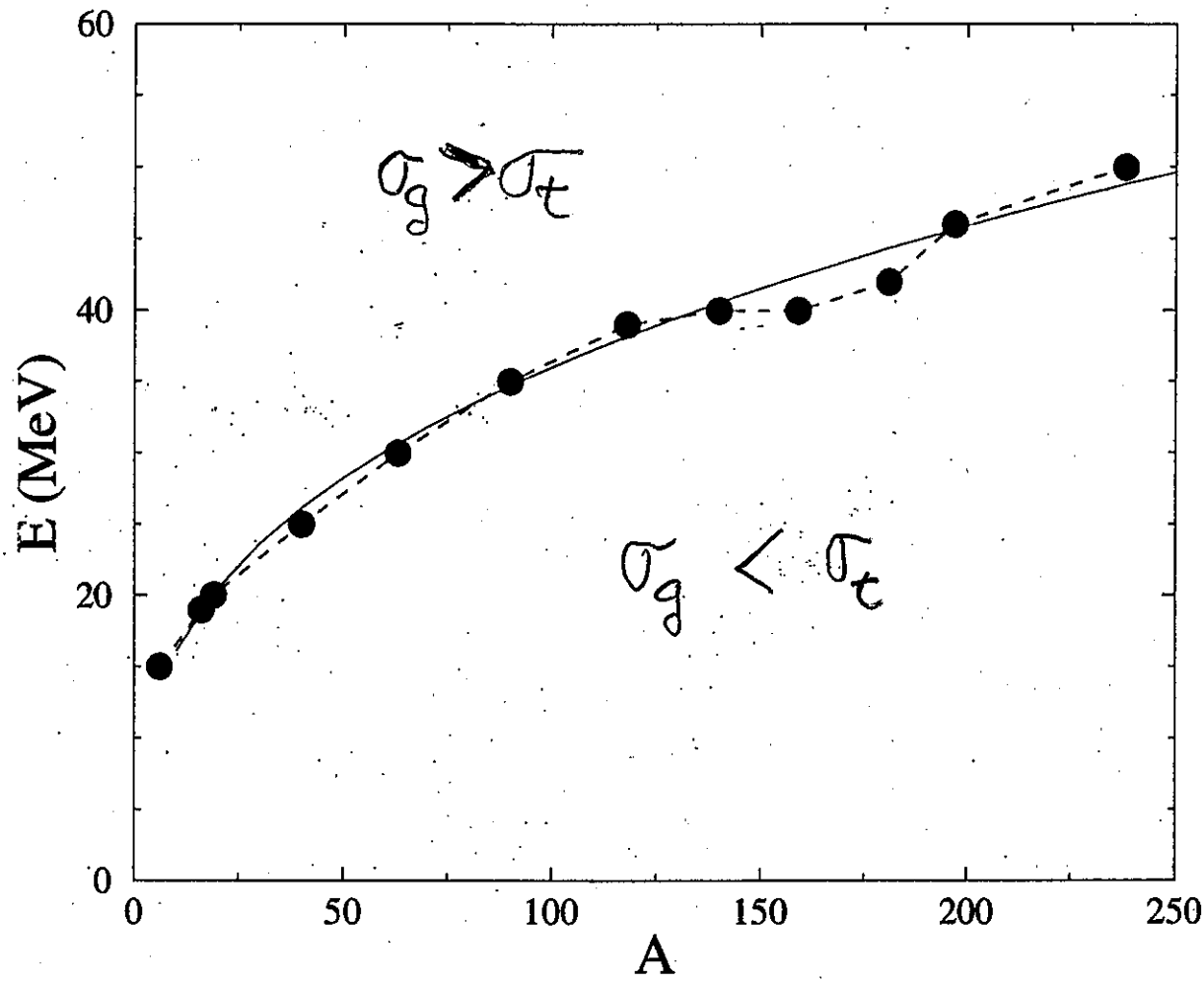

Energies where t- and g folding results are equal

—— $E = (280A)^{0.35}$

Integral observables ctnd.

Total neutron scattering cross sections

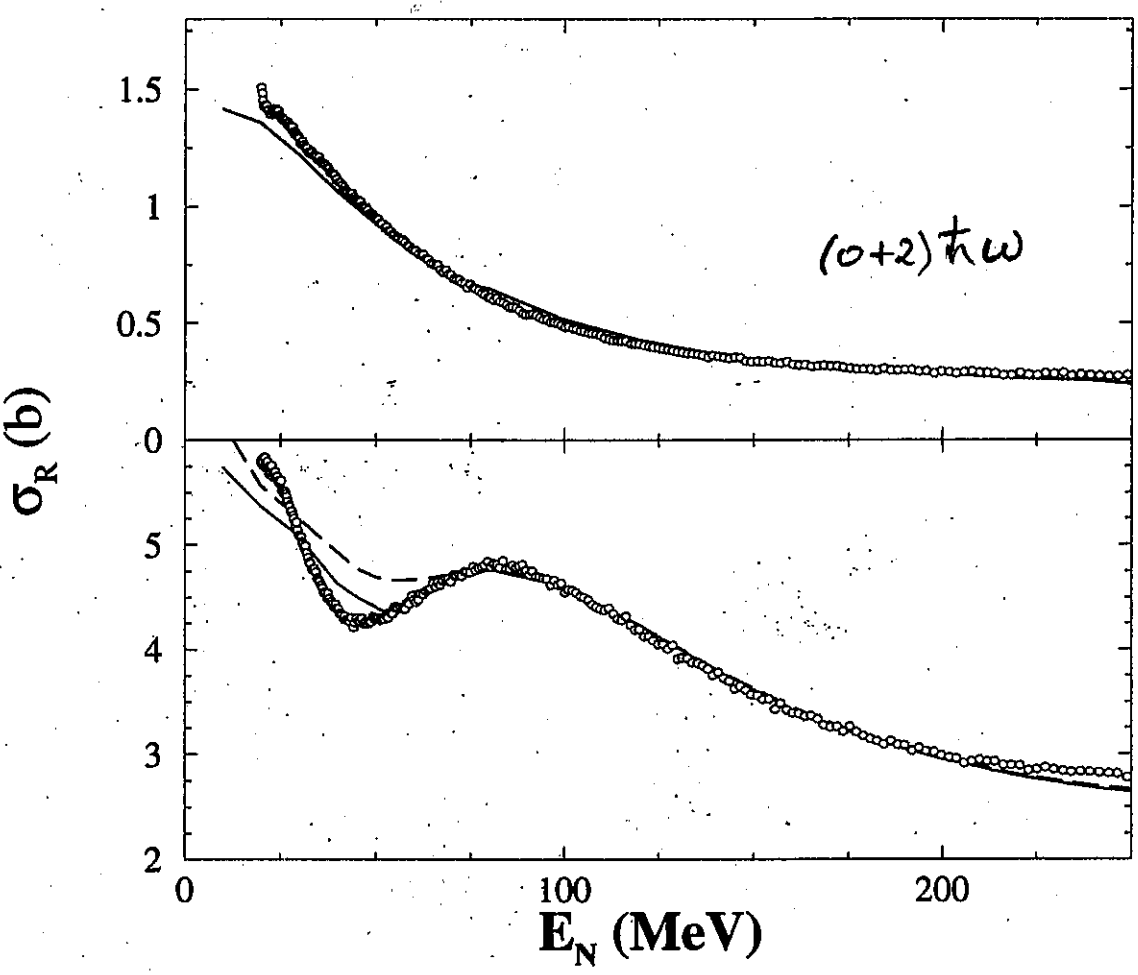

^{12}C (top) and ^{208}Pb (bottom)

—— SHF1 model

– – – $0\hbar\omega$ model

Integral observables ctnd.

partial wave elements

$$\sigma_R(E) = \frac{\pi}{k^2} \sum_{l=0}^{\infty} \sigma_R^{(l)}(E)$$

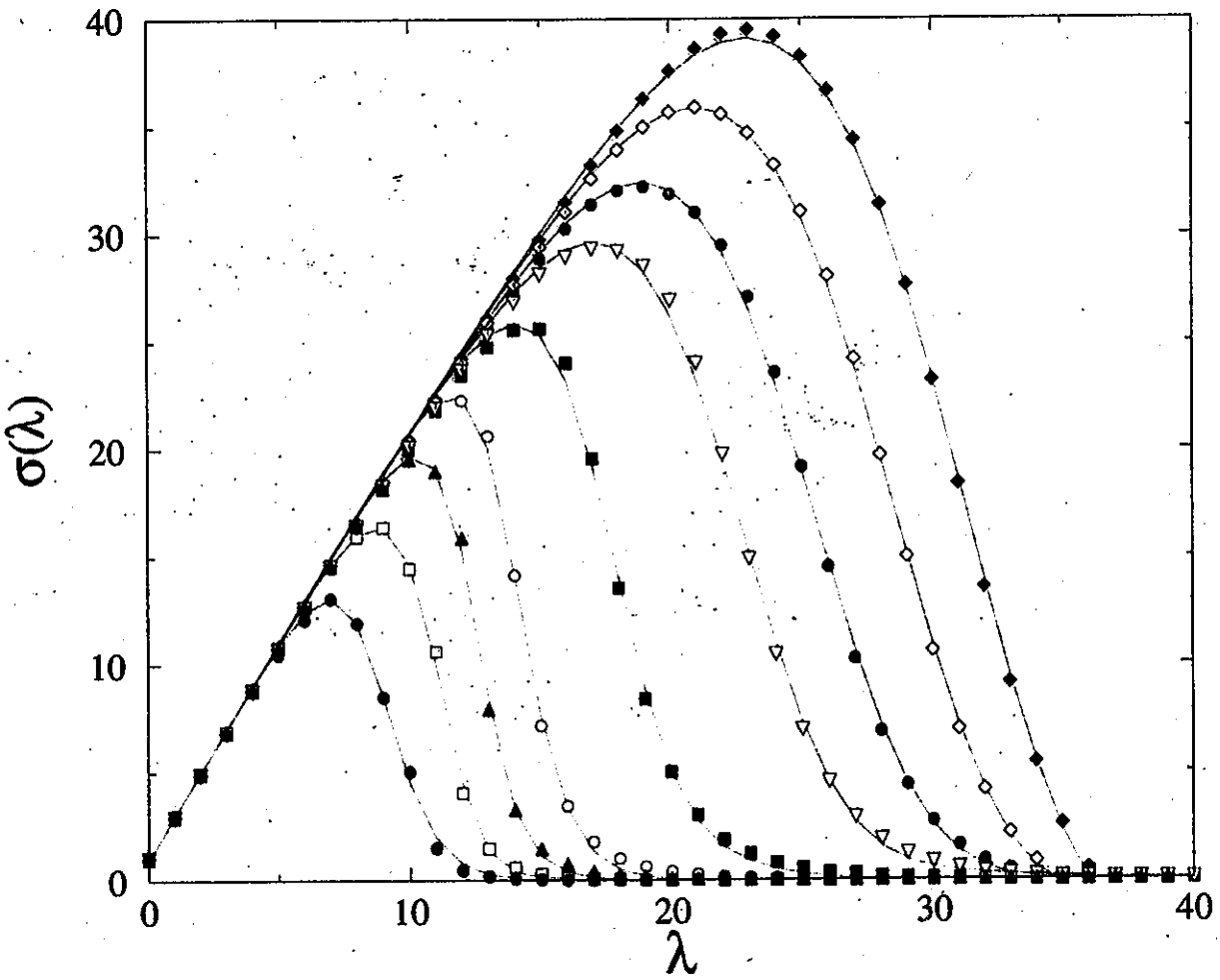

30 to 300 MeV protons on ^{208}Pb

Functional Form for $\sigma_R(E)$

⋆ Data from ^{208}Pb :

(30, 40, 50, 65, 100, 160, 200, 250, 300 MeV)

$\Rightarrow$ $\sigma_R^l(E)$ has a simple functional form

$$\sigma_R^l(E) = (2l+1)\left[1+e^{\frac{(l-l_0)}{a}}\right]^{-1} + \epsilon\,(2l_0+1)e^{\frac{(l-l_0)}{a}}\left[1+e^{\frac{(l-l_0)}{a}}\right]^{-2}$$

$l_0(E,A)$, $a(E,A)$ and $\epsilon(E,A)$ smooth functions.

⋆ Assume: $\epsilon = -1.5$ and

$$a(E,A) \sim 1.02k - 0.25 \quad \text{where} \quad k = \frac{1}{\hbar c}\sqrt{E^2 - m^2c^4}$$

$l_0(E,A)$; function form $\equiv$ measured $\sigma_R(E)$

⋆ high energy limit:

As total reaction cross section sum limited to l_{max}

For $l_{max}(E \to \infty)$, function $\approx$ a triangle so

$$\sigma_R \Rightarrow \frac{\pi}{2k^2} l_{max}(2l_{max}+1) \approx \frac{\pi}{k^2} l_{max}^2 \Rightarrow \pi R^2$$

the geometric cross section

Functional form ctnd.

Data fit values of l_0

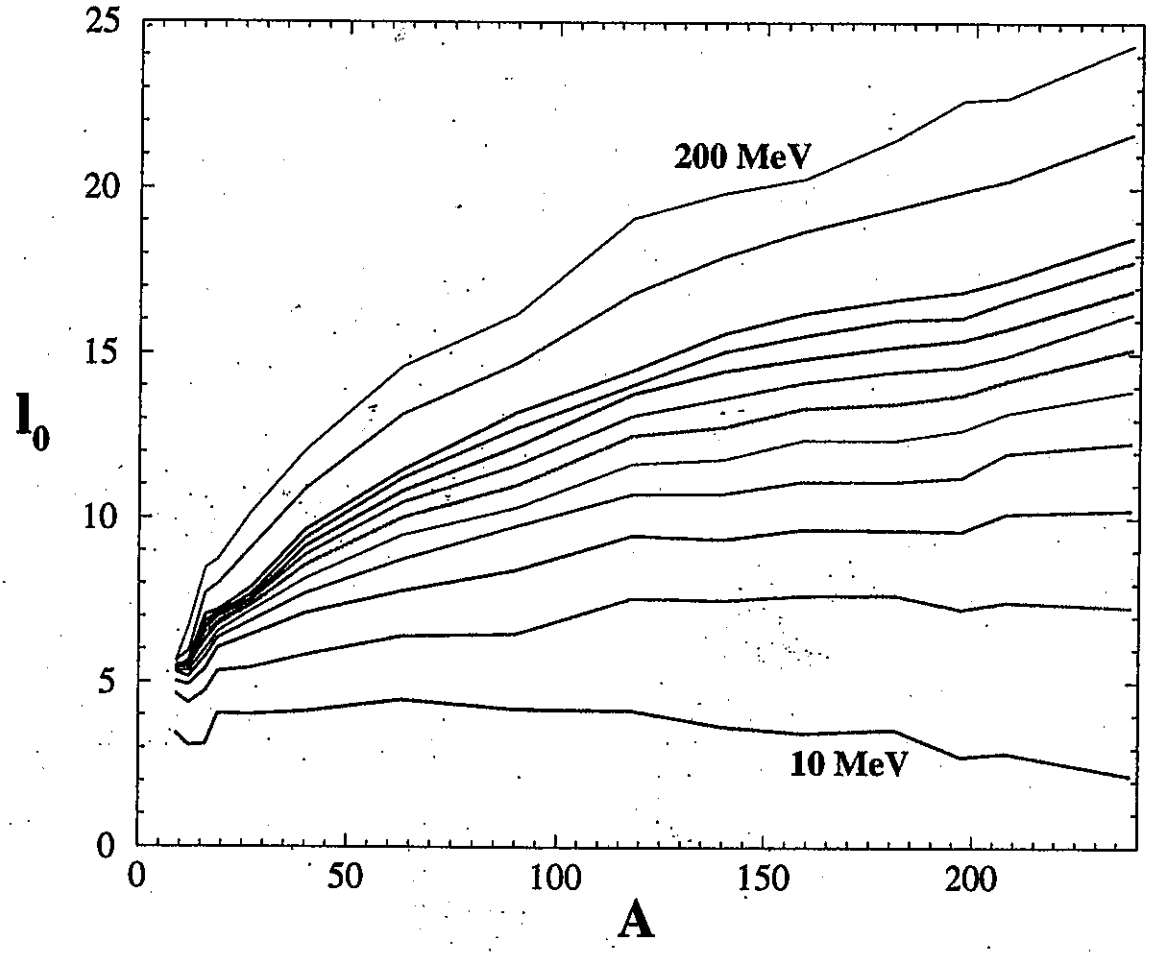

Values of l_0 given fixed values for ϵ, a
with which many measured reaction cross sections are fit
at diverse energies between 10 to 200 MeV

Functional form ctnd.

Reaction cross section fits

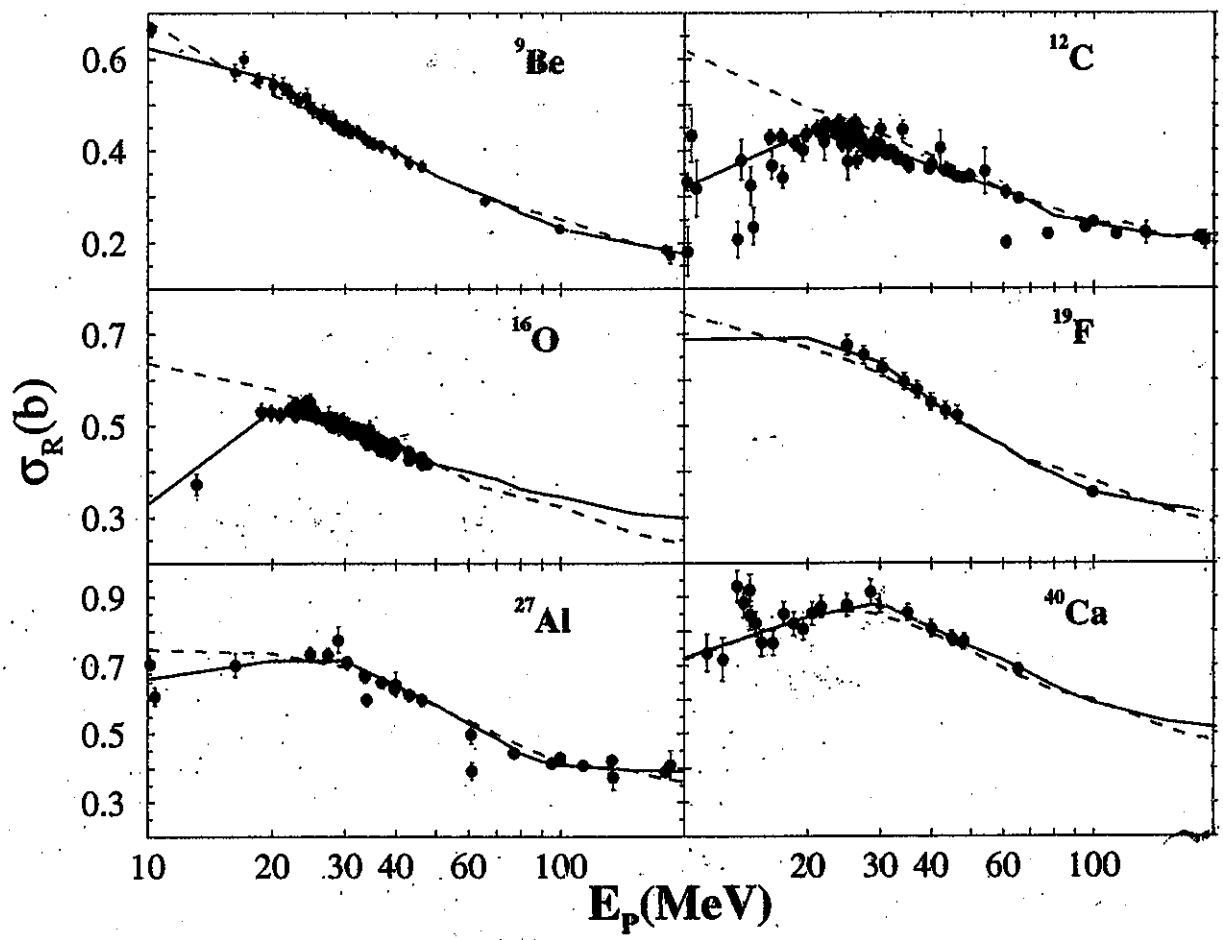

Reaction cross sections compared with predictions and function form fits

——— Function form

– – – – g-folding OMP

Inelastic Scattering

The D.W.A. and inelastic scattering

Elements in D.W.A. analyses:–

1. **Distorted Wave Approximation:–**
   Fully antisymmetrised theory
   involving nonlocal optical potentials

2. **An effective (NN) interaction:–**
   from a mapping of NN g matrices

3. **Nuclear spectroscopy:–** Shell model
   Example:– ^{12}C
   $J^{(+)}$ states – $(0+2)\hbar\omega$ basis
   $J^{(-)}$ states – $(1+3)\hbar\omega$ basis
   $\Downarrow$
   OBDME

4. **Single nucleon bound state functions:–**
   Fit electron scattering form factors
   or given with the Shell model states

Inelastic scattering ctnd.

- **The D.W.A. amplitudes:** $\mathcal{T} = T^{M_f M_i \nu' \nu}_{J_f J_i}(\theta)$

$$\mathcal{T} = \left\langle \chi^{(-)}_{\nu'}(\mathbf{k}_o 0) \right| \left\langle \Psi_{J_f M_f}(1 \cdots A) \right| A \mathbf{g}_{eff}(0,1) \times \mathcal{A}_{01} \left\{ \left| \chi^{(+)}_{\nu}(\mathbf{k}_i 0) \right\rangle \left| \Psi_{J_i M_i}(1 \cdots A) \right\rangle \right\}$$

⋆ Cofactor expand structure wave functions

$$\left| \Psi_{JM} \right\rangle = \frac{1}{\sqrt{A}} \sum_{j,m} \left| \varphi_{jm}(1) \right\rangle a_{jm} \left| \Psi_{JM} \right\rangle$$

⋆Expanded matrix elements

$$\mathcal{T} = \sum_{j_1, j_2} \left\langle \Psi_{J_f M_f} \right| a^{\dagger}_{j_2 m_2} a_{j_1 m_1} \left| \Psi_{J_i M_i} \right\rangle \times \left\langle \chi^{(-)}_{\nu'}(\mathbf{k}_o 0) \right| \left\langle \varphi_{j_2 m_2}(1) \right| \mathbf{g}_{eff}(0,1) \times \mathcal{A}_{01} \left\{ \left| \chi^{(+)}_{\nu}(\mathbf{k}_i 0) \right\rangle \left| \varphi_{j_1 m_1}(1) \right\rangle \right\}$$

- **The density matrix elements:**

$$\left\langle \Psi_{J_f M_f} \left| a^{\dagger}_{j_2 m_2} \; a_{j_1 m_1} \right| \Psi_{J_i M_i} \right\rangle = \sum_{I(N)} (-1)^{(j_1 - m_1)} \; C^{m_1, -m_2}_{j_1, j_2, I} \times \left\langle \Psi_{J_f M_f} \left| \left[a^{\dagger}_{j_2} \times a_{j_1} \right]^{IN} \right| \Psi_{J_i M_i} \right\rangle$$

Inelastic scattering ctnd.

Use the Wigner–Eckart theorem

$$\left\langle \Psi_{J_f M_f} \left| a^{\dagger}_{j_2 m_2} \; a_{j_1 m_1} \right| \Psi_{J_i M_i} \right\rangle = \sum_{I(N)} (-1)^{(j_1 - m_1)} C^{m_1,-m_2}_{j_1,j_2,I}$$

$$\times C^{M_i,N}_{J_i,I,J_f} \; \frac{1}{\sqrt{2J_f+1}} \; S_{j_1 j_2 I}$$

$S_{j_1 j_2 I}$ are the OBDME

- **The expanded D.W.A. amplitudes:**

$$\mathcal{T} \;=\; \sum_{j_1,j_2,m_1,m_2,I(N)} \frac{(-)^{(j_1-m_1)}}{\sqrt{2J_f+1}} C^{M_i,N}_{J_i,I,J_f} \; S_{j_1,j_2,I}$$

$$\times C^{m_1,-m_2}_{j_1,j_2,I} \left\langle \chi^{(-)}_{\nu'}(\mathbf{k}_o 0) \right| \langle \varphi_{j_2 m_2}(1)| \;\; \mathbf{g}_{eff}(0,1)$$

$$\times \mathcal{A}_{01} \left\{ \left| \chi^{(+)}_{\nu}(\mathbf{k}_i 0) \right\rangle \; |\varphi_{j_1 m_1}(1)\rangle \right\}$$

- Three ingredients:
  - a) $\mathbf{g}_{eff}(0,1)$ – transition operator
    effective interaction used to form g-folding potentials $\Rightarrow$ distorted waves
  - b) $S_{j_1,j_2,I}$ – OBDME from structure
  - c) φ_{jm} – Single particle bound states

Inelastic scattering: applications

Excitation of the 4.44 MeV 2^+ state in ^{12}C

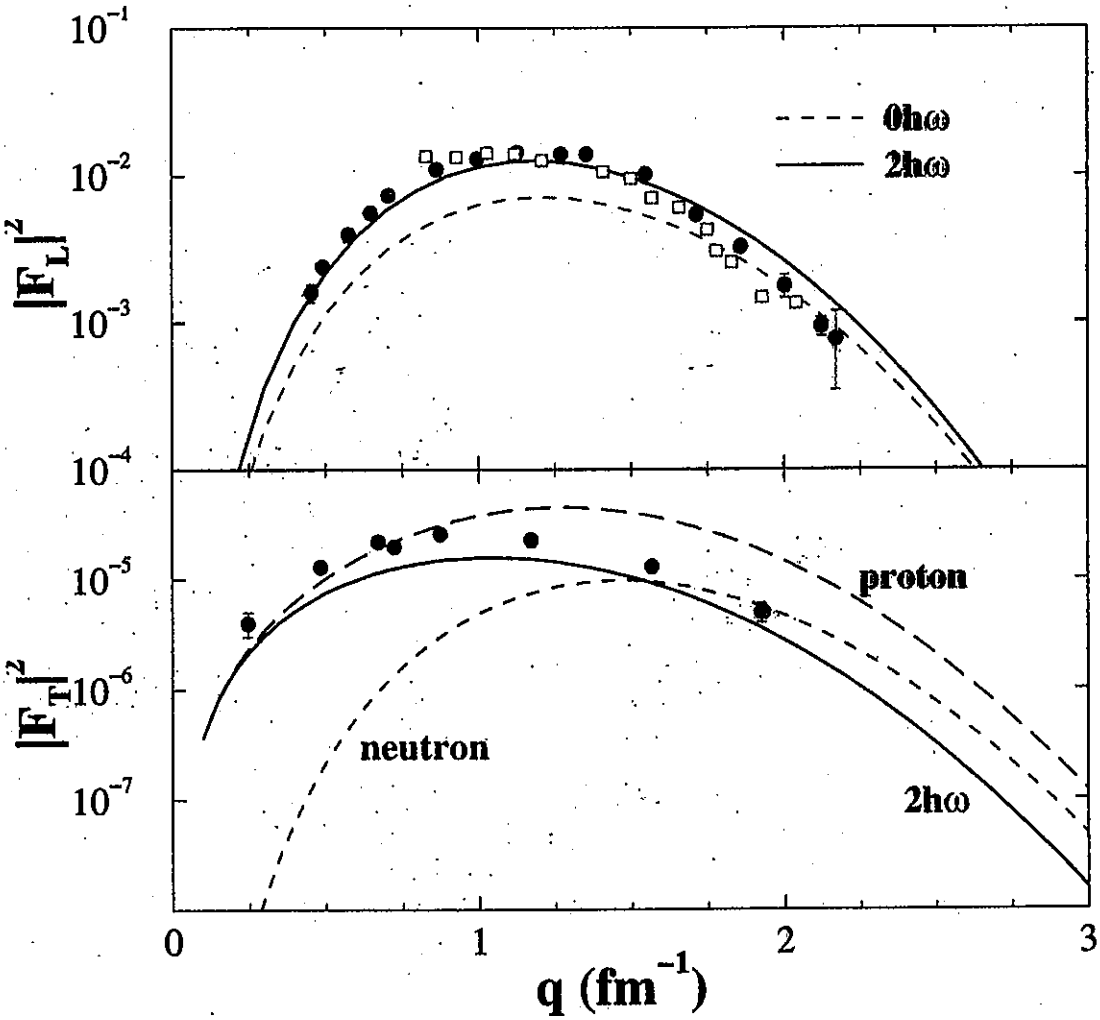

E2 Longitudinal (top) and transverse (bottom) form factors

(Model space and/or components as indicated)

Inelastic scattering: applications ctnd.

200 MeV p-^{12}C to the 4.44 MeV 2^+ state

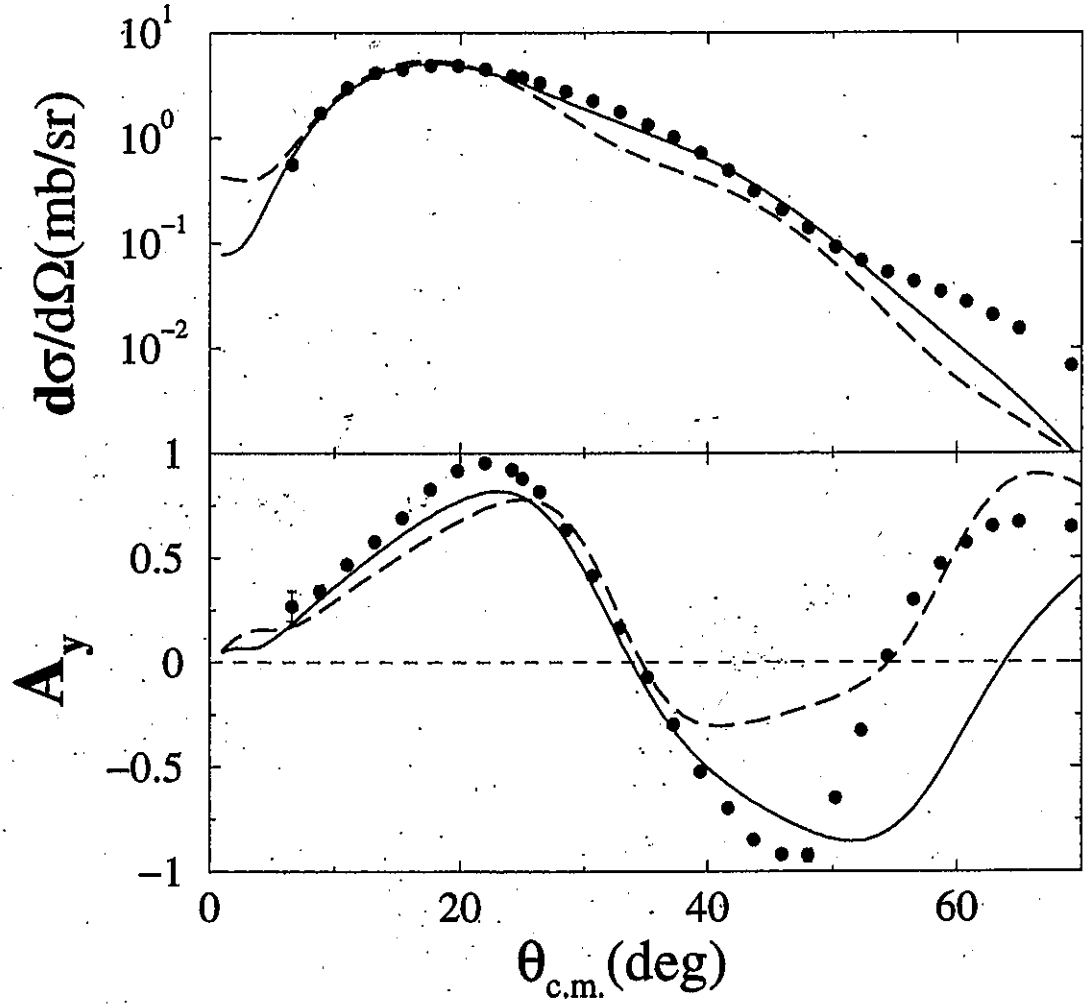

$2\hbar\omega$ predictions compared with data

—— g matrix

- - - t matrix

Inelastic scattering: applications ctnd.

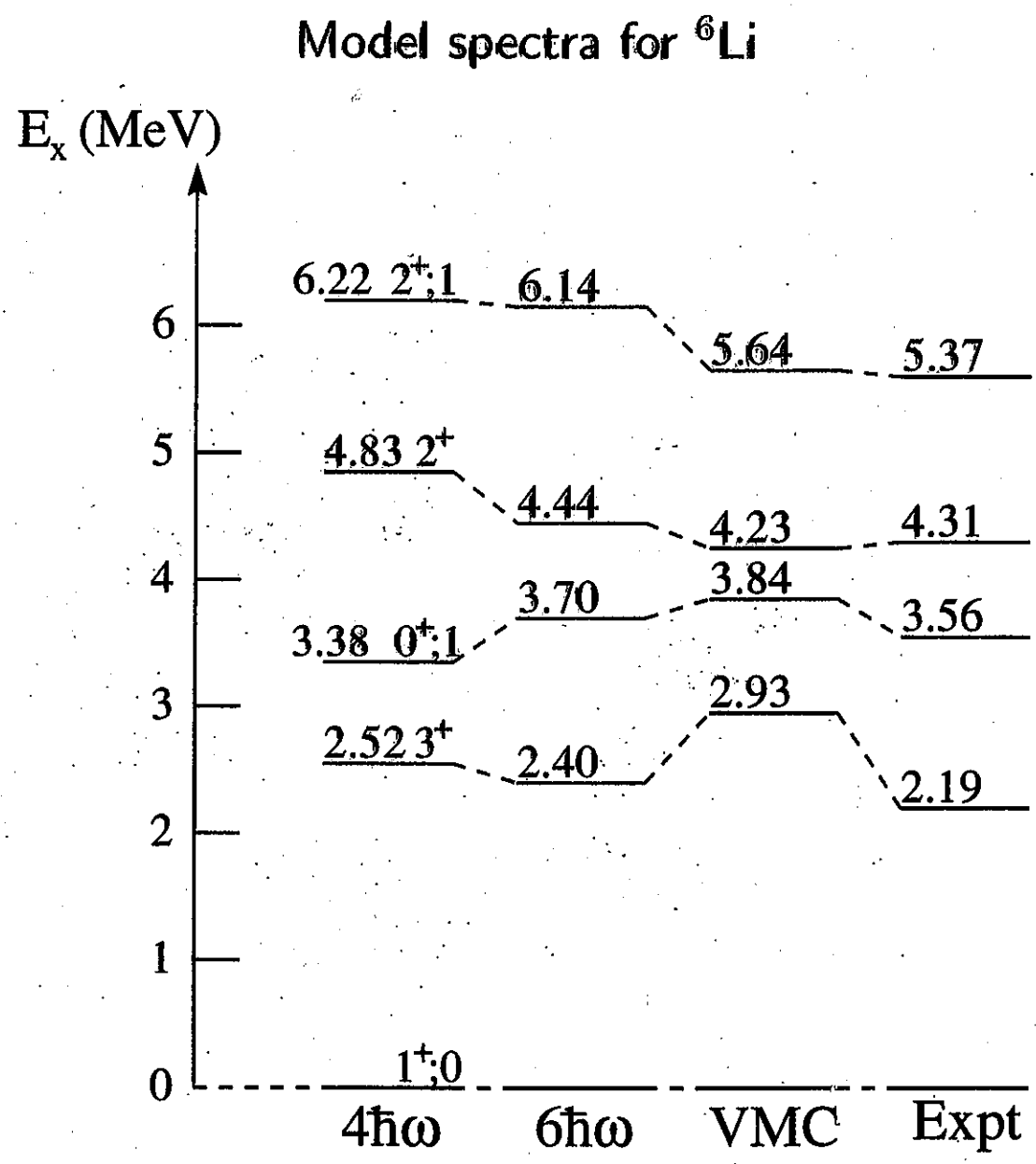

(Two shell models and a VMC result)

Inelastic scattering: applications ctnd.

Electron scattering to the 3_1^+ state in ^{6}Li

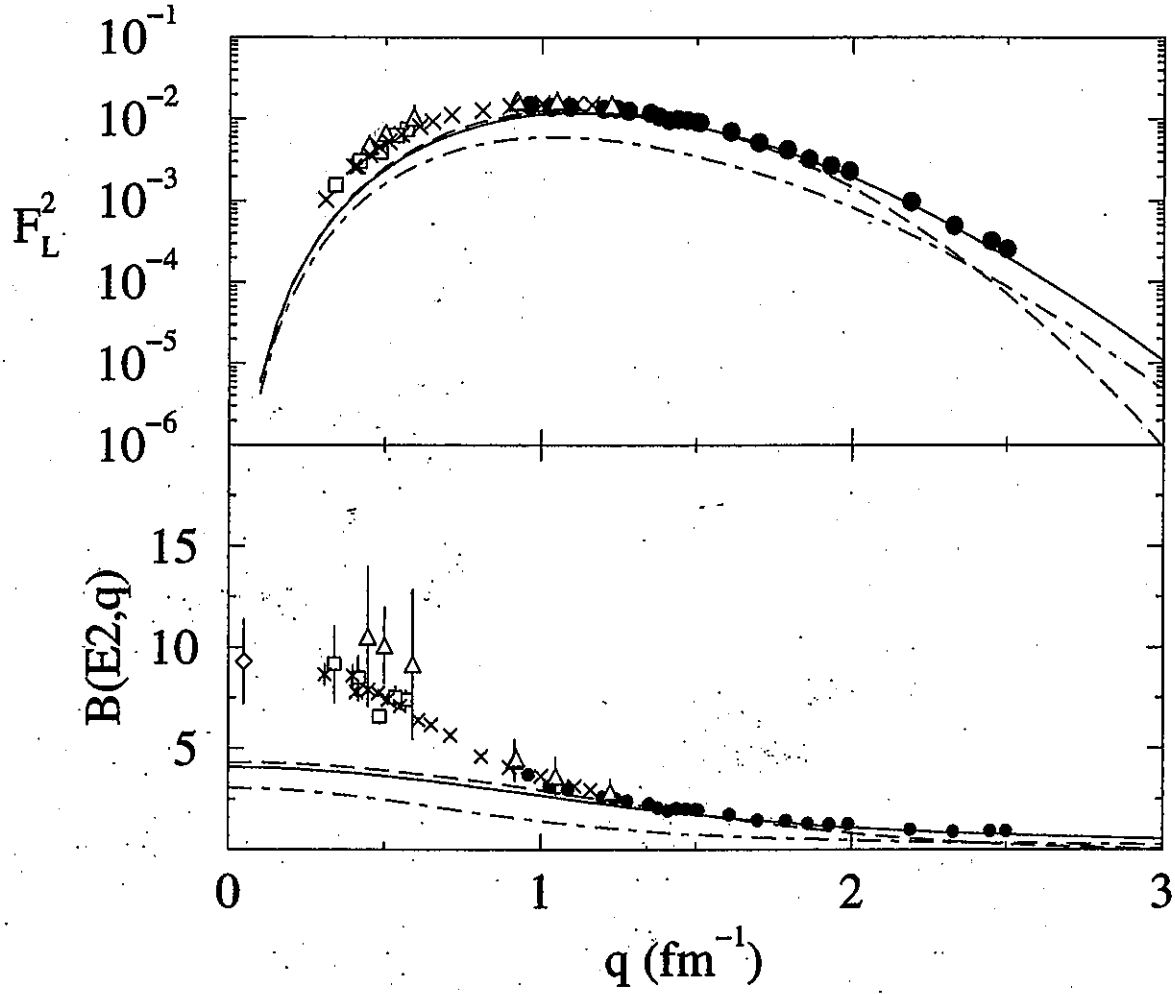

E2 Longitudinal form factor

——— $4\hbar\omega$ shell model

– – – $2\hbar\omega$ shell model

– · – · $0\hbar\omega$ shell model

Inelastic scattering: applications ctnd.

200 MeV p-^{6}Li to the 2.186 MeV 3^+ state

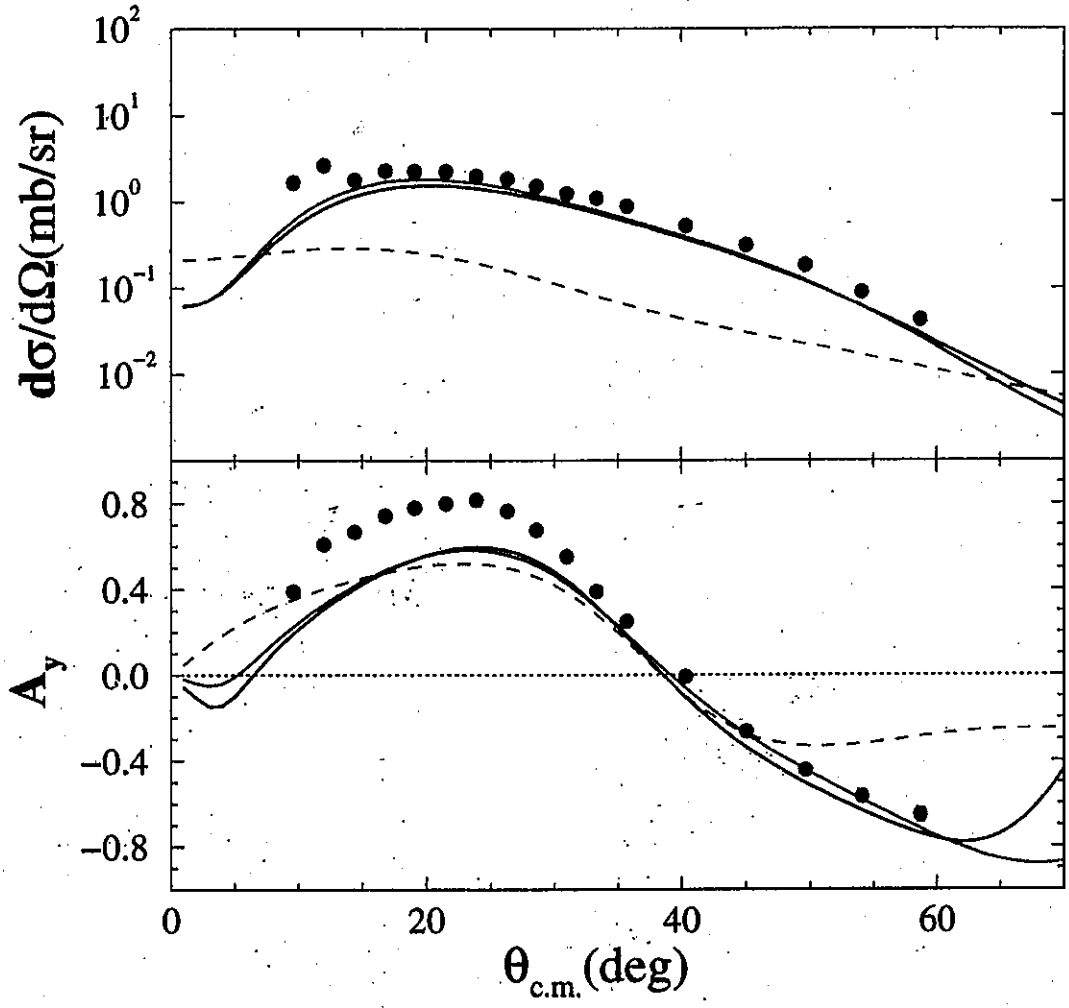

Predictions compared with data

—— $4\hbar\omega$ shell model

—— $2\hbar\omega$ shell model

– – $0\hbar\omega$ shell model

Inelastic scattering: applications ctnd.

40.9A MeV ^{6}He-p to the 2+ (1.8 MeV) state

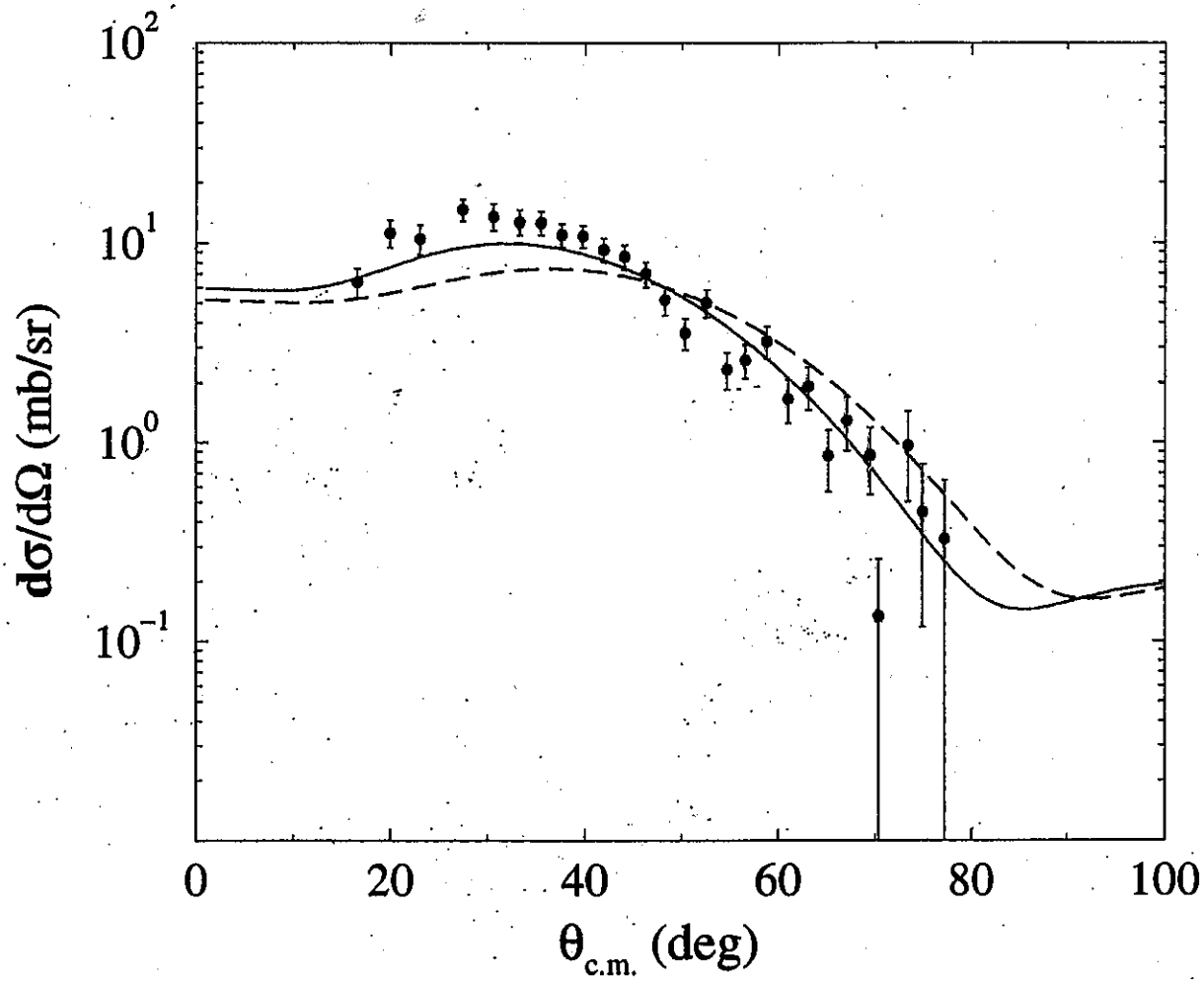

Predictions compared with data

——— Halo

– – – No-halo

Inelastic Scattering: applications ctnd.

^{6}He scattering from Hydrogen

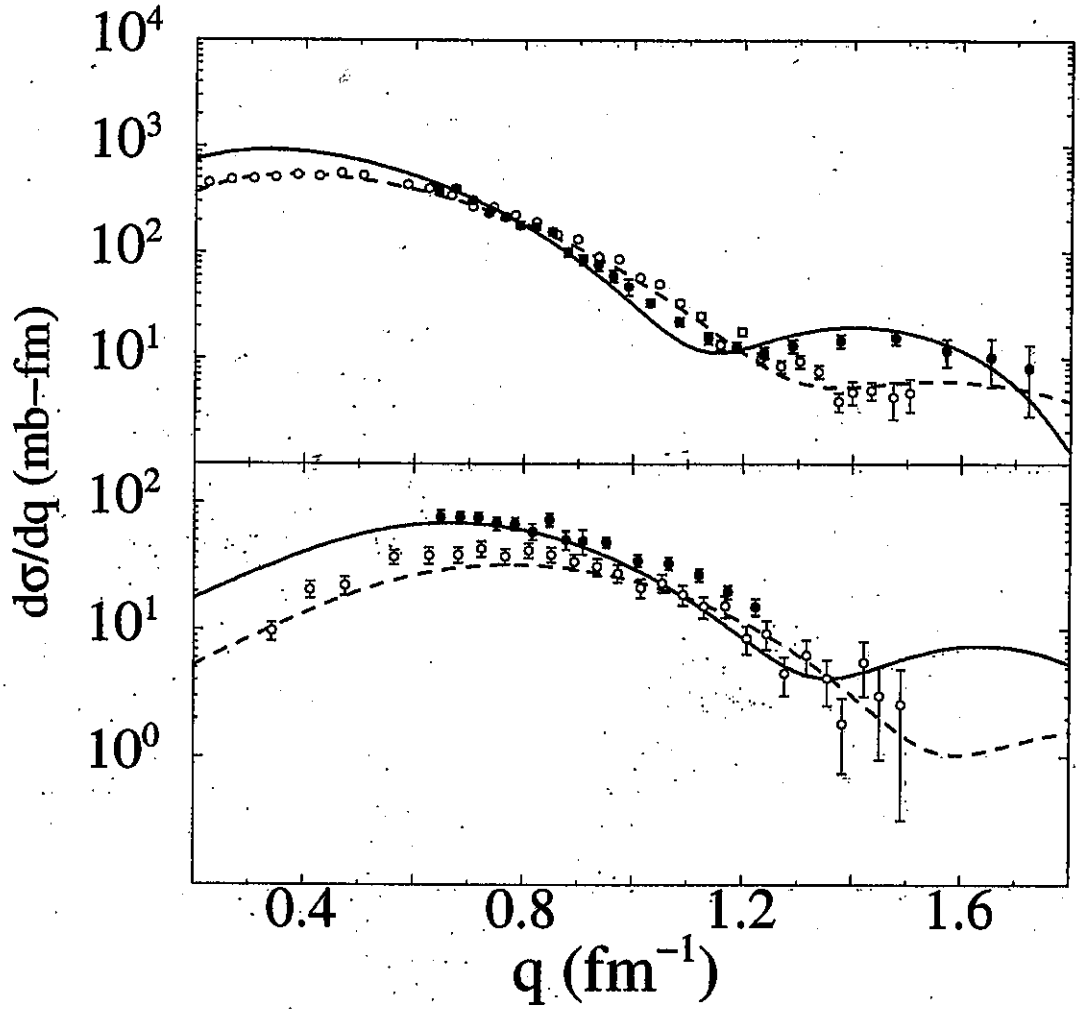

Elastic (top) and inelastic (bottom) scattering
(all results assuming a halo structure)

24.5A MeV:– filled circles, solid lines
40.9A MeV:– open circles, dashed lines